PART 1: CONTROLLING BARRIERS TO CHARGE TRANSFER IN DNA

PART 2: DNA-DIRECTED ASSEMBLY OF CONDUCTING OLIGOMERS

A Dissertation

Presented to

The Academic Faculty

by

Gözde Güler

In Partial Fulfillment
of the Requirements for the Degree
Doctor of Philosophy in the
School of Chemistry and Biochemistry

Georgia Institute of Technology

December 2008

PART 1: CONTROLLING BARRIERS TO CHARGE TRANSFER IN DNA

PART 2: DNA-DIRECTED ASSEMBLY OF CONDUCTING OLIGOMERS

Approved by:

Dr. Gary B. Schuster, Advisor
School of Chemistry and Biochemistry
Georgia Institute of Technology

Dr. Bridgette Barry
School of Chemistry and Biochemistry
Georgia Institute of Technology

Dr. David M. Collard
School of Chemistry and Biochemistry
Georgia Institute of Technology

Dr. Laren M. Tolbert
School of Chemistry and Biochemistry
Georgia Institute of Technology

Dr. Roger Wartell
School of Biology
Georgia Institute of Technology

Date Approved: 11/11/2008

This dissertation is dedicated to my family.

To my parents Emral and Ahmet Güler who have been the most supportive, most loving parents anyone could ask for.

To my sister Deniz Güler Sahin who has always been my rock, the voice of reason in my head.

Without your guidance and love none of this would be possible.

I love you all very much.

ACKNOWLEDGEMENTS

I have been extremely blessed to have the support of so many people during my time at Georgia Tech. First of all I would like to thank my advisor Gary B. Schuster for his never ending support, understanding and wisdom. Without his direction, patience and his trust in me when I didn't trust myself I would never be able to get through the tough times and finish this work. I will be eternally grateful to him.

I would also like to thank past and present Schuster lab members. A special thanks to Dr. Abraham Joy who has been my mentor when I started my doctorate degree and Dr. Joshy Joseph for picking up where Abraham left off. Abraham, Joshy and their wives Suguna and Suma opened their hearts and homes to me and their friendship means the world to me. I would like to thank Dr. Sriram Kanvah for all of his help through the years. I would also like to express my gratitude to Dr. Elizabeth Kuruvilla, Daniela Verga, Dr. Prolay Das, Dr. Lezah Roberts, Dr.Thabisile Ndlebe, Dr. Nathan Schlientz, Dr.Frank Onyemauwa, Dr. Bhaskar Datta, Dr. Rick Redic, Dr. Chu-sheng Liu, Dr. Wen Chen, Dr. Huachuan Cao for their friendship, support, invaluable input and making my years in this lab, so enjoyable.

I would like to thank my committee members for their suggestions, availability, encouragement and support. A special thanks to Dr. David

Collard and Dr. Cameron Tyson for their support during the first year of my doctorate and continuing encouragement since then.

It has been a hard 7 years for me at Georgia Tech. I would like to thank my girls Chiko Umeweni and Christy Charlton for the margaritas, the phone calls and for just being awesome overall. I love them to death!

An extra special thanks to my friends Melis Inan, Tuba Sural and Hale Asar Ogun for being the best girlfriends, sisters, a girl can ask for. They have stood by me for over 12 years now and the support, the love I got from them has always been priceless. I don't know what I would do without them and I hope I never learn.

I would like to thank the "Turkish mafia", my apprentices, Zeynep Turunc and Burcu Ishakoglu, my rocks Ozgul Persil Cetinkol and Ozlem Dogan Ekici, their rocks and overall great men Mehmet Cetinkol and Eylem Ekici, my good friends Mehmet Kutukcu, Asli Ovat (thanks for sharing your home with me), Alpay Kimyonok, Emel Eren, Selma Bakbak and Kagan Kuyu, Mustafa Burak Boz, Gungor Ozer for always being there when I needed them and for their friendship.

I'd like to thank Cihan Oguz for all the basketball games, for listening to my ramblings and for his friendship.

Gonca Basak Bayraktar for her encouragement and for just being so sweet all the time.

Big thanks to Aslihan Cortuk, Veronica DeSilva, Gamze Koseoglu, Gozde Coklu, Nevce Gurkan, Pinar Zaimoglu, Burc Tosyali, Sarp Centel, Ali Nejat Ipekci, Ilkay Yavrucuk and so many more for their friendship, support and for simply making Atlanta fun! I'll see you all in Istanbul!

Last but not least, I would like to thank my family, Emral and Ahmet Guler, Deniz Guler Sahin and Rafet Sahin. They've always believed in me, always supported me. Even though they lived thousands of miles away they were on a plane in a heart beat when I needed them. When the going got tough they got me going, I will live the rest of my life trying to do the same for them.

As Gary always said through "the series of unfortunate events" it was like I was walking with a black cloud over me for the past 7 years. I would like to thank God for always keeping me alive and keeping a light at the end of the tunnel.

TABLE OF CONTENTS

LIST OF TABLES

LIST OF FIGURES

LIST OF SYMBOLS AND ABBREVIATIONS

A	Adenine
APS	Ammonium per Sulfate
AQ	Anthraquinone
aq.	Aqueous
$B^{+\cdot}$	Base radical cation
C	Cytosine
CD	Circular Dichroism
$CdCl_2$	Cadmium Chloride
CH_3CN	Acetonitrile
cm	Centimeter
DBU	1,8-diazabicyclo[5.4.0]undec-7ene
DNA	Deoxyribonucleic Acid
EDTA	Ethylene Diamine Tetra Aceticacid
E_{ox}	Oxidation Potential
ESI	Electrospray Ionization
f	2,4-Difluorotoluene
G	Guanine
g	Gram
H_2O	Water
H_2SO_4	Sulfuric Acid

HCl	Hydrochloric Acid
HRP	Horse Radish Peroxidase
hrs	hours
k_{hop}	Rate constant for charge migration
KOH	Potassium Hydroxide
k_{trap}	Rate constant for irreversible trapping of the radical cation
M	Molar
mg	Miligram
Mg	Magnesium
$Mg(OAc)_2$	Magnesium Acetate
$MgSO_4$	Magnasium Sulfate
min	Minute
ml	Mililiter
mmol	Milimole
NaCl	Sodium Chloride
$NaHCO_3$	Sodium Bicarbonate
NaOH	Sodium Hydroxide
$NaSO_4$	Sodium Sulfate
NH_4OAc	Ammonium Acetate
nm	Nanometers
NMR	Nuclear Magnetic Resonance
P(PTHA)	Poly(6-(2,5-di(thiophen-2-yl)-1H-pyrrole-1-yl)hexan-1-

	amine)
PAGE	Poly Acrylamide Gel Electrophoresis
PANI	Polyaniline
PNK	Polynucleotide Kinase
SNS	3-(2,5-di(thiophen-2-yl)-1*H*-pyrrol-1yl)propan-1-amine
SNS1	2-(2,5-di(thiophen-2-yl)-1H-pyrrol-1-yl)ethanamine
SPS	Sulfonated Polystyrene
ssDNA	Single Strand DNA
t	3-Methyl-2-Pyridone
THF	Tetrahydrofuran
Tm	Melting Temperature
uM	Micromolar
UV	Ultraviolet
V	Volts
Vis	Visable
β	Beta
γ	Gamma
Δ	Delta
ε	Epsilon
μ	Micro
πß	Pi
°C	Degrees Celcius

SUMMARY

PART I

A series of anthraquinone-linked DNA oligonucleotides was prepared and the efficiency of long-distance radical cation migration was measured. In one set of oligonucleotides, two GG steps are separated by either a TATA or an ATAT bridge. In these two compounds, the efficiency of radical cation migration from GG to GG differs by more than an order of magnitude. Replacement of the thymines in the TATA or ATAT bridges with 3-methyl-2-pyridone (***t***, a thymine analog) results in the much more efficient radical cation migration across the bridge in both cases. This is attributed to a decrease in the oxidation potential of ***t*** to a value below that of A. In contrast, replacement of the thymines in the TATA or ATAT bridges with difluorotoluene (***f***, a thymine analog with high oxidation potential) does not measurably affect radical cation migration. These findings are readily accommodated by the phonon-assisted polaron-hopping mechanism for long-distance charge transfer in duplex DNA and indicate that DNA in solution behaves as a polaronic semiconductor.

PART II

Oligomers containing thiophene-pyrrole-thiphene (SNS) monomers were covalently linked to the nucleobases of DNA. Treatment of these oligomers with horseradish peroxidase and hydrogen peroxide lead to the formation of conducting oligomers conjoined to the DNA. The DNA template aligns the oligomers along one strand of the duplex and limits the intermolecular reaction of monomers. This method enables utilization of the unique self-recognizing properties and programmability of DNA to create tailored oligomers.

PART I: Controlling Barriers to Charge Transfer in DNA

CHAPTER 1: Introduction

Deoxyribonucleic acid (DNA) is the storehouse, or cellular library, that contains all the information required to build the cells and tissues of an organism.[1]

In 1943 Avery and coworkers identified DNA as the carrier of genetic information.[2] Almost a decade later, in 1952 Rosalind Franklin took a set of X-Ray diffraction images of DNA.[3] One of those images, named Picture 51 by Franklin, was shown to James D. Watson by Maurice Wilkins. This particular picture was the last piece of information needed for Watson and his colleague Francis Crick to build the first model of DNA structure that is still accepted today.[4] The discovery of the secondary structure of DNA has opened the door to an exciting new era in DNA research. With the knowledge of the base stacking nature of DNA, one of the most exciting questions was whether or not a charge could migrate through the DNA.[5,6] Decades of research have focused on understanding the charge transfer through DNA. It has been shown that charges moving through DNA may result in oxidative damage, which is believed to be responsible for aging, apoptosis and cancer.[7,8,9,10] A better understanding of the mechanism of charge migration through DNA may lead to the discovery of tools required for damage prevention and repair.[11] The

phenomena of charge migration through DNA have led to the hypothesis that DNA could be used as a "molecular wire".[12] It is now known that the poor conductivity of DNA prohibits its use as a molecular wire.[13,14] Although it is acknowledged that charge, in the form of radical cation or electron can migrate into DNA to a limited distance, the mechanism by which this migration process occurs has produced much controversy among researchers.

1.1 Structural overview of DNA

DNA is chemically a polymer composed of monomeric units called nucleotides. The polymerization of nucleotides forms nucleic acids. DNA's structure plays an important role in storing and transferring genetic information which is encoded in the sequence of its nucleotides.[15] A nucleotide consists of a phosphate group linked by a phosphodiester bond to a pentose which in turn is linked to a nitrogen containing organic base.[1] Nucleotides are connected to each other by a phosphate backbone form that forms each of the DNA strands. Two anti-parallel complementary DNA strands come together to form the DNA double helix structure. The double helical nature of DNA encloses the nucleotides and prevents them from damage[16] while conserving the integrity of the genetic information.[17]

1.1.1 Structural components of DNA

1.1.1.1 Bases

Four different bases make up the DNA structure: Adenine (A), Thymine (T), Guanine (G) and Cytosine (C). Adenine and guanine contain a pair of fused rings and are purines whereas thymine and cytosine contain a single ring and are pyrimidines (Figure 1).[1]

Purines adenine and guanine have a six-membered ring fused to a five-membered ring with two nitrogen atoms in each respective ring. Adenine contains an amino group ($-NH_2$) attached at the C6 position of the purine ring while guanine contains an amino group at the C2 position and a carbonyl group (-C=O) at the C6 position of the purine.

Pyrimidines thymine and cytosine have a six-membered aromatic ring with two nitrogen atoms. Cytosine contains a carbonyl group at the C2 position and an amino group at the C4 position of the pyrimidine whereas thymine contains two carbonyl groups at positions C2 and C4 as well as a methyl group ($-CH_3$) at the C5 position of the pyrimidine.[18]

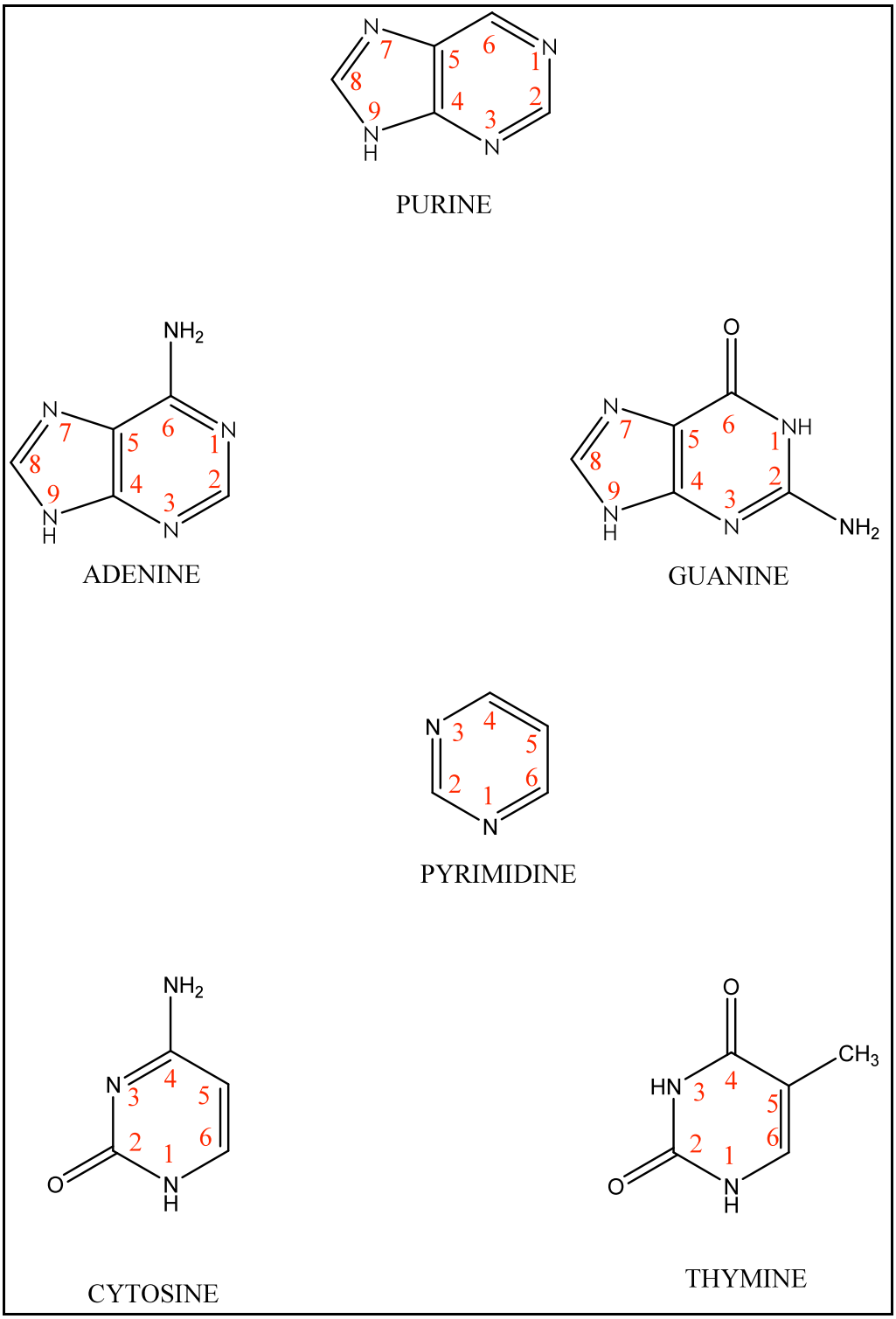

Figure 1 Structures of Purine, Pyrimidine and DNA bases

1.1.1.2 Sugar

The bases of DNA are linked to pentose groups. In DNA the pentose is 2-Deoxyribose which is an aldopentose (Figure 2).[1] The five-membered sugar ring is not planar for steric reasons; its conformation determines the shape of the DNA helix. One of the atoms in the ring tends to "pucker" out of the plane of the ring in order to conform to the tetrahedral arrangement of each carbon molecule affecting the overall conformation of the DNA. The conformation with a sugar pucker on the same side of the plane as the base and the C5' (See Figure 2) is commonly referred to as an *endo* conformation, while the conformation with the sugar pucker on the opposite side of the plane is referred to as an *exo* conformation. For DNA, the sugar pucker is mainly C2'-*endo*. This conformation lines up the oxygen and 3 carbon molecules in the same plane while C2' carbon puckers out of the plane. The exo conformation has not been found in DNA.[18]

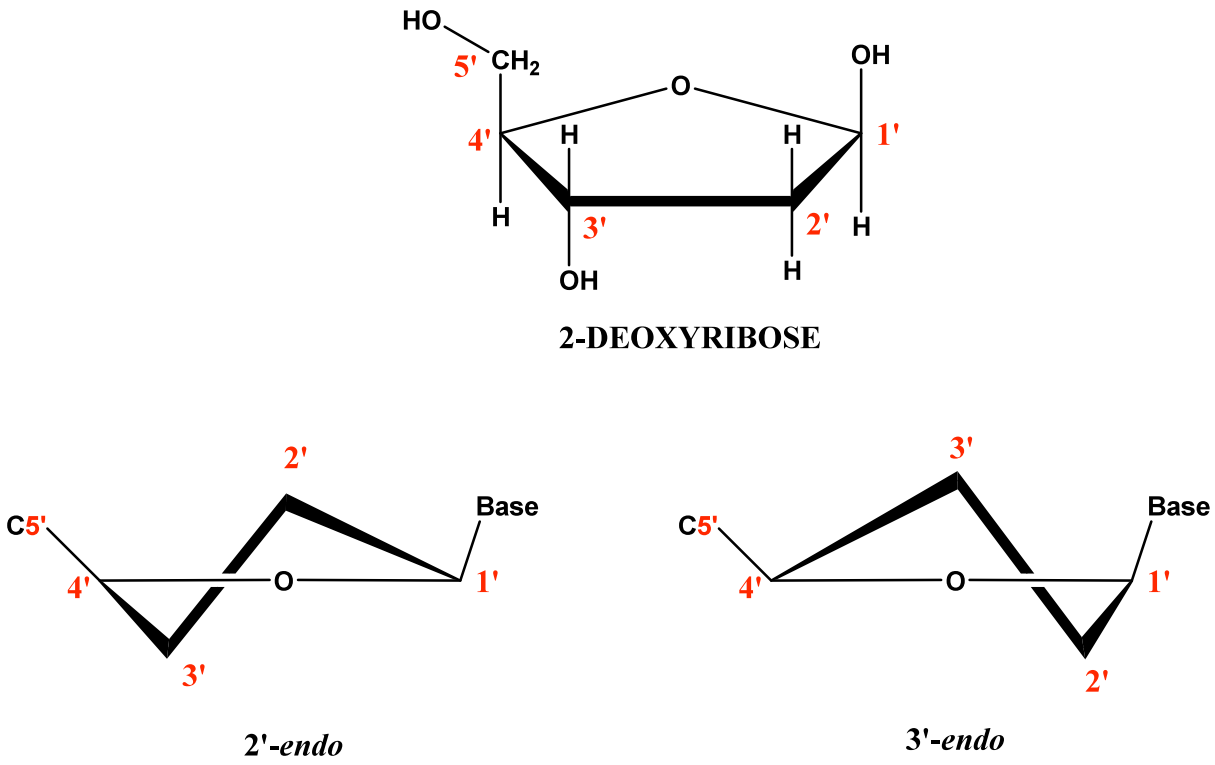

Figure 2 Structure of 2-Deoxyribose and Sugar Puckers

1.1.1.3 Glycosidic Bond

The sugar and base are linked to each other by a glycosidic bond forming nucleosides (Figure 3). In the purine bases, adenine and guanine, the glycosidic bond is between the N9 of the base and the C1 of the sugar. In the pyrimidine bases, cytosine and thymine, the glycosidic bond is between the N1 of the base and the C1 of the sugar.

1.1.1.4 Phosphate backbone and phosphodiester bonds

Phosphate groups are attached to 5'-CH_2OH and 3'-OH of the sugar, forming the backbone of DNA (Figure 3). As mentioned earlier the deoxyribose sugar, the base and the phosphate group form the nucleotide. Nucleotides are connected to each other via phosphodiester bonds. The end of the DNA strand where the phosphate is connected to C5' hydroxyl is termed as the 5'-end and the opposite end is termed as 3'-end.

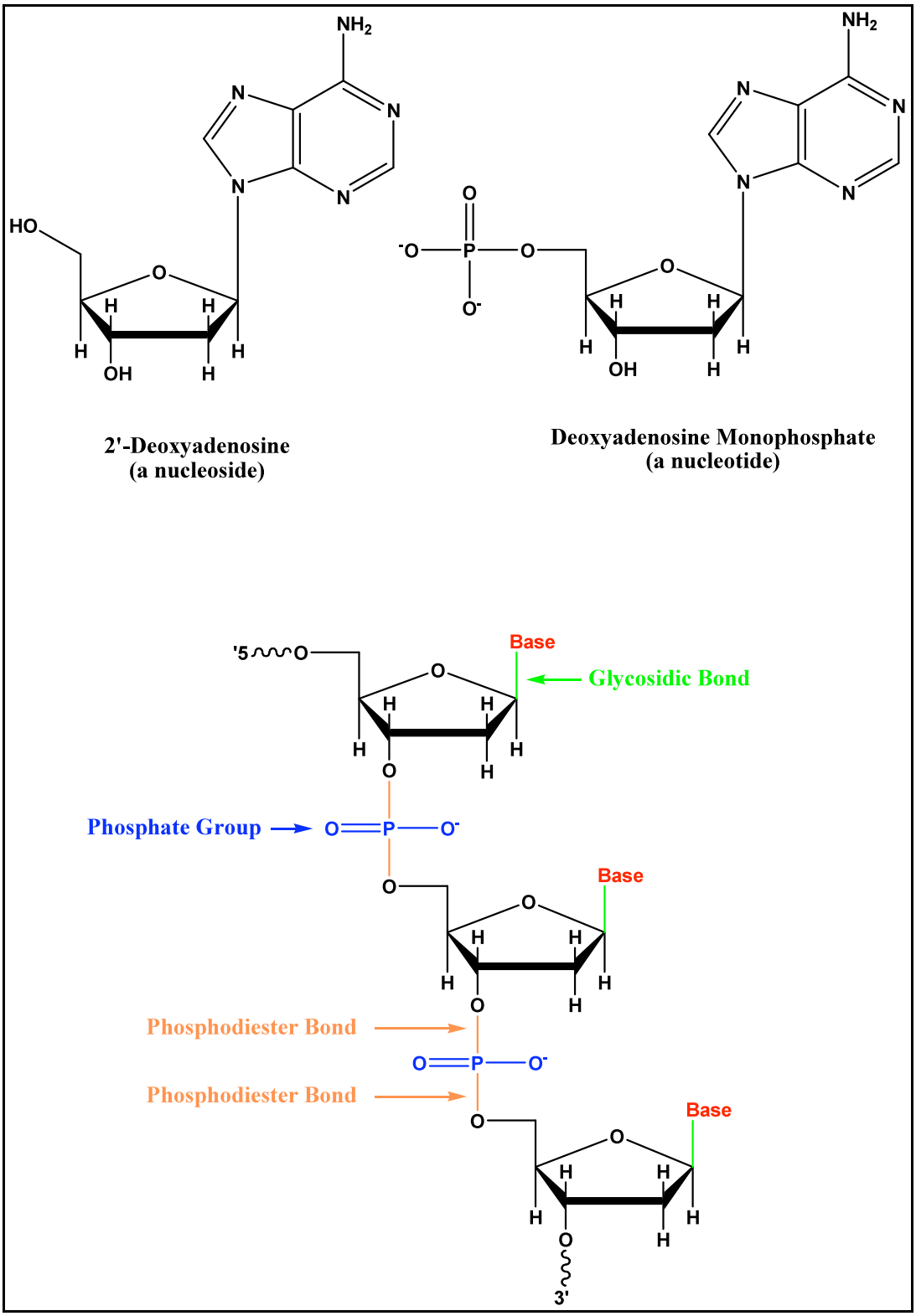

Figure 3 Structure of nucleosides and nucleotides

1.1.2 The DNA Double Helix

In 1953 Watson and Crick proposed the double helical structure of DNA.[4] According to their model, which is the accepted model for DNA today, two complementary strands of DNA line up anti-parallel to each other (their 5' → 3' direction is opposite) and twist around the same axis to form a right-handed helical structure called the DNA double helix. Two bases on opposing strands are held together by hydrogen bonds forming base pair.[19] The base pairs are complementary to each other as a consequence of their shape, size and chemical composition of bases.[1] Adenine (A) is paired with thymine (T) via two hydrogen bonds and guanine (G) is paired with cytosine (C) via three hydrogen bonds. Watson-Crick base pairing is the most common base pairing found in DNA. In this base pairing the C6-NH_2 of A forms a hydrogen bond with C4-O of T and N1 of A forms a hydrogen bond with N3-H of T. For G-C base pairs the three hydrogen bonds involve the C6-O of G with C4-NH_2 of C, N1-H of G with N3 of C and lastly C2-NH_2 of G with C2-O of C (Figure 4).

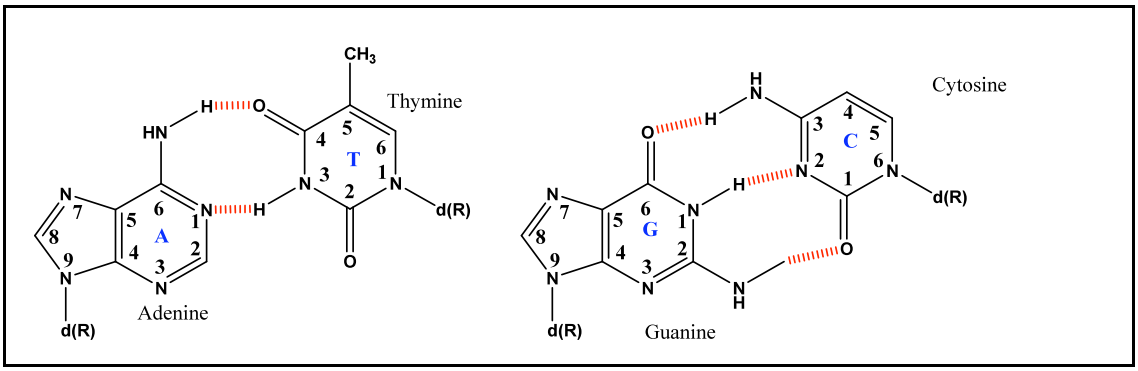

Figure 4 Watson-Crick Base Pairs. Hydrogen Bonds are shown in red.

The bases stack on top of each other in parallel planes facing towards the core of the helix and the individual sugar phosphate backbone chains run along the periphery, thereby minimizing the repulsions between the charged phosphate groups.

Although hydrogen bonds between bases add to the stability of the DNA duplex there are bigger forces that hold the strands of the double helix together. Hydrophobic forces are the major stabilizing factor in the DNA duplex[19] because the aromatic heterocyclic structures of the bases can not offer much hydrogen bonding alternatives to water molecules; water is excluded from the interior of the helix. Bases form stacking interactions with neighboring bases instead, thereby stabilizing the DNA duplex.[20] The negatively charged, hydrophilic phosphate groups are projected towards the cellular liquid and are surrounded by metal cations adding to the stability of the duplex. Lastly, water molecules cooperatively bind along

the major and minor groove of DNA adding further stability to the duplex structure.[21]

1.1.3 DNA Conformations

Depending on its environment, the DNA duplex is found in mainly three different conformations: A-Form, B-Form and Z-Form DNA.[22] The characteristics of these DNA conformations are listed in Table 1.

Table 1 Properties of Different DNA Conformations[22]

Helix Sense	Right Handed	Right Handed	Left Handed
Repeating Unit	1 base pair	1 base pair	2 base pairs
Rotation/Base Pair	33.6 ^{0}C	t_t : 38.0^{0}C (4.4^0)* t_g : 35.9^{0}C (4.2^0)*	60^{0}C /2
Mean Base Pairs/Turn	10.7	10.0 (1.2)*	12
Inclination of Base to Helical Axis	+19^0	-1.2^0 (4.1^0)*	-9^0
Rise/Base Pair Along Helical Axis	2.3 Å	3.32 Å (0.19 Å)*	3.8 Å
Pitch/Turn of Helix	24.6 Å	33.2 Å	45.6 Å
Mean Propeller Twist	+18^0	+16^0 (7^0)*	0^0
Glycosyl Angle Conformation	*anti*	*anti*	C: anti G: syn
Sugar Pucker Conformation	C3'-*endo*	C2'-*endo*	C: C2'-*endo* G: C3'-*endo*
Diameter	26 Å	20 Å	18 Å

* Mean and standard deviation over 36 bases or 33 base steps in three independently refined dodecamers: CGCGAATTCGCG with bent helix axis, and CGCGAATT^{Br}CGCG (where ^{Br}C is 5-bromocytosine) under conditions in which its axis is bent and straight. The quantity t_g is the global twist angle as measured from outside the helix, whereas t_t is the local value considering the two base pairs in isolation. They differ because the local helix axis frequently deviates from the best overall axis.[22]

1.1.3.1 B-FORM DNA

In its most common form DNA assumes a right-handed helical structure with bases facing the core of the duplex and the phosphate backbone along the periphery. The stacked bases are 3.4 angstroms apart and the helix makes a turn every 10 base pairs extending it to approximately 34 angstroms per turn. The bases are relatively flat and are perpendicular to the helical axis. This form of DNA is called the B-form DNA or B-DNA (Figure 5). Its glycosidic bonds form *anti* conformations and its sugar puckers are C2-*endo*. On the outside of the duplex there are two helical grooves of differing widths, the major groove and the minor groove. The grooves are almost equal in depth but the major groove is wider than the minor groove (Figure 5). The N7 and C6 of A and G, along with the C5 of C and T, point towards the major groove, while the N3 of A and G, along with the C2-O of C and T, point towards the minor groove. This helps facilitate the sequence specific recognition of DNA by DNA binding proteins.

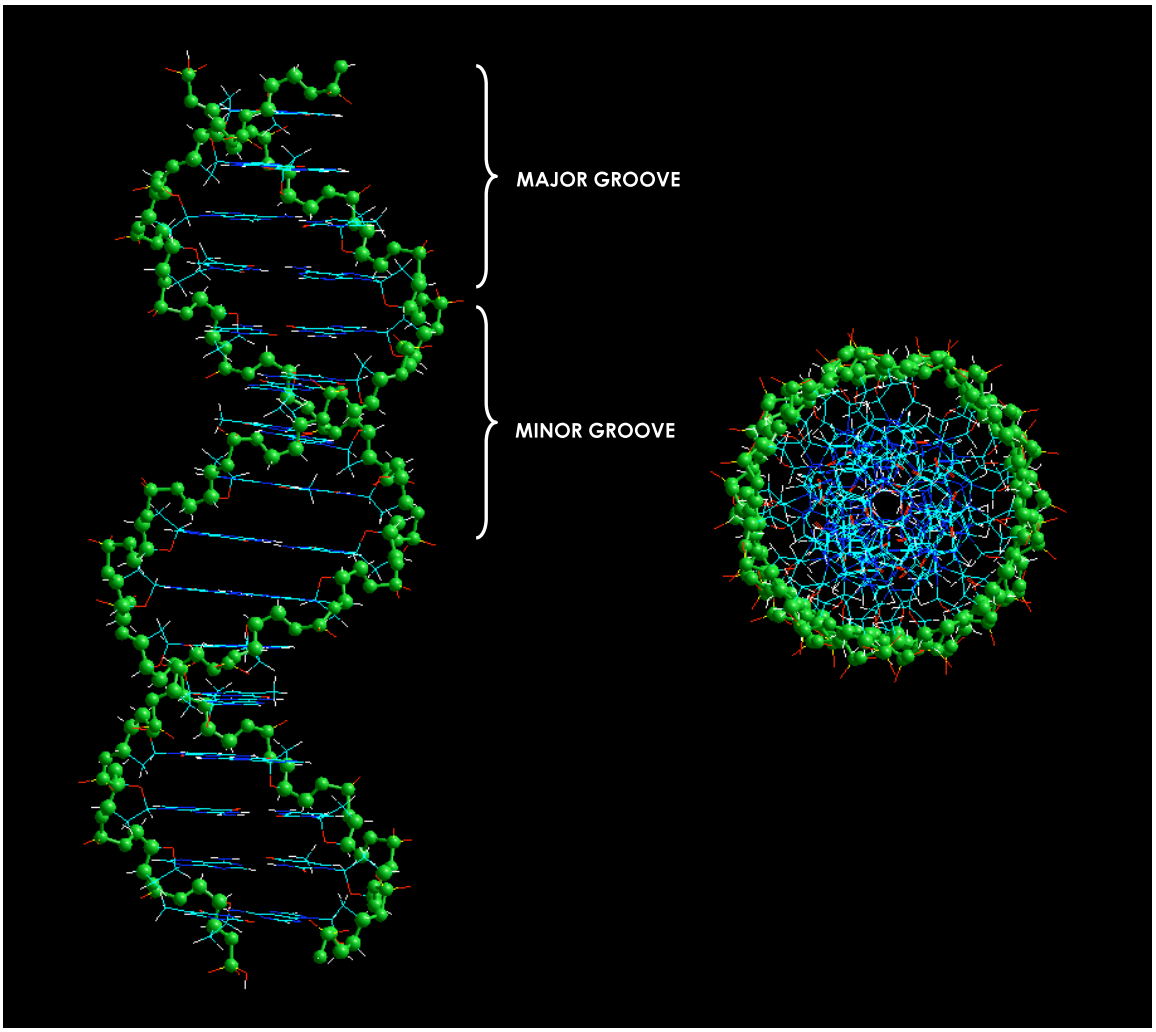

Figure 5 Hyperchem modeling of B-FORM DNA

1.1.3.2 A-FORM DNA

A form DNA (A-DNA) is formed under low humidity conditions (less than about %75) or in GC rich sequences under normal conditions. The helix is right-handed like B-DNA however each helical turn in A-DNA has 11 base pairs and is approximately 28 angstroms (Figure 6). The base stacking is tilted, with adjacent base pairs rotated by 32.7 degrees and 2.55 angstroms apart. The glycosidic bonds of A-DNA form the *anti* conformation and its sugar puckers favor the C3'-*endo* conformation. The major grooves of A-DNA are very deep and narrow, while the minor grooves are wide and very shallow. The deep major groove pushes bases toward the edge creating an empty core.[1,16,17,19]

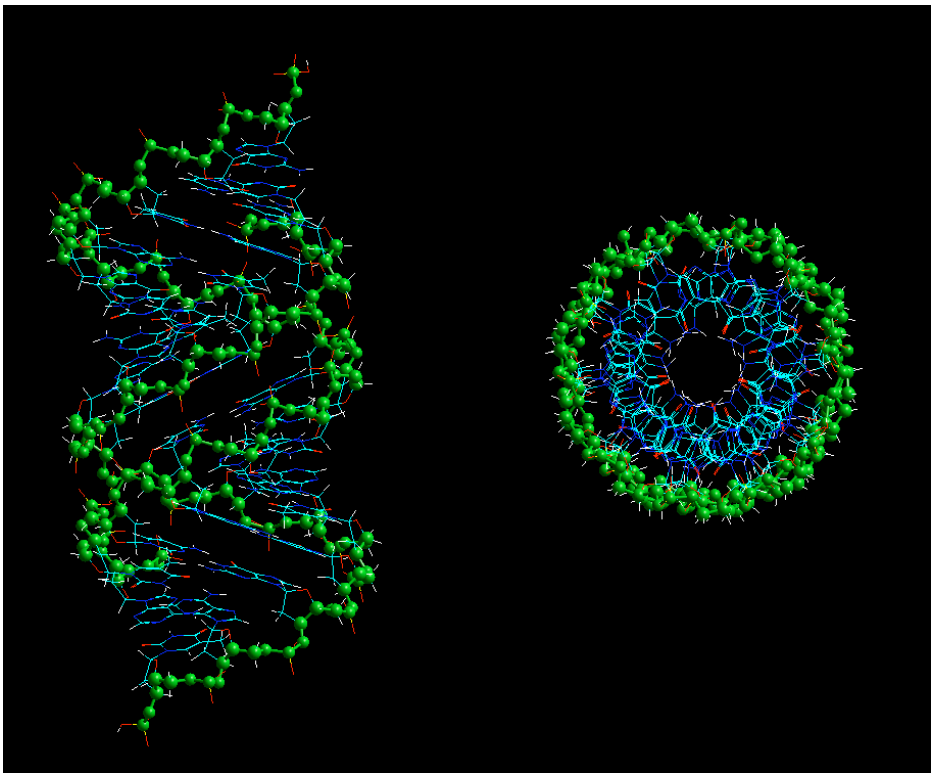

Figure 6 Hyperchem Modeling of A-DNA

1.1.3.3 Z-FORM DNA

Z-form DNA (Z-DNA) gets its name from its bases forming a zigzag-like structure (Figure 7). It is a left-handed helix with 12 base pairs per helical turn, making it approximately 45 angstroms. The base pairs are rotated by 30 degrees in opposing directions from each other. Z-DNA is composed of alternating purine-pyrimidine bases (especially Gs and Cs) and forms under high salt conditions. Purines are in *syn* conformation, while pyrimidines are in *anti* conformation. Z-DNA forms both C3' and C2' endo sugar puckers. Z-DNA has deep minor grooves, and a bulged convex surface for the major groove. Under biological conditions Z-DNA does not occur naturally under biological conditions but it is believed to provide relief from torsional strain during transcription.[23,24]

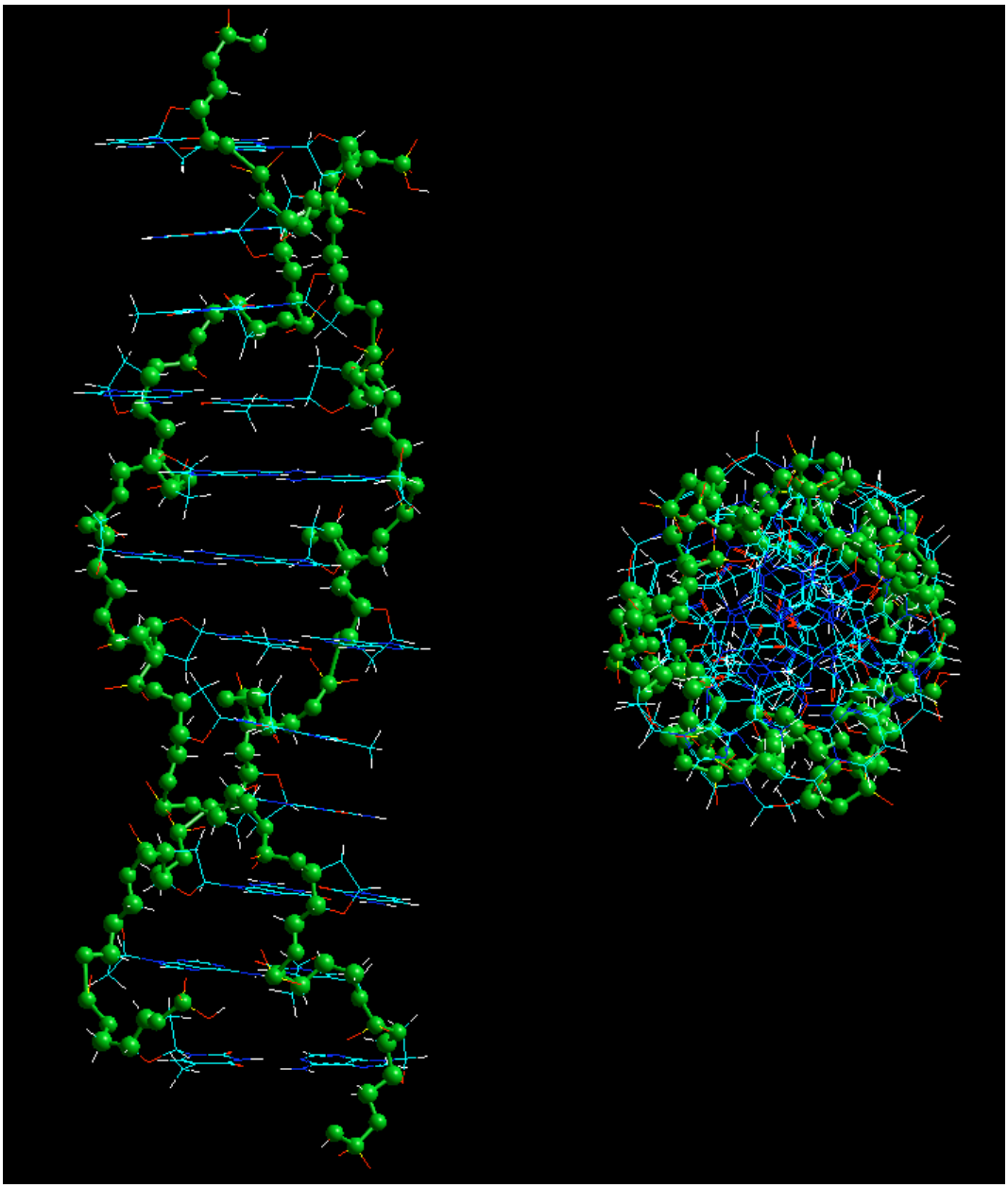

Figure 7 Hyperchem Modeling of Z-DNA

1.2 Charge Transfer in DNA

After the structure of DNA was understood[4], stacking nature of the bases raised the question of whether it was possible for the charges to be shuttled through DNA, making charge transfer possible.[25,26] Decades of research has been dedicated to answering this question.

Charge transport in DNA is biologically important due to its association with mutation and carcinogenesis.[27,28] As mentioned earlier, DNA is the carrier of information in living cells. Changes in DNA sequence introduced by DNA polymerases during replication process or changes to the molecular DNA by environmental factors may have fatal consequences. DNA polymerases correct copying errors by proofreading but errors that are left uncorrected may render the cells unable to function. Some of the environmental factors that modify DNA at the molecular level are mutagenic chemicals and certain types of radiation. The general types of DNA damage include missing bases, altered bases (due to ionizing radiation and alkylating agents), deletion or insertion of a nucleotide (by intercalating agents) , single or double strand breaks , cross-linked strands, 3'-deoxyribose fragments etc.

One of the most important causes for structural changes in DNA is oxidative damage.[29]

1.2.1 Oxidative Damage in DNA

DNA damage caused by oxygen-derived species is known as oxidative DNA damage. Oxygen derived species result from redox-cycling drugs, carcinogenic compounds, ionizing radiations and from cellular metabolism. Oxidative DNA damage can cause base and sugar lesions, strand breaks, DNA-protein cross-links and base-free sites.[27,30,31,32,33] It has been linked to multiple diseases including aging, neurodegenerative disorders, cancer, multiple sclerosis and arthritis.[34,35,36,37]

Beside biological processes various photosensitizers initiate oxidative damage in DNA. These include hydrogen atom abstraction from an intermediate free radical[38], generation of singlet oxygen or hydroxyl radical from an excited photonuclease[39] and electron transfer from a nucleobase generating a radical cation.[40]

In hydrogen abstraction, irradiation of a photosensitizer in the presence of a hydrogen donating substrate leads to the transfer of the hydrogen from the donating substrate to the excited photosensitizer[41], forming a radical pair. The deoxyribose sugar moiety in DNA has multiple hydrogen donating sites[30] and often acts as the hydrogen donor. The sugar radicals formed by hydrogen abstraction proceed to rapid rearrangement and ultimately lead to strand cleavage. Some examples of photosensitizers

that cleave DNA through hydrogen abstraction are photoactive rhodium (III) complexes[42], cationic metal porphyrins[43], and activated bleomycin.[44]

Singlet oxygen is the lowest excited state of molecular oxygen and is highly reactive.[30] Energy transfer between an excited photosensitizer and ground state oxygen leads to the formation of singlet oxygen provided the photosensitizer have enough triplet energy to generate singlet oxygen.[45] Singlet oxygen preferentially modifies guanine residues in DNA.[46] Some examples of photosensitizers that generate singlet oxygen are Ruthenium (III) complexes[47], porphyrins[48] and vanadium (V) complexes[49].

In electron transfer process a base donates an electron to an excited photosensitizer producing a radical cation (the base) and a radical anion (the photosensitizer). The process depends on the oxidation potential of the base and the reduction potential of the photosensitizer. The radical cation can migrate through DNA until it reacts at a low oxidation potential site which is most often guanine due to its lowest oxidation potential out of the four bases.[27,50] Some examples of photosensitizers that induce oxidative damage through electron transfer are riboflavin[50] and anthraquinones.[40]

Charge transfer in DNA starts with charge injection into the DNA.

1.2.2 Charge Injection into DNA

Several charge photosensitizers have been shown to initiate charge transfer in DNA.[30] The close interaction between the photosensitizer and the DNA is essential for the initiation of charge transfer. These photosensitizers either intercalate between the base pairs, bind in a groove or are attached to a DNA terminus where they "end-cap" the DNA.

Barton and coworkers developed and use rhodium and ruthenium metallointercalators.[51] Two of the most important intercalators they have developed are shown in Figure 8. However these intercalators may be unreliable due to aggregation[52,53] and complex electron transfer kinetics[54,55].

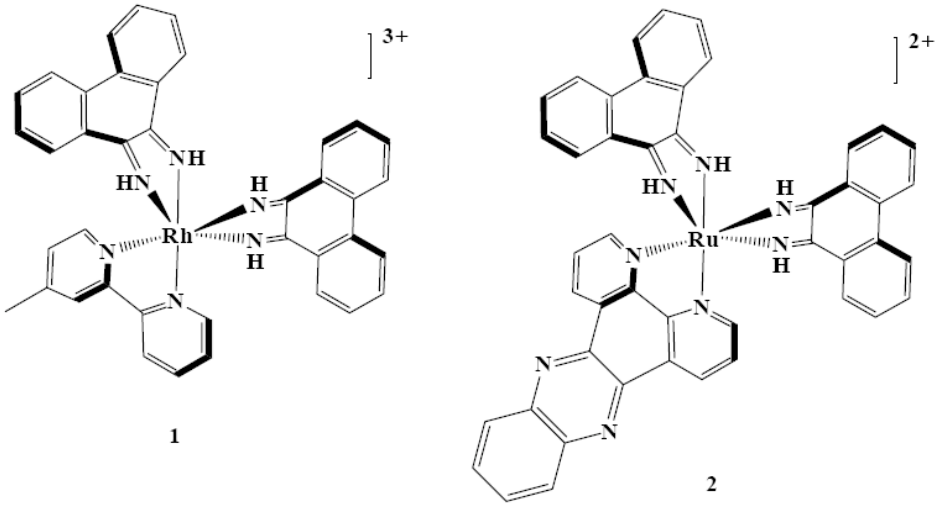

Figure 8 Structures of Bis (phenanthrenequinone diamine) (4,4'-dimethylbipyridine) rhodium (III) (1) , bis(phenanthroline) (dipyrido-phenazine) ruthenium(II) (2)

Trioxatriangulenium ion ($TOTA^+$, Figure 9) is another intercalator which acts by one-electron oxidation of DNA with a preference towards GC base pairs.[56] $TOTA^+$ has been shown to be a relatively weak sensitizer because it reacts from its singlet state.[57]

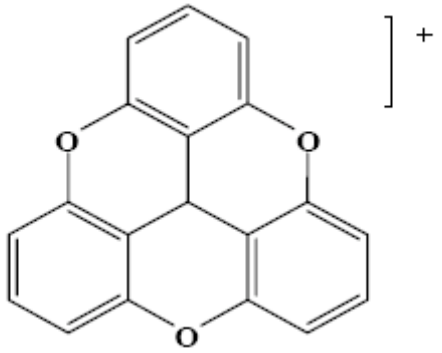

Figure 9 Structure of Trioxatriangulenium Ion

Lewis and Wasielewski use stilbene linked hairpins[58] which can only be used for short range electron transfer studies due to the singlet excited state of stilbene having a short lifetime (Figure 10).

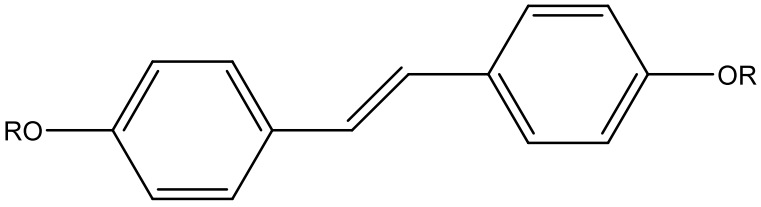

Figure 10 Structure of Stilbene

Bernd Giese utilizes a strand cleavage reaction to inject the radical cation into the duplex DNA.[59]

In our studies pertaining to this work we used anthraquinone as the photosensitizer for charge injection.

1.2.2.1 Anthraquinone

The photochemistry of anthraquinone derivatives is well established[60]. They are nearly perfect sensitizers for one-electron oxidation of DNA. They absorb light in the near-UV spectral region (350 nm) where DNA is essentially transparent. This permits the excitation of the quinine without subsequent absorption by the DNA which would complicate mechanistic and chemical analysis. Anthraquinones like AQC and AQS2 intercalate in DNA whereas AQ is covalently linked to DNA at the 5' end (Figure 11). The position of charge injection is controlled with the covalently linked AQ. Studies have shown that when AQ attached single-stranded DNA is hybridized with its complementary sequence, the AQ is "end-capped" to the duplex DNA. This permits electronic contact with the π-electron system of the DNA but does not disturb the structure like the intercalators do.[61]

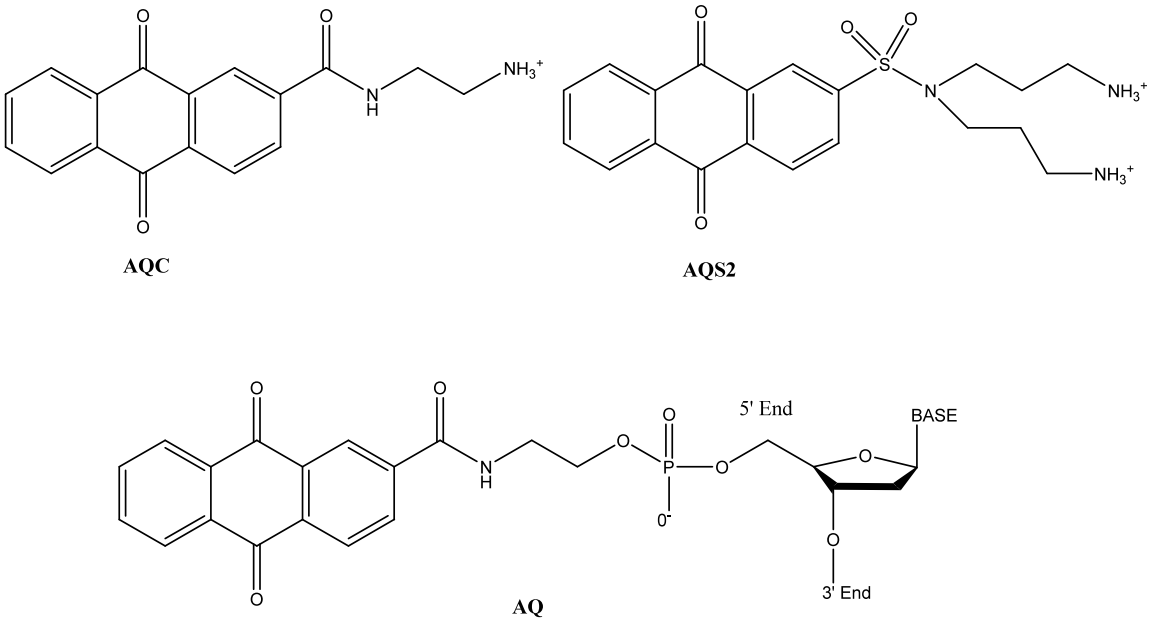

Figure 11 Structures of anthraquinone charge injectors

When the covalently linked AQ is irradiated at 350 nm it goes from its ground state to the singlet excited state. The singlet excited state rapidly intersystem crosses to the excited triplet state within picoseconds of excitation. Both the singlet and triplet excited states of anthraquinone are capable of one-electron oxidation of any of the four DNA bases to form the anthraquinone radical anion ($AQ^{-\cdot}$) and the base radical cation ($B^{+\cdot}$). In the triplex excited state back electron transfer is forbidden by spin conservation rules and the base radical cation has a longer lifetime whereas the singlet excited state radicals rapidly undergo back electron transfer to generate the starting materials.[38]

The radical cation generated by the triplet excited state AQ^{*3} reacts with O_2 to form superoxide ($O_2^{-\cdot}$) and the neutral AQ. The radical cation injected to the DNA can migrate through the bases until it is irreversibly trapped by reactions at different bases within DNA.[62]

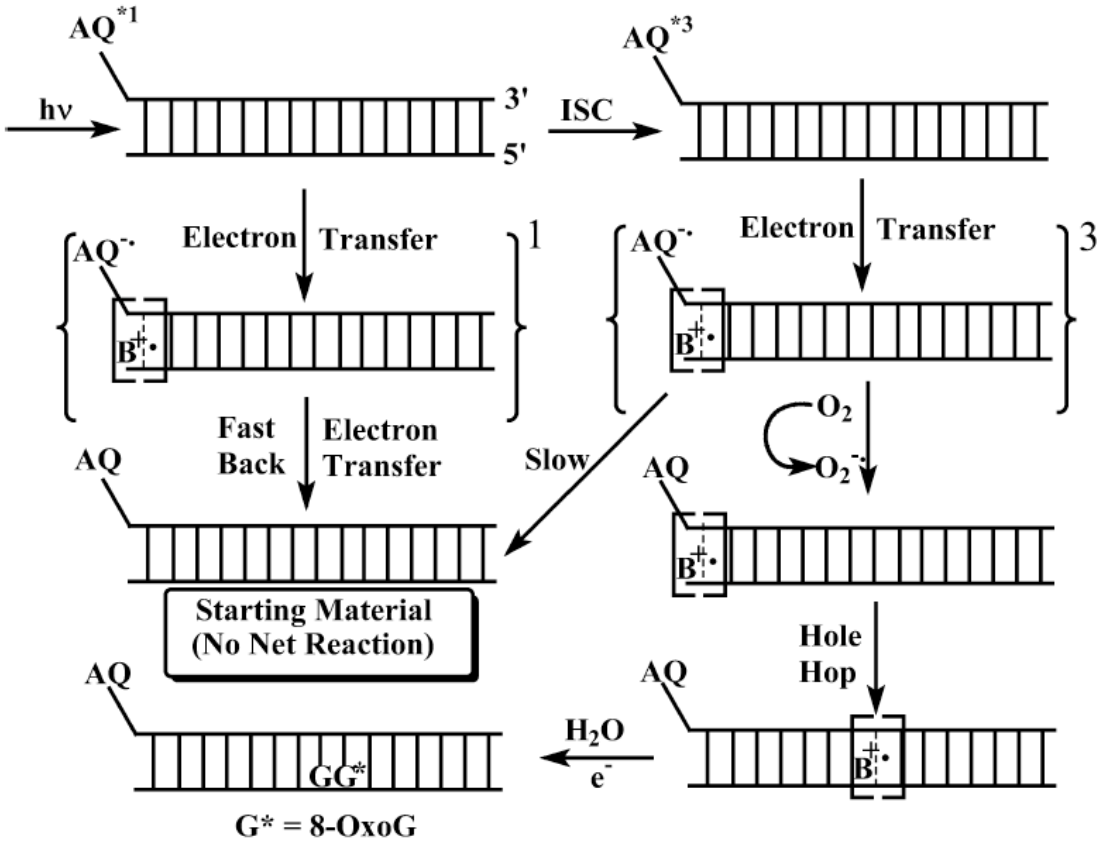

Figure 12 Schematic representation of charge migration through DNA[62]

1.2.3 Charge Migration Through DNA

As we have discussed earlier DNA is the instruction booklet that dictates all heritable information through generations; therefore maintaining its integrity is of utmost importance to the living cell. Changes in DNA structure have mostly deleterious effects and have to be corrected. Several things can cause changes in DNA structure, including but not limited to, mistakes introduced during replication by DNA polymerases, mutagenic chemicals and one-electron oxidation. Oxidation of DNA can occur naturally within the cell from the by-products of cellular metabolism or from exposure to ionizing radiation. Upon oxidation, DNA loses an electron, thereby creating a radical cation ("hole"), which resides primarily on the aromatic base moiety of nucleotides that make up the double helix. These radical cations are short-lived since they are quickly consumed by reacting with intracellular H_2O or O_2 causing oxidative damage of the base at the site of reaction. The aromatic base that eventually reacts with H_2O or O_2 (i.e. damaged base) is not necessarily the base that gets oxidized initially. It is known that charge migrates through the DNA duplex from its origination site until it is consumed by a reaction elsewhere. Considerable effort has gone into elucidating the mechanism of long-distance migration of radical cations (i.e. charge transfer) in DNA. Understanding charge transfer will provide further understanding of oxidative DNA damage, believed to be the cause of

prominent human conditions such as aging and cancer. Currently, there are 3 mechanistic models proposed to explain this phenomenon.

1.2.3.1 DNA as a Molecular Wire

The DNA double helix consists of two anti-parallel strands held together by interactions between two complementary bases (base pairs) on both strands. Adjacent base pairs along the helical axis are arranged in stacks, on top of each other, rotated by about 36^0 relative to each other. This highly ordered assembly, revealed by X-ray crystallographic studies, have raised the possibility that DNA may act as a molecular wire to mediate charge transfer between bases. Although not very clearly defined, the theory suggests that charge is transferred in a super-exchange process from a donor to an acceptor by continuous walking across a "π-way" formed by a bridge of perfectly stacked base pairs.[63]

The theory assumes an intact bridge of stacked base pairs; any imperfection in the bridge affects the rate and the efficiency of charge transfer.[64] This assumption originated from a series of experiments by Barton and coworkers, who looked at the effects of disrupting base stacking on subsequent charge transfer along DNA. In one set of experiments, they employed a DNA oligonucleotide where the donor and the acceptor are separated by a bulge (N-N-N) which disrupts base stacking.[65] They observed that the presence of the bulge was sufficient to prevent charge transfer beyond the bulge. This was confirmed further by

another set of experiments, where they heated a duplex DNA above its T_m, resulting in a loss of charge transfer, only to be restored after cooling the duplex down to re-assume proper base stacking.[66] Introducing C-A mismatches in DNA had the same effect, which suggests that charge transfer is dependent on the integrity of aromatic stacking of the base pairs of DNA.

Barton and coworkers also found that charge transfer depends on the distance between the donor and the acceptor.[67] However, they found that the rate of charge transfer stayed constant beyond a distance of 14 angstroms, which corresponds to only 3 bases and cannot explain the long-distance transfer (up to 200 angstroms) observed by other groups.

Although an attractive theory to explain charge transfer, DNA as a molecular wire cannot explain all of the observed results. The theory is currently regarded as invalid, since it does not take into account the dynamic nature of DNA in solution. Even though DNA in solution assumes a B-form on average, over long distances it assumes a somewhat disordered structure that would render charge transfer inefficient beyond 2-3 base pairs. Therefore DNA in solution cannot be a molecular wire.

1.2.3.2 Hopping models

The inability of the molecular wire theory to explain *in vitro* observations brought about new models to explain the apparent long-distance charge transfer. Giese and coworkers proposed one such model, the hole-resting site model.[68] According to the hole-resting site model, the cation is localized exclusively on individual guanines due to their lowest oxidation potential among the four bases. The charge then "hops" from hole to hole in an individual super-exchange between low-energy bases. Intervening A/T bases (bridge) between the donor and the acceptor do not act as charge carriers due to their higher oxidation potential. The extent of hopping is dependent on the distance between two holes, as the rate of charge transfer decreases by ten fold for each A/T base pair added to the bridge. This model cannot, once again, explain charge migration over 200 angstroms; however it is deemed valid for charge transfers over short distances of a few bases.

1.2.3.2.1 Phonon-Assisted Polaron Hopping Model

A major flaw (shortcoming) of the above-mentioned models is that they do not take into account that DNA has a dynamic nature in solution and that it responds to the thermal fluctuations in the system, making it a non-rigid molecule. Phonon-assisted polaron hoping model proposed by Schuster and coworkers, on the other hand, is a modified version of the hole-resting hopping model that takes into account the environment that the DNA duplex is in.[62] The major assumption in Phonon-Assisted Polaron Hopping Model is that upon the introduction of a base radical cation into the DNA, the system itself (including nearby bases, counterions and solvent molecules) will respond by structural changes to lower the energy of the system.

Once a highly electron-deficient radical cation is generated, the system will attempt to stabilize (delocalize) this extra positive charge by changing the structure of the nearby bases (distortion) to provide additional electron density to the radical cation, such as unwinding around the z-axis and increasing molecular orbital overlap between bases. The cation is self-trapped in the lowest energy base (hole) via instantaneous superexchange within the accompanying distortion (polaron). The extent of the distortion (i.e. size of the polaron) will depend on the nature of the surrounding bases and is usually between 5-7 base pairs. Thermal (phonon) motions of the base pairs in and near the structural distortion

lead to their leaving or joining the polaron, thereby moving it from one sequence to the next, followed by charge transfer via super-exchange to the new hole within the new polaron. The number of base pairs entering and leaving the polaron in a hop also depends on the local and surrounding sequence. The major differences between Phonon-Assisted Polaron Hopping Model and the others is that;

(1) it is this polaron harboring the radical cation that hops through the DNA duplex, rather than the individual cation as proposed by other models,

(2) The radical cation exists as a detectable entity during its migration through the bridge separating the donor and the acceptor, unlike the hole-resting model.

(3) Long-range migration can only happen with the assistance of the thermal fluctuations (phonons) of the medium the DNA is in.

Currently, Phonon-Assisted Polaron Hopping is the only mechanistic model that can explain long-range charge migration in DNA.

CHAPTER 2: Polaronic semiconductor behavior of long-range charge transfer in DNA oligomers in solution: controlling barriers to long-distance radical cation migration in DNA with thymine analogs

2.1 Introduction

DNA in solution has been described as a ''molecular wire''.[63,69] One challenge in assessing this claim has been uncertainty in the precise definition of a molecular wire. At one extreme, the term is limited to those specific cases of a conductor having an electronic transmission of unity that exhibits the Landauer resistance of $h/2e^2$ (12.9 kΩ).[70] A more liberal characterization of molecular wires identifies them as having bridges of many bond lengths through which charge moves rapidly and efficiently.[71] However, the problematic nature of such a qualitative definition has been noted,[72] and this difficulty has plagued discussion of the properties of DNA.

It is apparent now that consideration of the electrical properties of DNA requires a division into at least two main groups: ''dry'' and wet DNA. A careful assessment of the available data led to the explicit conclusion that DNA in the dry state is an insulator.[73] In contrast, long-distance charge transport through DNA oligonucleotides in appropriate aqueous buffer solutions has been observed and confirmed in several

laboratories.[74,75] These findings show that radical cations (holes) migrate in the DNA. However, these studies show that DNA oligomers in solution are not molecular wires or conductors in any sense. The behavior of DNA places it in the class of polaronic semiconductors. Over very short distances, holes may tunnel from guanine to guanine through bridges composed of A–T base pairs,[76,77] but over longer distances charge transfer occurs by the ion gated phonon-assisted polaron-like hopping mechanism.[78,79,80,81]

We have suggested that radical cations in DNA are stabilized by delocalization over some number of contiguous purine bases (forming a polaron) and that migration occurs when thermal motions (phonons) of the DNA and its solvent and ionic environment provide sufficient energy to overcome activation barriers formed around interposing pyrimidines.[78,79,82,83] Thus, the rate of radical cation hopping is determined by the sequence of base pairs that controls both the extent of delocalization and the nature of the barrier. A recent report by Rösch and co-workers supports this view.[81] Using quantum mechanics/molecular dynamics modeling, they show that structural and environmental fluctuations facilitate the transfer of a hole from a guanine to an adenine. The relative energies of adenine and guanine radical cations are modulated by fluctuations of the electrostatic interaction between DNA and its electrolyte environment thereby forming charge transfer effective

configurations[79] where a radical cation at an A has a lower energy than at a neighboring G. The formation of these configurations is thought to be the rate determining step that gates hole transfer from one polaron to the next. Recently, O'Neill and Barton[84] proposed an alternative to the ion-gated phonon-assisted polaron-hopping model that they identify as conformationally gated hopping through stacked domains. However, this proposal is part of the polaron hopping mechanism[85] and indistinguishable from it when intermediates and transitions states are considered properly and it is recalled that activation energy has both enthalpy and entropy as components.

A key postulate of the ion-gated phonon-assisted polaron hopping mechanism is the creation of barriers to charge transfer by pyrimidines, particularly thymine, between polarons. The oxidation potentials (E_{ox}) of C and T are both significantly greater than that of A, which is greater than for G.[86,87] A radical cation encountering an adjacent cytosine as part of a G–C base pair can migrate to the complementary guanine, but there is no especially low oxidation potential site for the radical cation when it encounters an adjacent thymine that is part of an A–T base pair. We examined the postulate that intervening thymines create barriers to charge migration by construction of DNA oligomers that contain the

thymine mimics 3-methyl-2-pyridone[88] and difluorotoluene[89] (**t** and **f**)[1]. See Figure 13.

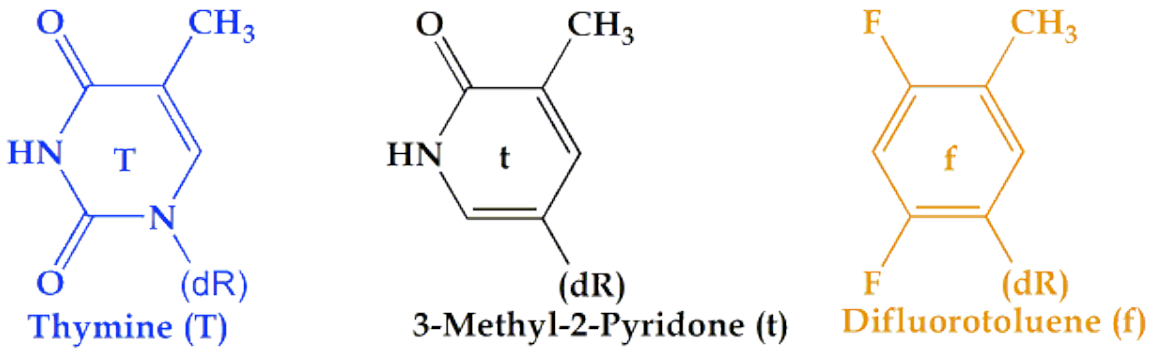

Figure 13 Structures of thymine, t and f analogs

These unnatural nucleobases maintain the stacking characteristic of the A–T base pair but provide different electronic and solvent environments. Investigation of long-distance charge transfer in these modified oligomers confirms the central role that thymine plays in the creation of barriers to radical cation migration in duplex DNA. In addition, the findings indicate that radical cations migrate to the complementary adenine when a T–A barrier is encountered.

[1] The experiments with 3-methyl-2-pyridone were conducted by Dr. Abraham Joy in our lab.

2.2 Experimental

2.2.1 Materials and methods

All the chemicals and solvents for the synthesis of 2,4-difluorotoluene AQ-phosphoramidite and 3-Methyl-2-Pyridone[88]. AQ-phosphoramidite were purchased from Sigma Aldrich and Fisher Scientific. All synthetic DNA oligonucleotides were synthesized in our laboratory on an Applied Biosystems Inc. Expedite DNA Synthesizer. Nucleotide phosphoramidites were obtained from Glen Research and used as received. UV/Vis studies on DNA oligonucleotides were conducted at 260 nm on a Hewlett-Packard Spectrophotometer. The extinction coefficients of the oligomers were calculated using a biopolymer calculator, and their concentrations were determined from the absorbance at 260 nm. The mass of each oligonucleotide was determined by a Micromass Quattro Electrospray Ionization (ESI) mass spectrometer. [γ-^{32}P] radioactive isotopes were purchased from Amersham Biosciences. T4 polynucleotide kinase was purchased from New England Biolabs. UV melting and cooling experiments were performed on a Cary 1E Spectrophotometer equipped with a multi-cell block, temperature controller and sample transport accessory. Circular Dichroism (CD) measurements were conducted on a JASCO-720 instrument. Kodak film for PAGE analysis was purchased from Aldrich. The quantitative analysis of autoradiograms was performed on a

FUJI 2340 BAS-Image system. Spin columns and centrifugal filters were obtained from Millipore.

2.2.1.1 Synthesis of 5-Bromo-2,4-Difluorotoluene[90] (1)

2,4-Difluorotoluene (13.2 g, 0.15 moles) and 200 mg of iron filings were added to a three neck round bottom flask equipped with an addition funnel, a condenser and a drying tube filled with KOH. The solution was heated to 60^0C followed by the addition of bromine (9.3 g, 0.12 moles) via the additional funnel in 2 hrs. The reaction was stirred in the dark for an additional hour.

The solution was poured into 10% aqueous NaOH. The organic layer was collected and the aqueous layer was extracted twice with benzene. The combined organic layers were washed with anhydrous MgSO4. The solution was concentrated to give a pale yellow liquid and was purified by Kugel–Rohr distillation under reduced pressure.

^{1}H NMR ($CDCl_3$, ppm): δ 7.35 (t, 1H), δ 6.8 (t, 1H), δ 2.23 (s, 3H)

2.2.1.2 Synthesis of 2'-Deoxy-3',5'-di-O-p-toluoyl-D-erythropentosyl-chloride[91] (3)

2-Deoxy-D-eryhtro-pentose (5.44 g, 0.04 moles) was dissolved in 98 ml of methanol. 11 ml of 1%HCl in methanol was added. The mixture was kept in a stoppered flask for 15 minutes. 2 g of silver carbonate was added and the mixture was stirred to stop the reaction. The solution was filtered and evaporated under reduced pressure followed by co-evaporation twice with 15 ml pyridine.

The syrupy brown compound was dissolved in pyridine (30 ml) and the solution was cooled to 0^0C in an ice bath followed by addition of p-toluoyl chloride (11.8 ml, 0.088 moles). The reaction mixture was stirred at 0^0C for an additional hour then gradually heated to 50^0C and kept at room temperature overnight.

The mixture was poured onto 200 ml crushed ice while stirring and after the ice melted the mixture was extracted multiple times with ethyl ether. The combined organic extracts were successively washed with H_2O, 10% H_2SO_4 and aq. $NaHCO_3$. The solution was dried over $NaSO_4$ and was concentrated under reduced pressure to obtain 16.4 g of compound (**2**) as thick yellow syrup (**2**). No purification was conducted at this stage.

54 g glacial acetic acid was saturated with HCl at 10^0C and added to compound (**2**) dissolved in 36 ml glacial acetic acid. HCl gas was passed

through the solution at 10^0C for 10 minutes to give white crystals. It was left to stand for 30 minutes and was washed with dry ether followed by suction filtration. The white crystals were dried overnight in a desiccator to yield pure compound (**3**) in %85 yield.

^{1}H NMR ($CDCl_3$, ppm) : δ 8.00 (dd, 1H) , δ 7.98 (dd, 1H), δ 7.91 (dd, 1H), δ 7.88 (dd, 1βH) , δ 7.25 (m, 4H), δ 6.48 (d, 1βH), δ 5.57 (m, 1H), δ 4.86 (dd, 1H), δ 4.66 (bd, 2H), δ 2.87 (m, 1H), δ 2.76 (dd, 1H), δ 2.42 (s, 3H), δ 2.41 (s, 3H)

2.2.1.3 Synthesis of 1',2'-Dideoxy-1'-(2,4-difluorotoluyl)-3',5'-di-O-toluoyl-α, β-D-ribofuranose[90] (4) :

Mg turnings (0.19 g) were activated in a dry 100 ml round-bottom flask equipped with a stirrer. 2 necks were closed and the third neck was equipped with a condenser, purged with dry argon gas and was cooled down to room temperature.

Dry THF (10 ml) was syringed into the flask, under argon. The flow of the argon was increased while the flask was opened for the addition of a few crystals of iodine.

Argon gas was bubbled through 5-bromo-2,4-difluoro toluene (2.19 g , 40.5 mmol) (**1**) for 10 seconds and was slowly syringed into the reaction flask. The color due to the iodine disappeared within a few minutes. The reaction was heated to 45^0C and was stirred for 2 hours. The colorless solution was observed to become increasingly yellow as the reaction progressed. After most of the Mg turnings disappeared 915 mg dry $CdCl_2$ was added and the reaction mixture was refluxed for 1 hour and slowly cooled down to room temperature. 2-Deoxy-3',5'-di-O-p-toluoyl-D-erythropentosyl-chloride (3.10 g, 7.7 mmol) (**3**) dissolved in THF was syringed into the reaction mixture in one portion at room temperature and was stirred overnight at this temperature.

The reaction mixture was concentrated under reduced pressure to yield thick yellow syrup. The solution was poured into 10% ammonium chloride

(50 ml) and extracted with methylene chloride. The organic layer was washed with saturated $NaHCO_3$, saturated NaCl and dried over anhydrous $MgSO_4$.

The solution was filtered, concentrated and purified by silica gel chromatography eluting with hexanes-ethyl acetate (80:20) to give **(4)** in 47% yield. The α and β anomers could not be separated at this stage. The α anomer was the dominant stereoisomer.

^1H NMR ($CDCl_3$, ppm) , α epimer : δ 7.98 (d, 2H), δ 7.68 (d, 2H), δ 7.40 (t, 1H), δ 7.26 (d, 2H), δ 7,19 (d, 2H), δ 6.74 (t, 1H), δ 5.61 (m, 1H), δ 5.55 (dd, 1H), δ 4.73 (m, 1H), δ 4.55 (t, 2H), δ 2.97 (m, 1H), δ 2.41 (s, 3H), δ 2.40 (s, 3H), δ 2.23 (s, 3H)

2.2.1.4 Synthesis of 1',2'-Dideoxy-1'-(2,4-difluorotoluyl)-3',5'-di-O-toluoyl-β-D-ribofuranose (5)[92]

To 500 mg (**4**) dissolved in 50 ml toluene, 120 mg excess benzenesulfonic acid, 5 drops of concentrated H_2SO_4 and 5 drops of H_2O were added. The reaction mixture was refluxed for 28 hours.

The mixture was poured onto 5% $NaHCO_3$ (aq.), extracted with ethyl acetate, dried over $MgSO_4$ and concentrated under reduced pressure. The β isomer was separated in 30% yield by slow silica gel column chromatography eluting with ethyl acetate-hexane (5:95).

The reaction was repeated several times to get the desired β-nucleoside.

^{1}H NMR ($CDCl_3$, ppm), β epimer: δ 7.97 (d, 2H), δ 7.92 (d, 2H), δ 7.30-7.20 (m, 5H), δ 6.72 (t, 1H), δ 5.62 (dd, 1H), δ 5.44 (dd, 1H), δ 4.75 (dd, 1H), δ 4.62 (dd, 1H), δ 4.51 (m, 1H), δ 2.59 (m, 1H), δ 2. 43 (s, 3H), δ 4.40 (s, 3H), δ 2.19 (m, 1H), δ 2.08 (s, 3H)

2.2.1.5 Synthesis of 1'2',-Dideoxy-1'-(2,4-difluorotoluoyl)- β-D-ribofuranose (6)[90]

The literature was followed with minor modifications. Complete deprotection was achieved only when the reaction was stirred for 24 hours and the product was purified with silica gel chromatography eluting ethyl acetate-hexane (40:60).

Compounds **7** and **8** were synthesized as described previously.[93]

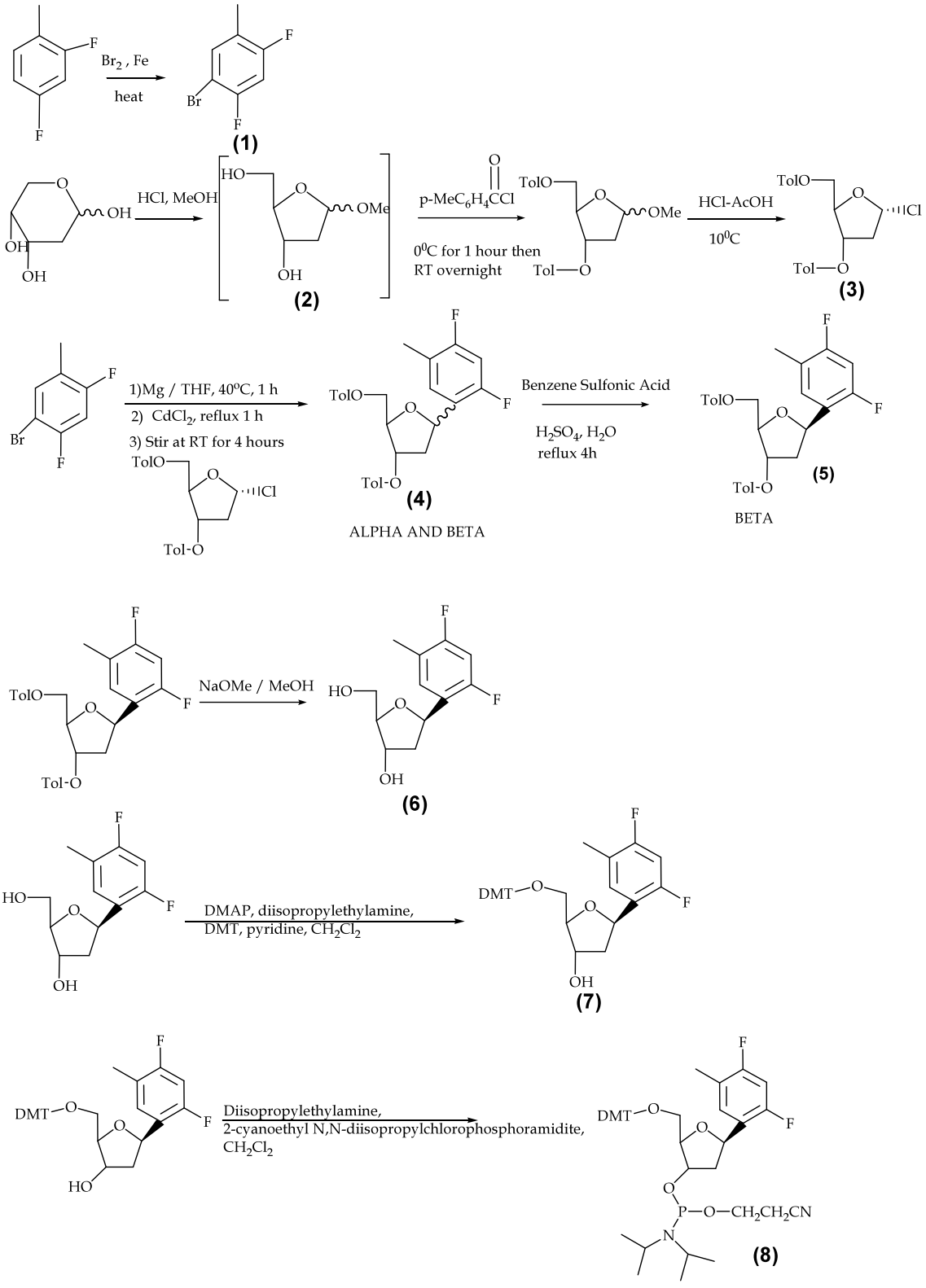

Figure 14: Synthesis of 2,4-difluorotoluene nucleoside

2.2.1.6 Synthesis of 3-Methyl-2-pyridone (t) [88]

The modified ***t***, (3-methyl-2-pyridone), was synthesized according to the published procedure[88], except that for the palladium mediated Heck coupling between the base and protected glycol, reagent grade CH_3CN, instead of anhydrous CH_3CN, was used. Use of anhydrous CH_3CN decreased the yield of the desired product substantially. ^1H NMR ($CDCl_3$): δ 8.10 (2H,d, ArH), δ 7.94 (1H, s, ArH), δ 7.56–6.82 (16H, m, ArH), δ 5.08 (1H, m, $H_{1'}$), δ 4.60 (2H, t, CH_2), δ 4.58 (1H, m, $H_{3'}$), δ 4.22 (1H, s, $H_{4'}$), δ 3.78 (6H, s, OCH_3), δ 3.58–3.75 (4H, m, OCH_2CH_2CN), δ 3.24 (2H, d, $H_{5'}$), δ 3.20 (2H, t, CH_2), δ 2.14 (2H, m, $H_{2'}$), δ 2.00 (3H, s, CH_3), δ 1.21–1.23 (12 H, m, iPr)}

2.2.1.7 Synthesis of DNA single strands

The DNA oligomers, shown in Table 2, were synthesized on a standard Applied Biosystems Expedite Nucleic Acid Synthesis system. A modified protocol was used for deprotecting the oligomers containing p-nitrophenyl protected 3-methyl-2-pyridone. This protecting group was removed as the first step after sequence assembly by treating the solid support with a solution of 40% TEA/anhydrous pyridine for 2 h. The support was then treated with a solution of 0.5 M 1,8-diazabicyclo[5.4.0]undec-7ene (DBU) in anhydrous pyridine for 48 h and finally washing the sample three times with acetonitrile. The wash was followed by ammonium hydroxide treatment by heating the oligonucleotide overnight at 60^0C to

cleave the oligomer from the support and to deprotect the remaining groups. Oligomers containing 2,4-difluorotoluene were cleaved from the calcium pectinate gel solid support and deprotected by conventionally heating the oligonucleotide overnight at 60^0C.

Table 2 Modified and unmodified DNA duplexes

DNA(1) TTTC **GG_1** TATA **GG_2** CATC TTG*-5' AQ-5'-AAAG CC ATAT CC GTAG AAC -3'
DNA(2) TTTC **GG_1** ***t***A***t***A **GG_2** CATC TTG*-5' AQ-5'-AAAG CC ATAT CC GTAG AAC -3'
DNA(3) TTTC **GG_1** ATAT **GG_2** CATC TTG*-5' AQ-5'-AAAG CC TATA CC GTAG AAC -3'
DNA(4) TTTC **GG_1** A***t***A***t*** **GG_2** CATC TTG*-5' AQ-5'-AAAG CC TATA CC GTAG AAC -3'
DNA(5) TTTA **GG_1** TATA **GG_2** TATA **GG_3** TATA **GG_4** TACG*-5' AQ-5'-AAAT CC ATAT CC ATAT CC ATAT CC ATGC -3'
DNA(6) TTTA **GG_1** ***t***A***t***A **GG_2** TATA **GG_3** TATA **GG_4** TACG*-5' AQ-5'-AAAT CC ATAT CC ATAT CC ATAT CC ATGC -3'
DNA(7) TTTA **GG_1** ***f***A***f***A **GG_2** TATA **GG_3** TATA **GG_4** TACG*-5' AQ-5'-AAAT CC ATAT CC ATAT CC ATAT CC ATGC -3'
DNA(8) TTTA **GG_1** ATAT **GG_2** ATAT **GG_3** ATAT **GG_4** TACG*-5' AQ-5'-AAAT CC TATA CC TATA CC TATA CC ATGC -3'
DNA(9) TTTA **GG_1** A***t***A***t*** **GG_2** ATAT **GG_3** ATAT **GG_4** TACG*-5' AQ-5'-AAAT CC TATA CC TATA CC TATA CC ATGC -3'
DNA(10) TTTA **GG_1** A***f***A***f*** **GG_2** ATAT **GG_3** ATAT **GG_4** TACG*-5' AQ-5'-AAAT CC TATA CC TATA CC TATA CC ATGC -3'

These synthetic DNA oligonucleotides were purified by HPLC on a Hitachi 7000 preparative HPLC system equipped with a Varian Dynamax 25x21.4 mm reverse-phase C-18 column using 5-20% Acetonitrile in 0.5 M Triethylammonium Acetate buffer at pH 7 and then desalted by using sep-pak column.

The concentrations of the DNA single strands were determined using absorption spectroscopy and applying Beer-Lambert Law.

$$A = \varepsilon \cdot c \cdot l$$

Where **A** is the absorbance at 260 nm, ε is the extinction coefficient (calculated using a biopolymer calculator), **l** is the path length, and **c** is the concentration of the DNA. AQ was substituted by an adenine; ***t*** and ***f*** were substituted by a thymine in the extinction coefficient calculations.

2.2.1.8 Characterization of DNA duplexes

The mass of each oligonucleotide was determined by a Micromass Quattro Electrospray Ionization (ESI) mass spectrometer.

2.2.1.8.1 Thermal Denaturation Studies

The samples for thermal denaturation studies were prepared by mixing 25 μM of unlabeled complementary DNA single strands in 10 mM sodium phosphate buffer (pH 7). The samples were hybridized at 90^0C for 10 minutes and cooled down to room temperature gradually. Hybridized samples were transferred to UV transparent quartz cells with 1cm path length. The melting temperatures of the samples were monitored by their UV absorption at 260 nm using CARY 1E Spectrophotometer. Several melting ramps starting from 15^0C to 90^0C at 1^0C/min rate were recorded. The plot of wavelength vs. 1st derivative of the absorbance gave us the melting temperatures shown in Table 3.

Table 3 Melting Temperatures of the duplexes studied

DNA	Tm/°C	Modified/Unmodified
1	48	U
2	42	M (with ***f***)
3	49	U
4	42	M (with ***f***)
5	50	U
6	44	M(with ***f***)
7	40	M (with ***f***)
8	48	U
9	42	M (with ***f***)
10	37	M (with ***f***)

2.2.1.8.2 Circular Dichroism Studies

The samples used in thermal denaturation studies were used in CD experiments to determine the secondary structure of the DNA (1-10). The spectral resolution was 0.2 nm and the bandwidth was 1 nm. The CD spectra shown in Figures 3 and 4 are the average of 5 scans (scan rate 200-400 nm).

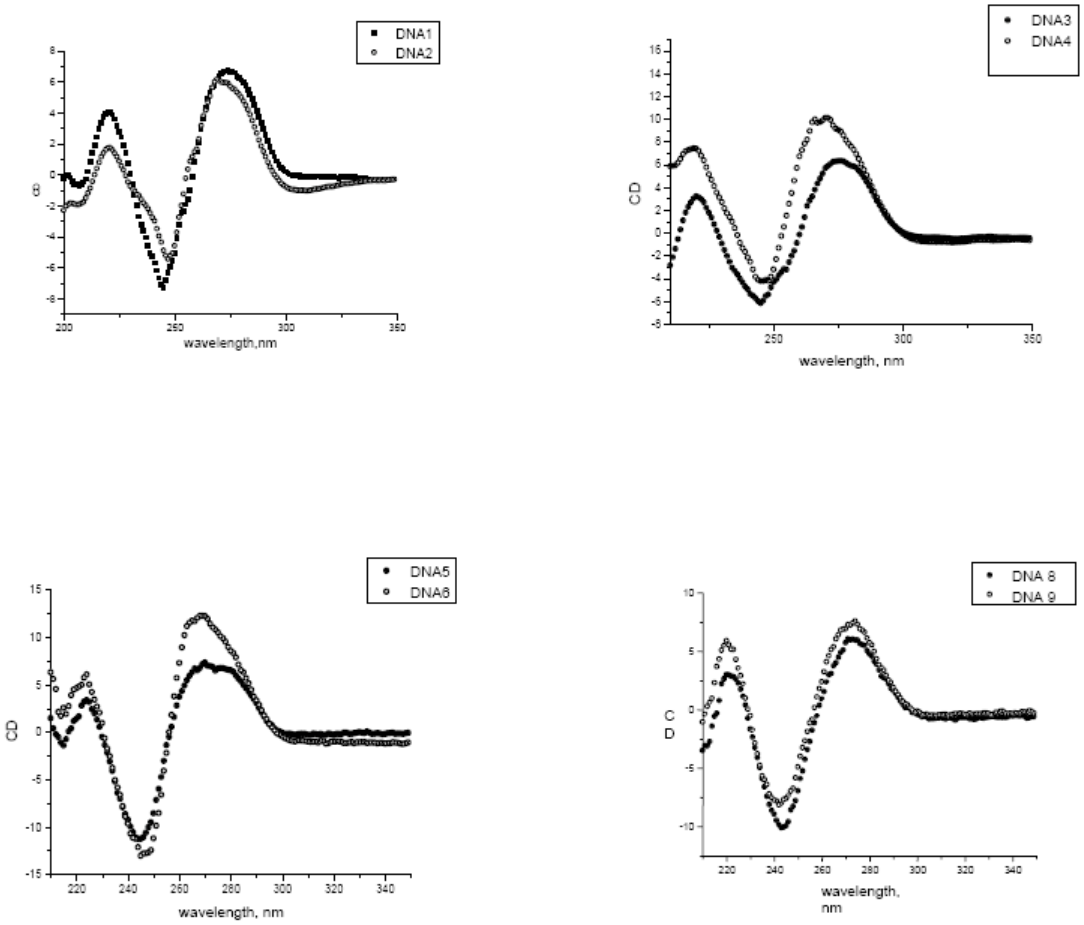

Figure 15 Circular Dichroism Spectra of DNA (1-6) and DNA (8,9)

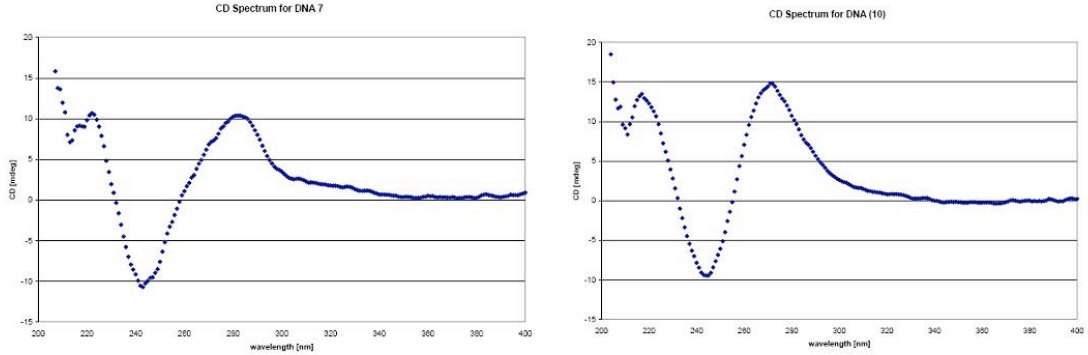

Figure 16 Circular Dichroism Spectrum of DNA (7) and DNA (10)

2.2.1.9 Preparation of Radiolabeled DNA

DNA single strands that did not contain the AQ were labeled at their 5' end using [γ-^{32}P]ATP and T4-Polynucleotide Kinase (PNK) enzyme.

5 µL of 200-300 µM of the desired ssDNA, 2 µL of PNK buffer, 1 µL of [γ-^{32}P]ATP, 2 µL of T4-PNK enzyme and 10 µL nano pure water were incubated at 37^{0}C for 45 minutes. After incubation the DNA sample was suspended in 10 µL of denaturing loading dye composed of 3',3'',5',5''-tetrabromophenolsulfonphthalein (bromophenol blue) in 4:1 water-formamide for visualization purposes. The labeled DNA was purified on a 20% polyacrylamide denaturing gel. Purified DNA was visualized by autoradiography and the desired band was cut from the gel. The excised gel piece was eluted with 800 µL of elution buffer (0.5 M NH_4OAc, 10 mM $Mg(OAc)_2$, 1.0 mM EDTA and 0.1% SDS) at 37^{0}C for 12 hours. The DNA was precipitated from the elution buffer by adding 2 µL of glycogen and 800 µL of 100% ethanol and centrifuging at 13000 rpm for 1 hour. The nonradioactive supernatant was removed, and the DNA was twice washed with 100 µL of 80% ethanol and air dried. Nanopure water was added to adjust the counts to 10,000 cpm/µL.

2.2.1.10 UV Irradiation and Gel Electrophoresis

The samples for irradiation were prepared by hybridizing a mixture of the unlabeled (5 μM) and radiolabeled (10,000 cpm) oligonucleotides with the AQ-linked complementary strands (5 μM) in 10 mM sodium phosphate buffer (pH 7) at 90^0C and slowly cooling to room temperature. Samples were irradiated at 350 nm at room temperature in microcentrifuge tubes in a Rayonet photoreactor (Southern New England Ultraviolet Company, Barnsford, CT). 5 min of irradiation with 2 lamps for DNA(5), DNA(7), DNA(8) and DNA(10) was shown to be satisfactory for maintenance of single-hit conditions. After irradiation, the samples were precipitated with cold ethanol (100 μL) in the presence of glycogen (1.25 μL, 20 mg/mL), washed with 80 % ethanol (2 x 100 μL), dried and treated with piperidine (50 μL, 1 M) at 90^0C for 30 min. After evaporation of the piperidine, lyophilization and dissolution in formamide-dye solution, the samples were run on a 20 % 19:1 acrylamide:bis-acrylamide gel containing urea (7 M) at 70 watts. The gels were dried and the cleavage sites were visualized by autoradiography.

2.2.1.11 Quantitative Analysis

The amount of damage at each GG step is relative to the efficiency of charge transfer through DNA. The damage was quantified using a FUJI phosphorimager. The gel was exposed on a FUJI imaging plate for 5 hours and read in the FUJI 2340 BAS-Image system. The damaged sites were revealed as dark spots due to radioactivity and were "counted" using Image Gauge software.

2.3 Results

2.3.1 Radical cation migration across 3'–TATA–5' and 3'–ATAT–5' bridges

The DNA oligomers shown in Table 2 were prepared, purified and characterized by standard procedures. Each contains an anthraquinone group (AQ) linked covalently to a 5'-terminus and a ^{32}P-radiolabel (* in Table 2). We have shown previously that UV irradiation of AQ at 350 nm[38] results in one-electron oxidation of an adjacent nucleobase that injects a radical cation into the DNA.[61] The radical cation migrates through the DNA and reacts irreversibly with H_2O or O_2 at GG steps resulting in damage that is detected as strand cleavage when the irradiated samples are treated with piperidine.[85] These experiments were carried out under ''single-hit'' (low conversion) conditions. In this circumstance, on average each DNA oligomer reacts once or not at all, and the number of duplexes that contain two or more damaged bases is insignificant. Under these conditions the amount of strand cleavage is linked with the probability that a radical cation will encounter a particular GG step. Thus, in DNA oligomers that contain more than one GG step, the amount of strand cleavage usually decreases as the distance from the AQ to the GG step increases. The relative amount of strand cleavage at each GG step in oligomers containing several GG steps is determined by the magnitudes of the rate constant for charge migration (k_{hop}) and for irreversible trapping of the radical cation (k_{trap}), the latter of which is largely

independent of the identity of the bases around the GG step.[83] If hopping is much slower than trapping, all of the strand cleavage will occur at the GG step that is closest to the AQ. On the other hand, if hopping is much faster than trapping, then the amount of strand cleavage is determined by thermodynamic equilibration of the radical cation among all of the available GG steps, and the amount of reaction is independent of distance from the AQ. For cases where the hopping and trapping rates are comparable, the amount of strand cleavage will decrease approximately exponentially with distance from the AQ.[94]

The DNA duplexes shown in Table 2 were characterized spectroscopically and by analysis of their thermal stability. Each of these duplexes exhibits a circular dichroism (CD) spectrum that is characteristic of B-form DNA.[95] The melting temperatures (Tm) of these compounds decrease when ***t*** or ***f*** is substituted for T, see Table 3. For ***t***, this has been attributed to the absence of the O_2 carbonyl group in the minor groove and the concomitant destabilization of the spine of hydration.[96] Similarly, the decrease in Tm observed when ***f*** replaces T is attributed to uncompensated desolvation of the complementary adenine during base pair formation.[93] X-ray crystallography has shown that the conformation of the A–T base pair is not affected by replacement of T with ***t***.[97] Similarly, NMR spectroscopy shows that the ***f***–A base pair very closely resembles the T–A base pair in the same context.[98] These findings indicate that

substitution of ***t*** or ***f*** for T does not significantly alter the local or the global structure of the modified oligomers.

As expected, irradiation of a DNA(1) sample to low conversion and its subsequent treatment with piperidine leads to cleavage of the DNA strand at GG_1 and at GG_2. Gel electrophoresis and phosphorimagery of irradiated DNA(1) reveal that the amount of reaction at GG_1 is 4.5 times that at GG_2 (see Figure 17 and Table 4).

Table 4 Melting temperature and reaction rates at GG steps

DNA	Tm/°C[a]	GG_1/GG_{tot}[b]	GG_2/GG_{tot}	GG_3/GG_{tot}	$(GG_1+GG_2)/GG_3$
1	48	0.82	0.18		
2	42	0.48	0.52		
3	49	0.98	0.02		
4	42	0.33	0.67		
5	50	0.95	0.05	0.005	200
6	44	0.50	0.47	0.03	30
7	44	0.95	0.05	0.003	
8	48	0.96	0.04	<0.005[c]	>200
9	42	0.50	0.48	0.02	50
10	40	0.95	0.04	0.01	

[a]Melting temperature of the DNA duplex. [b]Fraction of reaction that occurs at GG_n, errors are typically 10% of the reported value. [c]Reaction at GG_3 is not significantly above background.

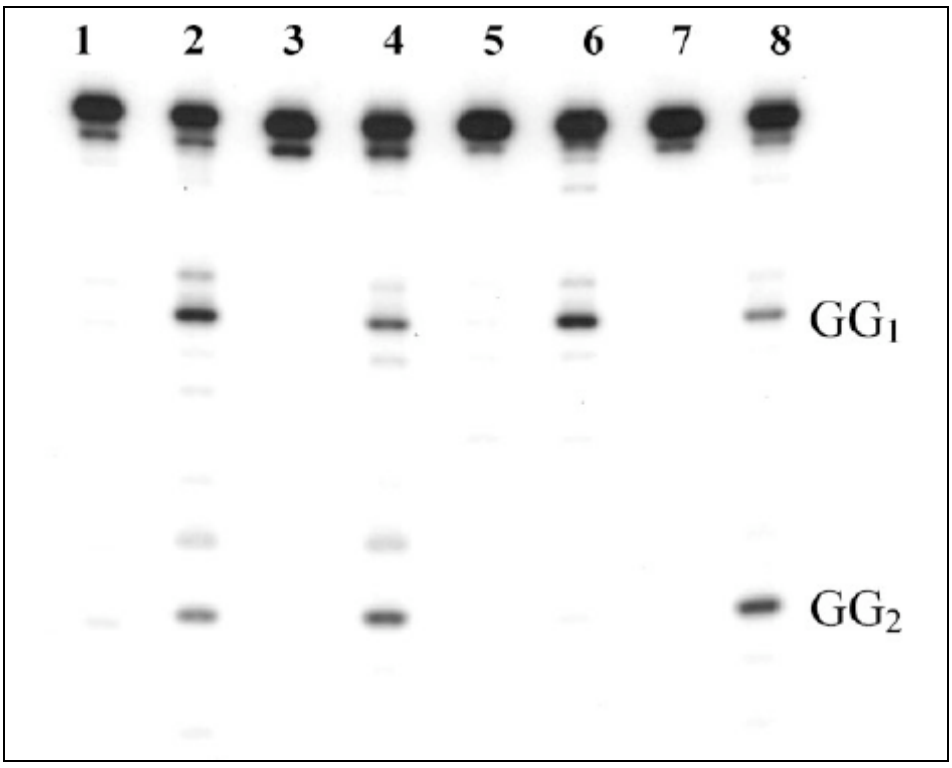

Figure 17 Autoradiogram resulting from the irradiation of DNA(1) (lanes 1,2), DNA(2) (lanes 3,4), DNA(3) (lanes 5,6) and DNA(4) (lanes 7,8). In lanes 2,4,6,8, the samples were irradiated at 350 nm (pH 7, phosphate buffer) and worked up with hot piperidine (1 M). Lanes 1,3,5,7 are control experiments (no irradiation).

This result indicates that the 3'–TATA–5' bridge presents a modest barrier to radical cation hopping. In contrast, for DNA(3), the 3'–ATAT–5' segment introduces a more significant barrier to radical cation migration from GG_1 to GG_2. In this case, GG_1 reacts 50 times more often than GG_2. These results allow the comparison of polaron stabilization and barrier creation with computational predictions.

2.3.2 The effect of replacing T with t on radical cation hopping

DNA(2) contains a 3'-***t***A***t***A-5' bridge in place of the 3'–TATA–5' bridge of DNA(1). The irradiation of DNA(2) leads to readily detected strand cleavage at both GG_1 and GG_2. However, unlike the 3'–TATA–5' bridge of DNA(1), the radical cation readily crosses the 3'-***t***A***t***A-5' bridge in DNA(2). Substitutions of T with ***t*** in this bridge causes the ratio of cleavage at GG_1 to GG_2 to go from 4.5:1 in DNA(1) to about 1:1 in DNA(2). The effect of substituting ***t*** for T in the bridge is even more striking when DNA(3) is compared with DNA(4). In this case the ratio of reactivity goes from 50:1 for DNA(3) to approximately 1:2 in DNA(4). Because the absorption spectrum of ***t*** tails beyond 300 nm, we considered the possibility that the portion of the irradiating light directly absorbed by this chromophore could result in reaction of the DNA that leads to strand cleavage. However, control experiments showed that irradiation of the duplex oligomer that contains the modified ***t*** but lacks the AQ, [DNA(2)-AQ] results in no detectable strand cleavage. In addition, even extensive (10 fold excess) irradiation of DNA(2)-AQ caused no change in the Tm of the duplex or in its absorption spectrum in regions characteristic of ***t***.

Clearly, though structurally similar to T, the replacement of thymine with ***t*** has a profound effect on the ability of the radical cation to traverse bridges composed of A–T base pairs. In principle, this might be due to an enhancement of k_{hop} from GG step to GG step, or this substitution might modify k_{trap} by H_2O or O_2 at nearby guanines. We prepared and investigated duplexes DNA(5, 6, 8, 9) to extend this analysis and differentiate between these two possibilities. DNA(5) contains four GG steps separated by a 3'–TATA–5' bridging sequence. Its irradiation leads to measurable amounts of strand cleavage at GG_1 through GG_3, the amount of reaction at GG_4 is too small to quantify reliably. See Figure 18.

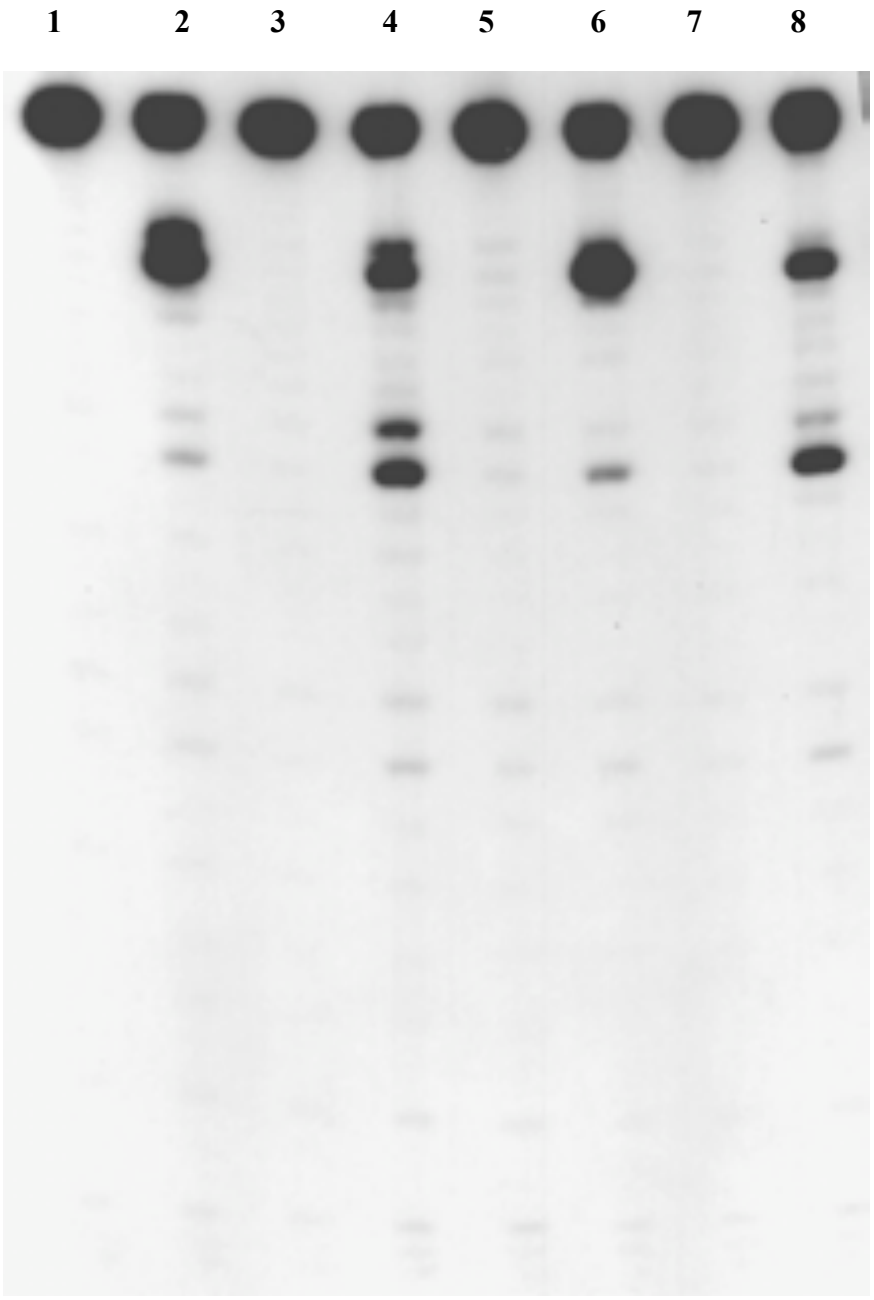

Figure 18 Autoradiogram from the irradiation of DNA duplexes **5** (lanes 1,2) **6** (lanes 3,4) **8** (lanes 5,6) and **9** (lanes 7,8). Lanes 1, 3, 5, 7: Dark Controls. Lanes 2, 4, 6, 8: samples irradiated using 2 x 350 nm Rayonet lamps and subsequently worked up with hot 1M piperidine

DNA(6) is identical to DNA(5) except that ***t*** has been substituted for T in the bridge between GG_1 and GG_2. If this substitution causes an increase in k_{hop} between GG_1 and GG_2, this will result in a greater reaction at GG_3 in DNA(6) than in DNA(5). In contrast, if changing T to ***t*** increases k_{trap} for nearby GG steps, less strand cleavage will occur at GG_3. The experimental results (Table 4) support the first possibility; more reaction is seen at GG_3 in DNA(6) than in DNA(5). Similar results are obtained from comparison of DNA(8) with DNA(9); more strand cleavage results at GG_3 when ***t*** replaces T in the 3'–TATA–5' bridge between GG_1 and GG_2. Introduction of a radical cation into DNA results from the one-electron oxidation of a base. Because G and A have lower oxidation potentials than C and T,[99] it is expected that radical cations in duplex DNA will reside primarily on the purine partner of normal Watson–Crick base pairs. Despite its structural similarity to thymine, electronically ***t*** is not a pyrimidine. In particular, we surmised that the replacement of N1 of T with a carbon atom in ***t*** would lower its E_{ox} significantly.

2.3.3 The E_{ox} of N-methyl-2-pyridone

Thymine, with an E_{ox} of ca. 2.1 V vs. NHE[87] is the most difficult to oxidize of the four common DNA nucleobases. The E_{ox} of N-methyl-2-pyridone (see Figure 19), which has an electronic structure analogous to that of ***t***, was determined by cyclic voltammetry in an acetonitrile solution containing tetrabutylammonium tetrafluoroborate as the supporting electrolyte. The oxidation wave shows a peak potential at 1.68 V vs. NHE.

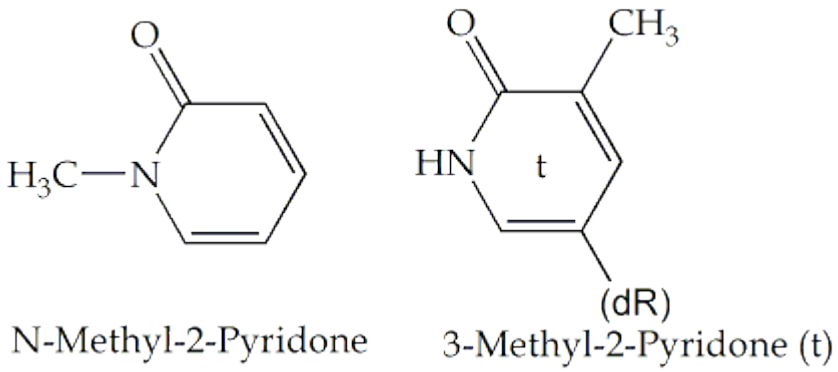

Figure 19 Structures of N-Methyl-2-Pyridone and ***t***

Under similar conditions, we showed that 2',3',5'-tris(t-butyldimethylsilyloxy) guanosine[100] has a peak potential of 1.5 V. This compares well with the value obtained by Seidel and co-workers[88] for guanine (1.49 V). They determined the E_{ox} of adenine to be 1.96 V under these conditions. Thus, the E_{ox} of ***t*** is greater than guanine but is ca. 0.28 V less than that of adenine. Consequently, it may be anticipated that in an A–***t*** base pair the

radical cation will reside on the ***t*** rather than on the A as it does in a normal A–T base pair. This matter is discussed further below.

2.3.4 The effect of replacing T with f on radical cation hopping

It is clear that replacement of T with ***t*** in bridges between GG steps increases the charge transfer efficiency. As suggested above, this may be attributable to the reduced E_{ox} of ***t***. However, it may also be a consequence of disruption to the normal hydration of the duplex DNA.[101] To distinguish between these two possibilities we examined duplexes DNA(7) and DNA(10) in which the thymines in bridging base pairs between GG steps were replaced by difluorotoluene(***f***). Both ***t*** and ***f*** disrupt the hydration of the DNA, but the E_{ox} of ***f*** should be well above 2.37 V vs. NHE (the E_{ox} of toluene[102]), which is significantly greater than that of adenine.

In contrast to the results obtained by substitution of ***t*** for T in the bridge, substitution with ***f*** in DNA(7) gives strand cleavage results (Table 4) that are indistinguishable from those obtained from irradiation of DNA(5), which contains only normal nucleotides (see Figure 20).

Similarly, irradiation of DNA(10), which also has ***f*** in place of T in the bridge, gives results that are the same as from irradiation of DNA(8), which has A–T base pairs in the bridge (See Figure 21).

On the basis of these findings, the effect of substitution of ***t*** for T on radical cation migration efficiency is attributed primarily to electronic

perturbation of the charge transfer pathway and not a consequence of structural modification of the DNA or its solvent environment.

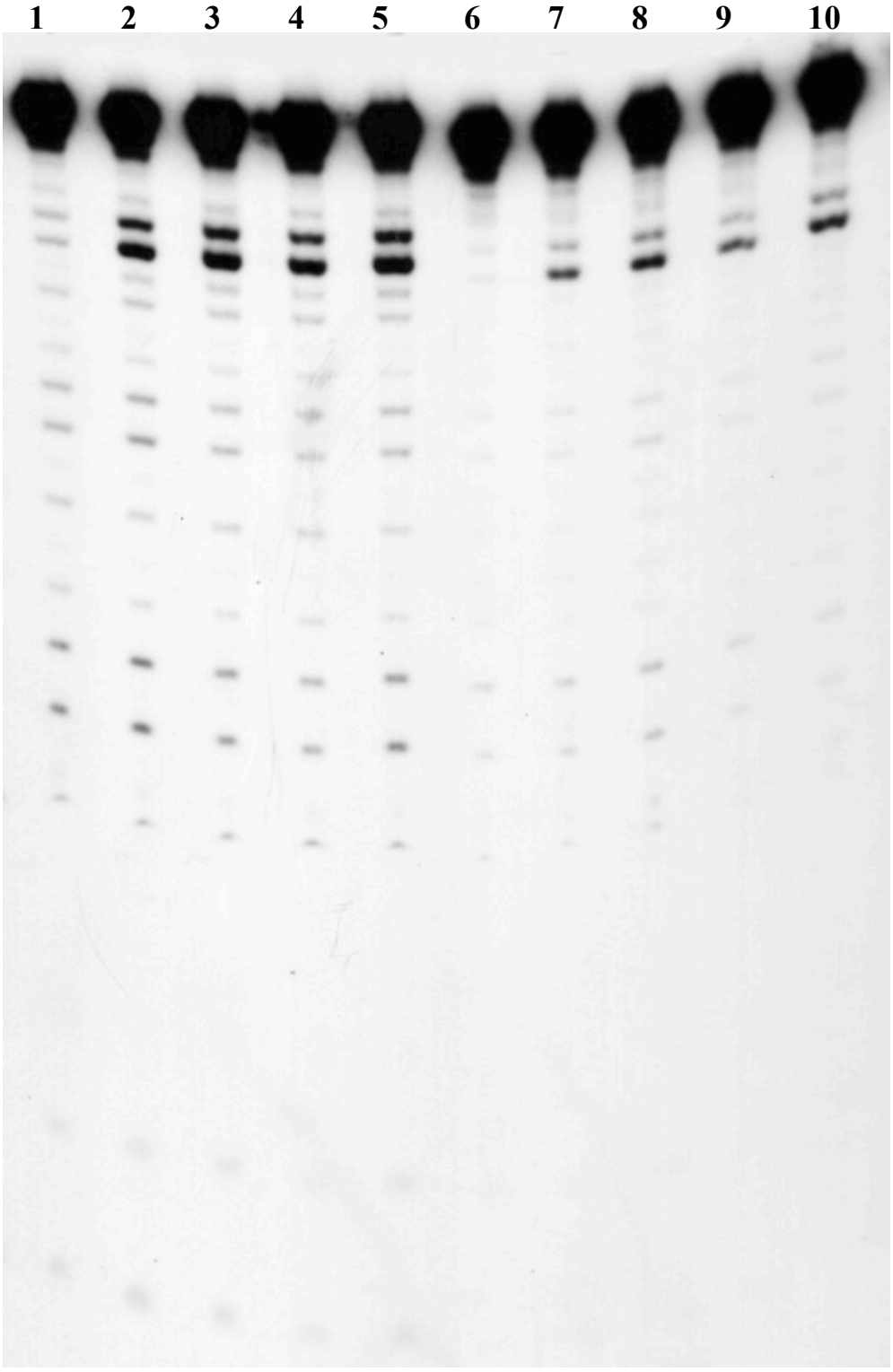

Figure 20 Autoradiogram from the irradiation of DNA(5): Lanes 1-5 and DNA(7): Lanes 6-10. Lanes 1 and 6 are dark controls. Lanes 2,4,7,9: samples irradiated for 3 minutes. Lanes 3,5,8,10: samples irradiated for 5 minutes.

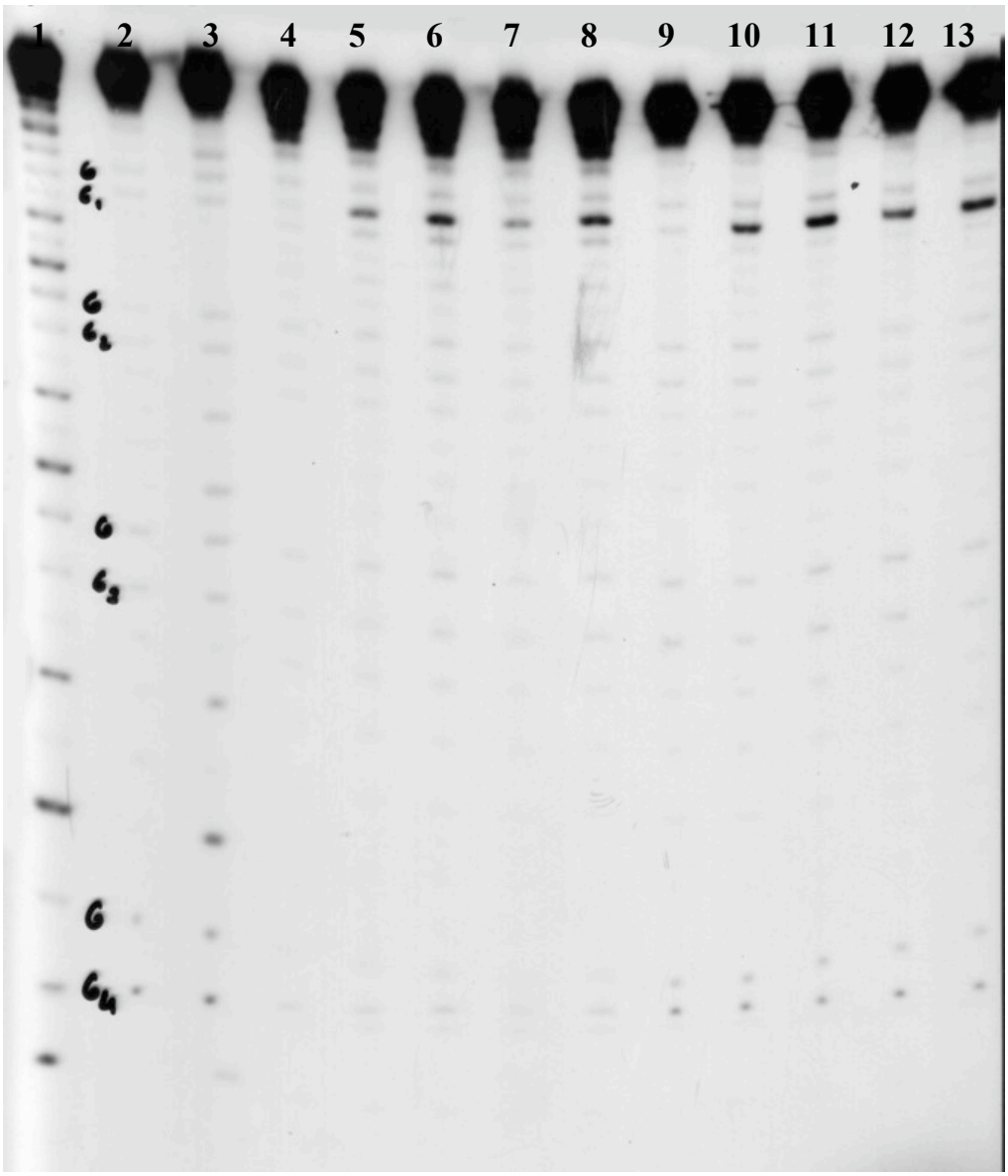

Figure 21 Autoradiogram from the irradiation of DNA(8): Lanes 1,4-8 and DNA(10): Lanes 2,3,9-13.Lanes 1, 3: T sequencing, Lane 2: A/G sequencing. Lanes 4,9: Dark controls. Lanes 5, 7,10,12: samples irradiated for 3 minutes. Lanes 6,8,11,13: samples irradiated for 5 minutes.

2.4 Discussion

2.4.1 Stabilization of radical cations in DNA by polaronic delocalization

The results from irradiation of DNA(1) and DNA(3) demonstrate again that long-distance radical cation migration occurs in duplex DNA. Light absorbed by the AQ chromophore creates an electronically excited singlet state that intersystem crosses[103] rapidly to a triplet. This is a critical step. Excited singlet states are generally inefficient sensitizers of DNA oxidation because of rapid charge annihilation of the resulting radical ion pair,[57,104] which reduces the quantum efficiency and can complicate mechanistic interpretations.[55] Energy transfer from triplet AQ to ***t*** or ***f*** is energetically impossible, but the AQ triplet readily oxidizes an adjacent nucleobase to form the AQ radical anion and base radical cation.[38] In the oligonucleotides investigated here, three A–T base pairs follow the AQ. Sanii and Schuster have shown[105] that this arrangement promotes efficient reaction because the radical cation is rapidly delocalized. Delocalization of the radical cation further slows charge annihilation in the (overall) triplet radical ion pair and this allows consumption of the AQ radical anion by reduction of molecular oxygen to superoxide to proceed more efficiently.[38] After the AQ radical anion has been consumed, the base radical cation can exist in the DNA for hundreds of microseconds,[83,106] which permits the long distance migration of the radical cation to occur.[107]

Numerous investigations have shown that radical cations in DNA react predominantly at $(GG)_n$ sequences where n=2,3.[74,75] In both DNA(1) and DNA(3), the radical cation encounters GG_1 after an identical four base pair sequence. As expected, strand cleavage is observed at GG_1. The second GG sequence in these duplexes (GG_2) is separated from GG_1 by bridges composed of A–T base pairs arranged in different sequences, and the efficiency of radical cation migration across the bridge depends dramatically on that detail. Simply put, the bridge is crossed about 10 times more efficiently in DNA(1) than it is in DNA(3). The phonon-assisted polaron-hopping model can explain this effect.

A polaron is a distortion in the DNA structure that is formed as a result of delocalization of the radical cation over nearby bases. We have suggested that polaronic delocalization occurs primarily among adjacent purines on one strand of the DNA duplex because that is adequate to explain radical cation migration data.[83] Thus, for DNA(1), delocalization of the polaron at GG_1 is restricted to the GG step (P_1 in Figure 22) because it is surrounded on its 3' and 5'-sides by pyrimidines. Similarly, polaron P_2 at GG_2 in DNA(1) is presumed to be delocalized over the 3'-AGG-5' sequence. The more limited delocalization of P_1 results in a somewhat higher energy polaron than for P_2. A related circumstance is encountered in DNA(3). In this case, P_1 is assigned to a 3'-GGA-5' polaron that is somewhat lower energy than P_2, which is delocalized only over the GG

step. The nucleobases between the assigned polaronic sites create the activation barrier (‡) to charge migration from one site to the next. This barrier for both DNA(1) and DNA(3) is formed by a TAT sequence.

One-electron oxidation of DNA(1) or DNA(3) introduces a radical cation adjacent to the AQ group. From the structure of these duplexes, this radical cation must encounter GG_1 before it migrates as far as GG_2. The activation energy for migration from GG_1 to GG_2 ($\Delta G^{\ddagger}_{1,2}$) in DNA(1) is less than $\Delta G^{\ddagger}_{2,1}$, because P_2 is more stable than P_1, see Figure 22. Consequently, for DNA(1) $\Delta\Delta G^{\ddagger}_{1,2}$ is negative. In contrast, for DNA(3) $\Delta\Delta G^{\ddagger}_{1,2}$ is positive and this difference accounts for the factor of ten difference in relative reactivity observed for the two GG steps of DNA(1) and DNA(3). Simply put, the radical cation has a harder time getting from GG_1 to GG_2 in DNA(3) than it does in DNA(1), so it is trapped more often at GG_1 in DNA(3). This analysis is consistent with calculations of the relative ionization potentials of three-base sequences where it is found that the identity of the base on the 3' side has a greater effect on the ionization potential of G than the base on the 5' side.[108,109]

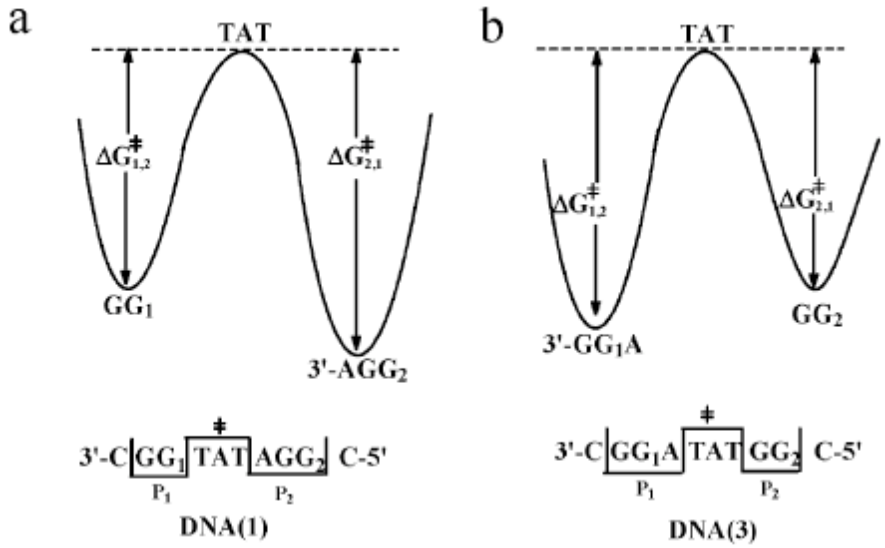

Figure 22 Reaction coordinate diagrams representing DNA(1), a, DNA(3), b. For DNA(1), GG_1, the first GG step encountered by the radical cation after injection by the AQ, is somewhat higher in energy than GG_2 because of delocalization to adjacent adenine. For DNA(3), the situation is reversed. This differential stabilization affects the activation barriers for charge hopping $\Delta G^{\ddagger}$.

2.4.2 The pathway for radical cation migration

The substitution of ***t*** for T may affect both the extent of charge delocalization of the radical cation and the energy of the activation barrier encountered when it hops from one polaronic site to another. The results reported above show that the preferences for reaction at GG_1 in DNA(1) and DNA(3) are absent for DNA(2) and DNA(4), where the bridges contain no thymines. The experiments also show that this occurs because the magnitude of k_{hop} increases. The variation of k_{hop} could be due to a disruption of the hydration environment of the DNA in the vicinity of the modified base, but the experiments where ***f*** replaces T show that this is not

an important factor. Moreover, in contrast to the factor of ten decrease observed between reaction at GG_1 and GG_2 when the 5'–ATAT–3' sequence of DNA(1) is changed to 5'–TATA–3' in DNA(3), reactions at GG_1 and GG_2 are of nearly equal efficiency for the 5'-A***t***A***t***-3' and 5'-***t***A***t***A-3' sequences of DNA(2) and DNA(4), respectively. These findings are attributed to the reduction of the oxidation potential of ***t*** compared to T.

The oxidation potential of ***t*** is much lower than T, greater than guanine, but less than that of adenine. Consequently, when a radical cation encounters a ***t***–A base pair, we conclude that it will reside primarily on the ***t*** rather than on the A as it does in a normal A–T base pair. Since the ***t***–A base pairs are part of the barrier to charge hopping between the GG-containing sites, the reduced oxidation potential of ***t*** relative to A lowers the activation energy for hopping so that k_{hop} is significantly greater than k_{trap}. As a result, the amount of reaction at the GG steps in DNA(2) and DNA(4) is determined by the relative energies of the polarons at GG_1 and GG_2, which are evidently nearly the same. These findings are fully consistent with the polaron-hopping model for long distance charge migration in DNA. It has been concluded on the basis of calculation that unnatural nucleobases of low oxidation potential facilitate charge transfer.[110]

The substitution of ***f*** for T illuminates an additional aspect of the mechanism for long-distance radical cation migration in DNA. The

oxidation potential of ***f*** is far greater than that of T. However, the experiments reported above show that there is no detectable effect on the relative reactivity at GG sites when ***f*** replaces T in the bridges of DNA(7) and DNA(10). This finding indicates that the radical cation in an A–T base pair resides primarily on the adenine whether or not that adenine is adjacent to a purine or in the complementary strand. Consequently, the increase in barrier height observed when the bridge separating GG sites is changed from AAAA to 5'–TATA–3', for example,[111] can be attributed to decreased delocalization associated with reduced electronic overlap of adenines when they are in complementary strands.

2.5 Conclusion

We have shown that radical cations migrate across ATAT and TATA bridges in DNA(1) and DNA(3) with different efficiency. This is attributed primarily to the difference in stabilization energy of radical cations in CGGA and CGGT sequences. Substitution of ***t*** for thymine in these bridges lowers the barrier to radical cation migration. This result is ascribed to an electronic effect. The E_{ox} of ***t*** is lower than A, so in an A–***t*** base pair the radical cation will reside primarily on the ***t***. In contrast, substitution of ***f*** for A has no measurable effect on radical cation migration through ATAT or TATA bridges because the radical cation resides primarily on the A. These sequence and structural effects can be applied generally to DNA because the efficiency of radical cation hopping is predictable[83] and easily understood within the phonon-assisted polaron-hopping model.[78,85] DNA in solution is not a conductor. It behaves like a polaronic semiconductor with thermal barriers to radical cation transport formed by A–T base pairs.

Part II: DNA-Directed Assembly of Conducting Oligomers

CHAPTER 3: Intoduction to DNA Directed Assembly of Conducting Oligomers

3.1 Introduction

DNA is the carrier of genetic information and as we have discussed in Chapter 1 the discovery of the structure of DNA opened the doors to the modern era of chemistry, biochemistry and genetics.[4] Apart from the biological aspects, the structural properties of DNA led to the creation of DNA nanotechnology[112] and the use of DNA as a template for more ordered reactions, compound synthesis, reaction discovery.[113,114,115]

The highly sequence specific self recognition and self assembly properties of DNA proved to be a very useful tool in creating well-defined functional nanoscale materials.[112,116,117,118,119] In 2000 Yurke and his colleagues built the first DNA hybridization based nanomotor (a molecular device that converts energy into movement).[120] Thus far one of the most exciting accomplishments came from Seeman and co workers who have created a fully functional robot arm by using the nucleobase recognition properties of DNA.[121]

As we have mentioned in chapters 1 and 2, DNA by itself is not a good conductor, can not be considered a "molecular wire" and this prevents its direct use in electrical curcuits.[13,14] However the unique structural

properties of DNA make it a good candidate as a scaffold for the assembly of nanowires of conducting materials. One strategy is to deposit metals along the DNA strands. Braun and coworkers hybridized DNA with surface bound oligonucleotides to stretch it between two gold electrodes. They used the stretched DNA as a template for the vectoral growth of a 12 μm long, 100 nm wide conductive silver wire. They used the recognition capabilities of DNA for the targeted attachment of conductive nanowires.[122]

In another approach replacement of sodium as the DNA counter-ion with Palladium led to the formation of metal nanowire along the path of the DNA.[123]

However the conductance of these metal wires is not controllable so the use of DNA/metal nanostructures as active circuit elements is restricted.

3.2 Templated Conducting Polymer Synthesis

Polymer synthesis is the coupling of small monomeric units. There is little control over the branching and the size of the polymer. The charge/hole transport in a doped conducting polymer is limited by the formation of a disordered structure.[124] Conducting polymers are insoluble in most solvents and they decompose without melting when heated.[125] To overcome these issues researchers turned to templated synthesis of polymers. The

template serves as an anchor, aligns the monomers and ultimately controls what form of oligomer is obtained during the reaction.

Matyjaszewski and coworkers templated the conducting polymer polyaniline (PANI) via self-assembly of block copolymers to achieve less brittle, more conductive and soluble polyanilines (PANI).[126]

In 2003, Liu and coworkers used sulfonated polystyrene (SPS) as a template and enzymatically synthesized water-soluble, conducting polyanilines.[127] SPS promoted para-directed polymerization, provided the necessary counterions for doping and prevented branching by aligning the monomers. This paper also introduced a milder polymerization technique. They used the enzyme horseradish peroxidase (HRP) in the presence of hydrogen peroxide to generate free radicals and start the polymerization process. (Figure 23)

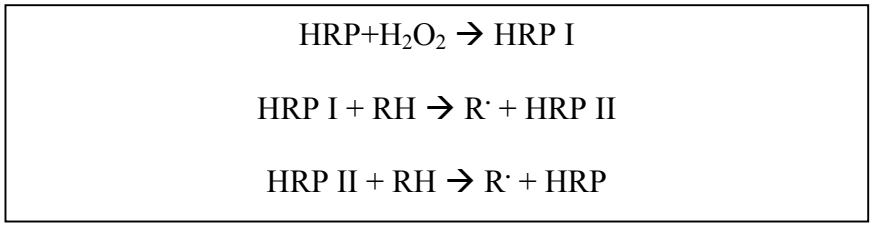

Figure 23 The horse radish peroxidase/H_2O_2 catalytic cycle. RH is the substrate and R· is the radical species formed.

The radical R· produced goes on to form dimer and the cycle continues and forms the polymers.[128] This new approach provided the mild conditions required for the use of biological templates like DNA.

Nabid and coworkers also used sulfonated polystyrene (SPS) as a template to synthesize water soluble polypyrrole.[125] Their enzymatic polymerization (with HRP/H_2O_2) approach with the template aligned the monomers onto the anionic SPS template and branching was controlled.

Apart from polyelectrolytes like SPS and polymers (like the block copolymers) the template can be a micelle, an oligomer etc. The template can be positively charged to accommodate negative charges on the polymer during polymerization or it can be negatively charged to accommodate positive charges on the polymer.

3.3 DNA as a Template for Conducting Polymer Synthesis

Apart from the self-organizing and self-recognizing properties, DNA has been proven to be a good candidate for templated synthesis because of it's negatively charged phosphate backbone and the stack of electrons the base pairs create.

Bae and coworkers created superstructural poly(pyrrole) morphologies using DNA as a polyelectrolyte template.[129] Others used DNA's surface negative charge to assemble materials with specific electronic properties on DNA.[130,131,132]

Nagarajan and coworkers used DNA as a template to biologically assemble conducting polyaniline. They have exploited the inherent molecular order as well as the polyelectrolyte behavior of DNA to synthesize the polymer from its precursor monomer.[133] The DNA/polyaniline complex was water soluble where the polymer was wrapped around the DNA strands. Their later work showed that the formation of the polyaniline caused the DNA-PANI strands to agglomerate[134] which prohibits its use in electronics.

Ma and coworkers used DNA as a template to fabricate PANI nanowires on silicon substrates.[135] First they immobilized the double stranded DNA on silicon surface by molecular combing then they utilized the phosphate backbone of the DNA to emulsify and align aniline monomers. They facilitated the polymerization with HRP/H_2O_2.

The problem with all of these approaches was that although the negatively charged phosphate backbone of DNA served as a template the electrostatic interactions that held the monomers and the DNA together were weak. Agglomeration and branching was inevitable and the sequence programmability of DNA was not being used.

In 2006 Datta and Schuster reported the synthesis of a PANI oligomer covalently linked to the nucleobases of duplex DNA.[136] They covalently attached aniline monomers to modified cytosine residues and initiated the oligomerization by use of HRP/H_2O_2. They synthesized the homopolymer PANI having the properties of a conducting polymer.

In 2008, Datta and Schuster, reported the DNA-directed synthesis of aniline and 4-aminobiphenyl oligomers where they used the programmability of DNA to create heteropolymers.[137]

Unique nanoscale materials with tailored electronic properties can be created by using the sequence programmability of DNA. The covalent attachment of monomers to the DNA template provides a much needed control over polymerization of molecules.

CHAPTER 4: DNA Directed Assembly of Conducting Oligomers

4.1 Introduction

Development of techniques for the creation of molecular electronics at the nanometer scale requires "atomic level" control. One challenge in creating functional nanoscale materials is the development of general techniques for the construction of designed molecular assemblies having nonrecurring, irregular structures.[136] As we have discussed in the previous chapter, DNA offers unique advantages for the preparation of such materials.[119]

DNA as a template is being used for the fabrication of nanowires. One dimensional structures that form self organizing connections between functional electronic components[138,139] and DNA templated metallization[122,140,141] are some examples.

Datta and Schuster developed a new technique for the synthesis of conjoined polymer nanowires.[136] They covalently attached aniline monomers to the nucleobases of DNA. Upon hybridization with the complementary strand, the monomers aligned themselves in the major groove of the duplex. After enzymatic hybridization with HRP/H_2O_2 they achieved DNA-conjoined PANI oligomers. Since there was only one type of monomer homopolymers were produced.

In their later work aniline and 4-aminobiphenyl monomers were attached to the oligonucleotides of DNA.[137] Using the self-recognizing, self-organizing and programmability of DNA they achieved oligomerization on the DNA template that had conducting properties and was a heteropolymer with different monomeric units. This work was a breakthrough in the preparation of conjoined polymer nanowires.

Srinivasan and Schuster covalently attached thionopyrrole monomers to the oligomers and showed that monomers other than aniline could be used in this technique.[142]

Covalent attachment of the monomer units to the nucleobases circumvents problems faced by other methods.

- DNA acts as the template and aligns the monomer units which makes the polymerization process more efficient.
- Since the number of monomers attached can be controlled the length of the resulting polymer chain can be controlled with high precision.
- Utilizing DNA's sequence programmability, the monomer attachment point can be varied depending on the size of the monomer.
- The parasitic branching of the polymer can be eliminated leading to well defined linear polymers.

- The solubility problem that most polymers face can be circumvented in this method. DNA linked monomers are soluble and easier to process.

The oligomers synthesized by Datta and Schuster have the properties of conventional conducting polyanilines. However detailed molecular modeling by Amanda McCook and Steve Harvey suggested that upon oligomerization DNA is distorted with reduced inter-base hydrogen bonding.

We have started looking for other possible monomers. The first one we examinedwas 2-(1H-pyrrol-1-yl) ethylamine (Figure 25). Polypyrrole has been proven to be a good conducting polymer[143] and it's been shown to polymerize under HRP/H_2O_2 enzymatic conditions.[125] The molecular modeling studies showed that although pyrrole could be a good candidate, 3-(2-(1H-pyrrol-2-yl)-1H-pyrrol-1-yl)propan-1-amine (

Figure *24*) was less disruptive to the DNA structure when oligomerized. Calculations also suggested that the use of the monomers, 3-(2,5-di(thiophen-2-yl)-1*H*-pyrrol-1yl)propan-1-amine (SNS) and 2-(2,5-di(thiophen-2-yl)-1H-pyrrol-1-yl)ethanamine (SNS1) (Figure 26) would not disrupt the DNA-duplex structure.

In this work we have synthesized and studied the DNA templated oligomerization of different monomers.

4.2 Experimental

4.2.1 Materials and methods

All the chemicals and solvents for the synthesis of 3-2-(1*H*-pyrrol-2yl)-1*H*-pyrrol-1-yl)propan-1-amine, 2-(1H-pyrrol-1-yl)ethylamine,3-(2,5-di(thiophen-2-yl)-1*H*-pyrrol-1yl)propan-1-amine and 2-(2,5-di(thiophen-2-yl)-1H-pyrrol-1-yl)ethanamine were purchased from Sigma Aldrich, Fisher Scientific and VWR. All synthetic DNA oligonucleotides were synthesized in our laboratory on an Applied Biosystems Inc. Expedite DNA Synthesizer. Nucleotide phosphoramidites including O4-triazolyl-deoxyuridine phosphoramidite were purchased from Glen Research and used as received. UV melting and cooling experiments as well as UV/Vis studies on DNA oligonucleotides were conducted at 260 nm on a Cary 1E Spectrophotometer equipped with a multi-cell block, temperature controller and sample transport accessory. The extinction coefficients of the oligomers were calculated using a biopolymer calculator, and their concentrations were determined from the absorbance at 260 nm. The mass of each oligonucleotide was determined by a Micromass Quattro Electrospray Ionization (ESI) mass spectrometer. [γ-^{32}P] radioactive isotopes were purchased from Perkin Elmer. T4 polynucleotide kinase was purchased from New England Biolabs. Circular Dichroism (CD) measurements were conducted on a JASCO-720 instrument. Kodak film

for PAGE analysis was purchased from Aldrich. Spin columns and centrifugal filters were obtained from Millipore.

4.2.2 Synthesis of the monomers

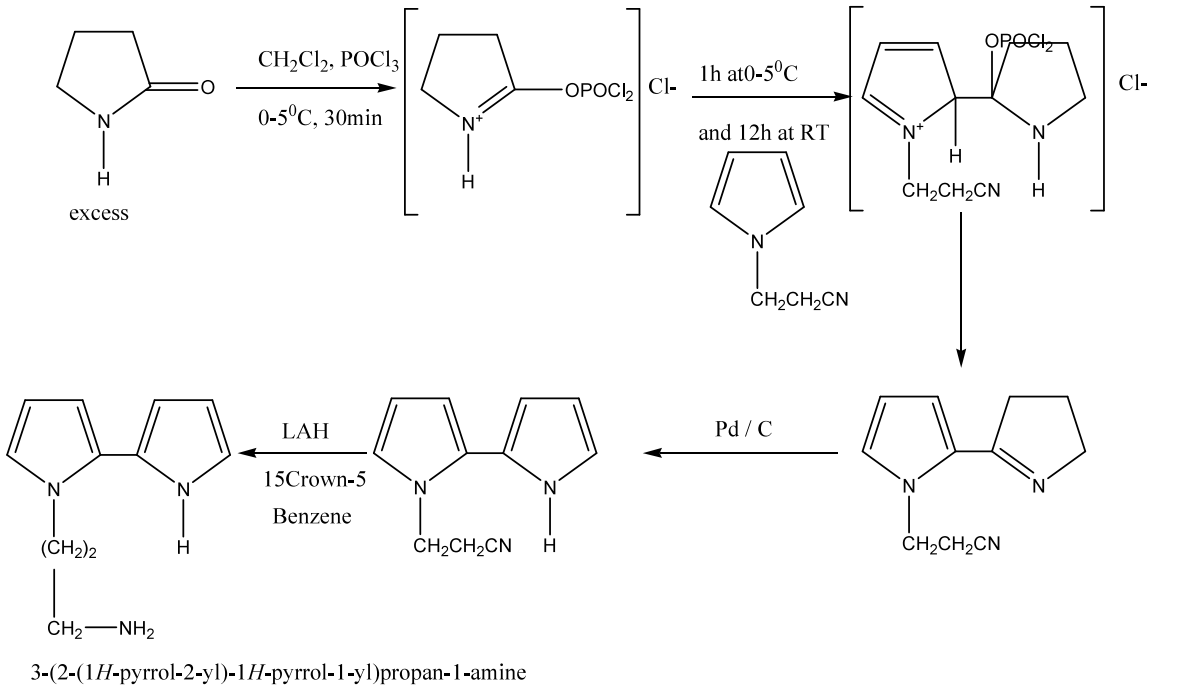

Figure 24 Synthesis of 3-(2-(1H-pyrrol-2-yl)-1H-pyrrol-1-yl)propan-1-amine[144]

The synthesis of the asymmetric bipyrrole, 3-(2-(1H-pyrrol-2-yl)-1H-pyrrol-1-yl)propan-1-amine, was achieved with 1% yield. It would take an enormous amount of time and work to get enough monomer so we turned our focused to the synthesis of 2-(1H-pyrrol-1-yl)ethylamine. (Figure 25)

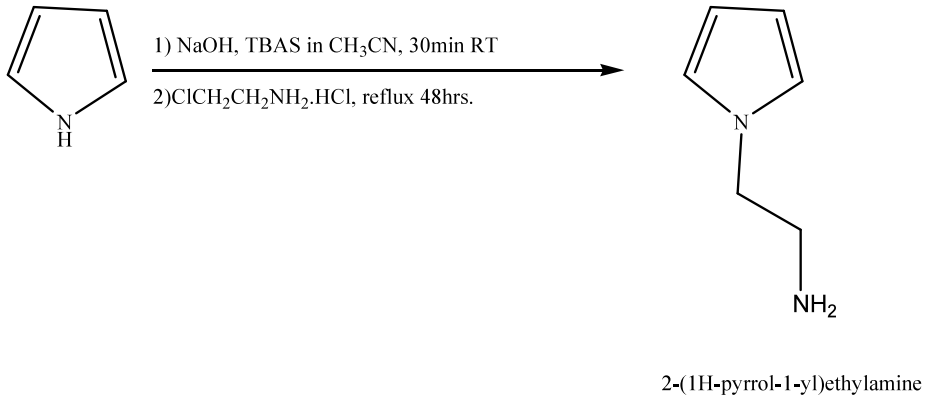

Figure 25 Synthesis of 2-(1H-pyrrol-1-yl)ethylamine[145]

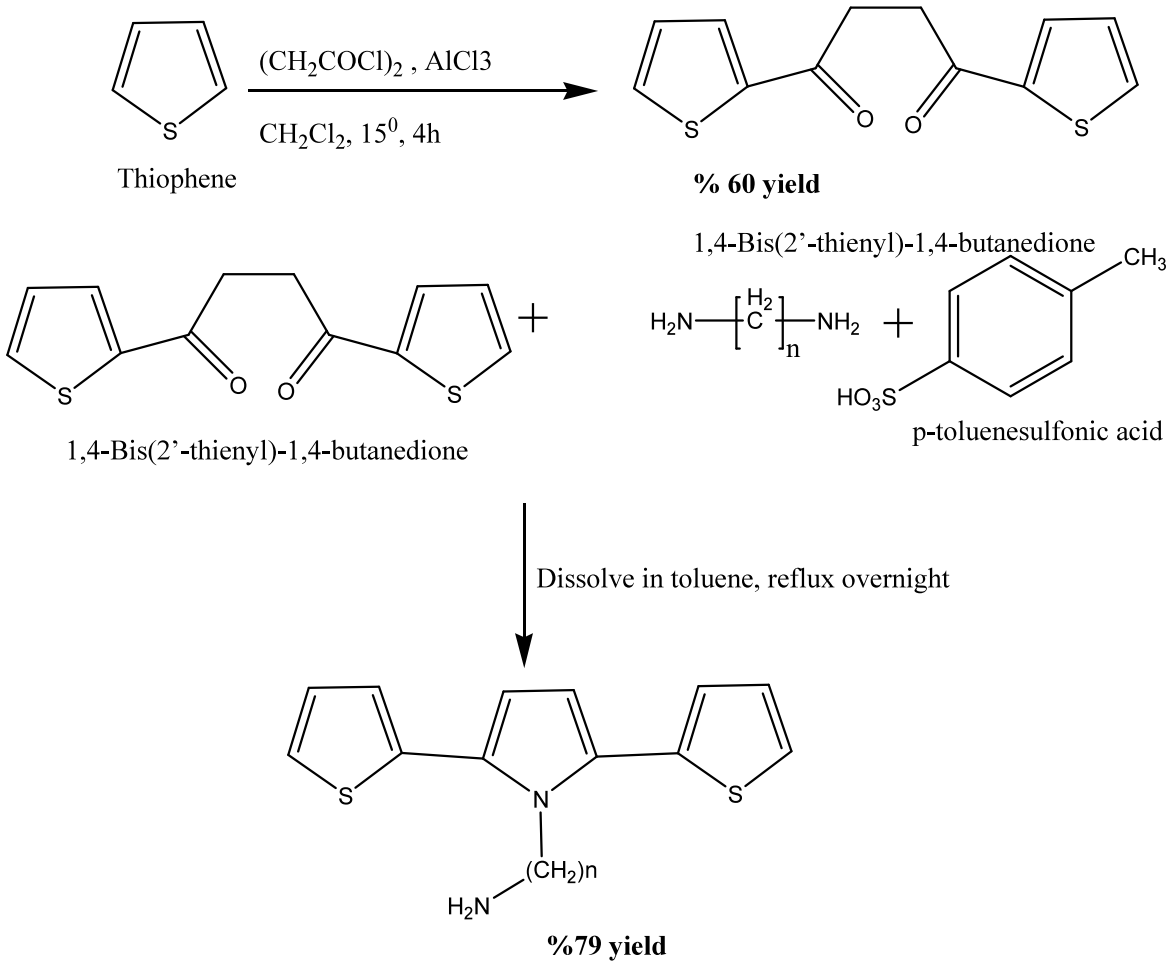

Figure 26 Synthesis of 3-(2,5-di(thiophen-2-yl)-1*H*-pyrrol-1yl)propan-1-amine and 2-(2,5-di(thiophen-2-yl)-1H-pyrrol-1-yl)ethanamine

4.2.3 Preparation of Modified DNA Oligonucleotides

DNA oligonucleotides were synthesized on an Expedite 8909 DNA synthesizer by the convertible nucleotide approach[146] using O4-triazolyl-deoxyuridine phosphoramidite along with PAC phosphoramidites. The resin bound oligonucleotides containing the convertible nucleotide were treated with150 uL of 1M (in anhydrous CH_3CN) solution of the appropriate amines for 42 h at 65^0C.(Figure 27) After the 42 h period the resin bound oligonucleotides were washed with anhydrous acetonitrile repeatedly to remove any unreacted amine. The amine treated DNA oligonucleotides were cleaved from the resin by treatment with 5 ml concentrated ammonium hydroxide at room temperature for 12 hours. The resin was separated from the ammonium hydroxide solution by Acrodisc LC 25 mm syringe filter with 0.45 um PVDF membrane. The solution was dried on a Speed Vac and the samples were dissolved in water for purification by HPLC. The modified DNA oligonucleotides were purified by HPLC on a Hitachi 7000 preparative HPLC system equipped with a Varian Dynamax 25x21.4 mm reverse-phase C-18 column using 5-20% Acetonitrile in 0.5 M Triethylammonium Acetate buffer at pH 7 and then desalted by using sep-pak column.

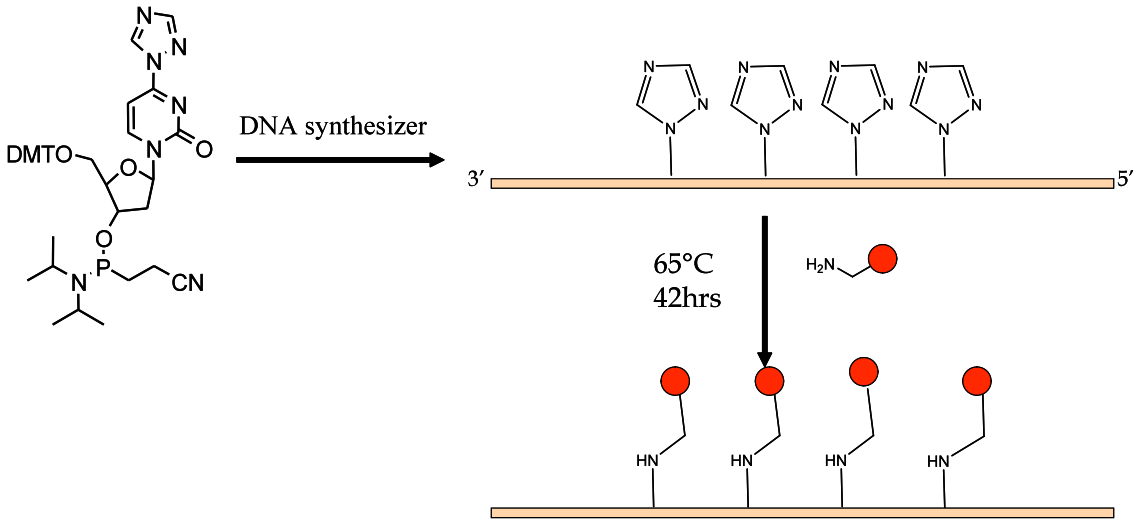

Figure 27 Scheme for Post Synthetic Modification of the DNA by the convertible nucleotide approach.[146] The red circles represent the various monomers used.

The concentrations of the DNA single strands were determined using absorption spectroscopy and applying Beer-Lambert Law. The modified nucleosides were substituted with cytosine in the extinction coefficient calculations.

4.2.4 Characterization of DNA duplexes

DNA duplexes were characterized by mass spectroscopy, thermal denaturation and circular dichroism studies.

4.2.4.1 Mass Spectroscopy

The mass of each oligonucleotide was determined by a Micromass Quattro Electrospray Ionization (ESI) mass spectrometer.

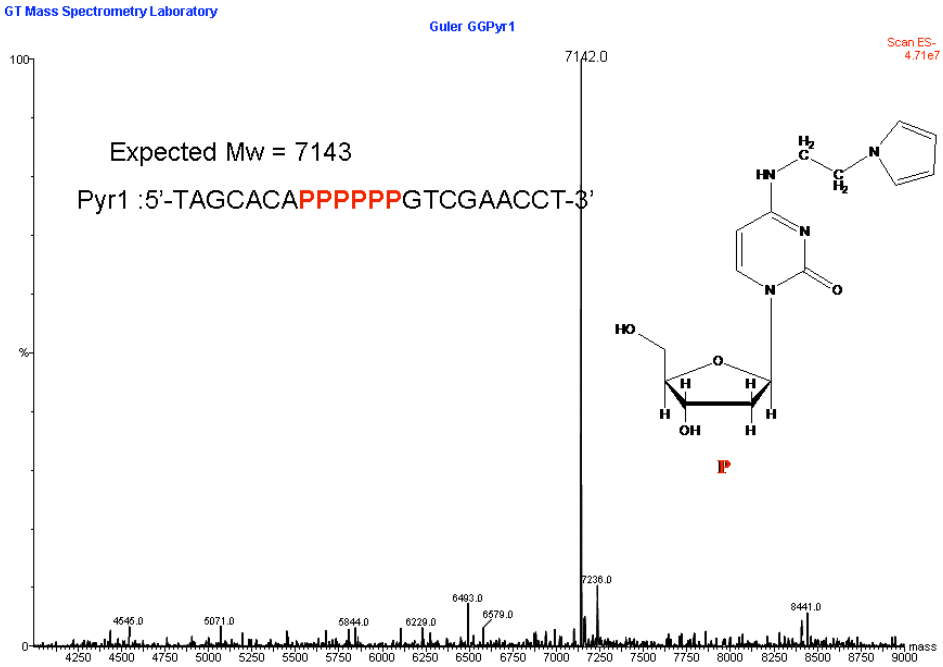

Figure 28 ESI Mass Spectrum of Pyr1

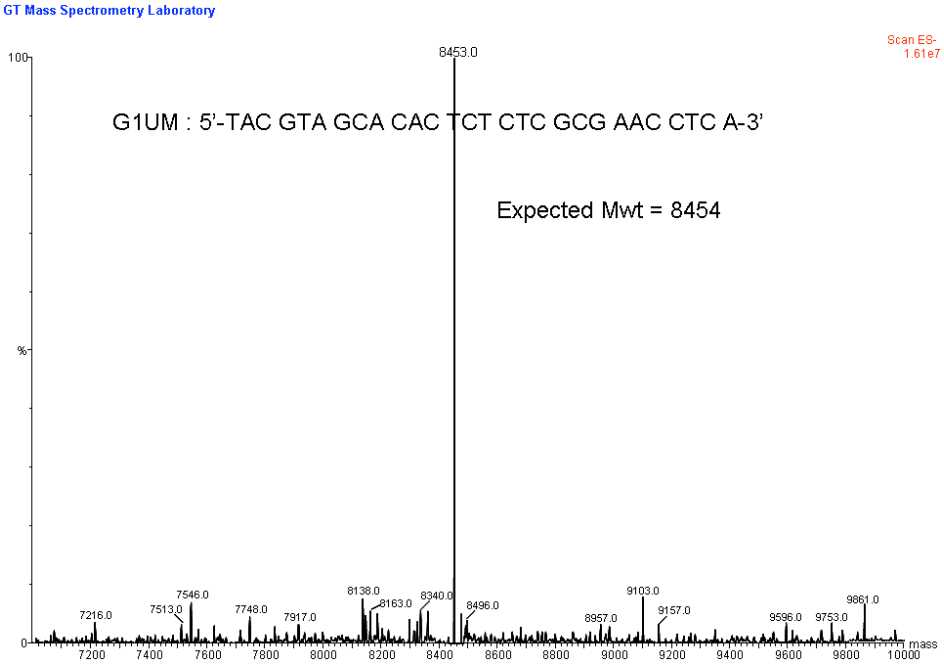

Figure 29 ESI Mass Spectrum of G1UM

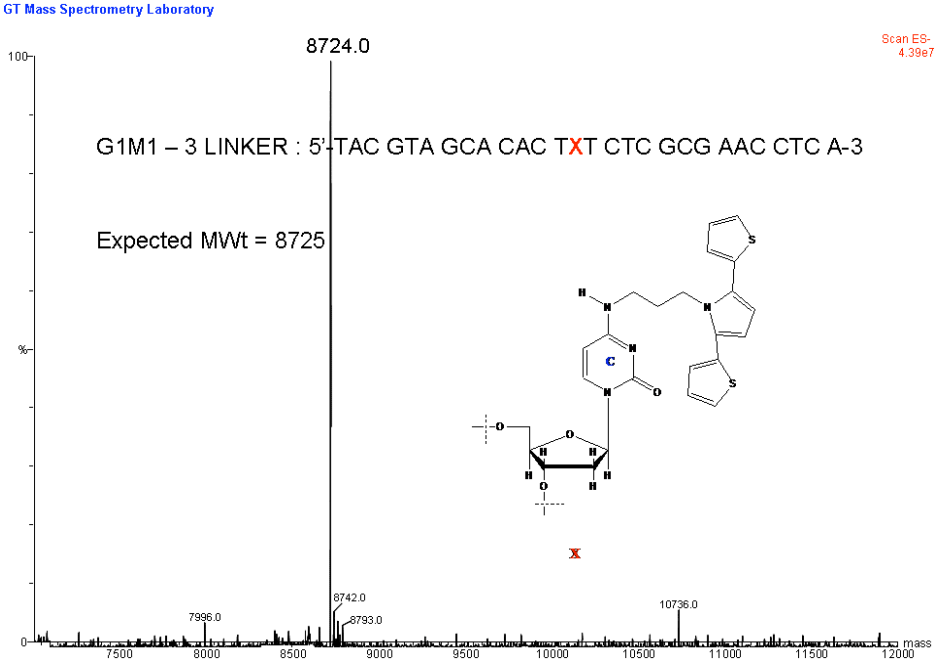

Figure 30 ESI Mass Spectrum of G1M1

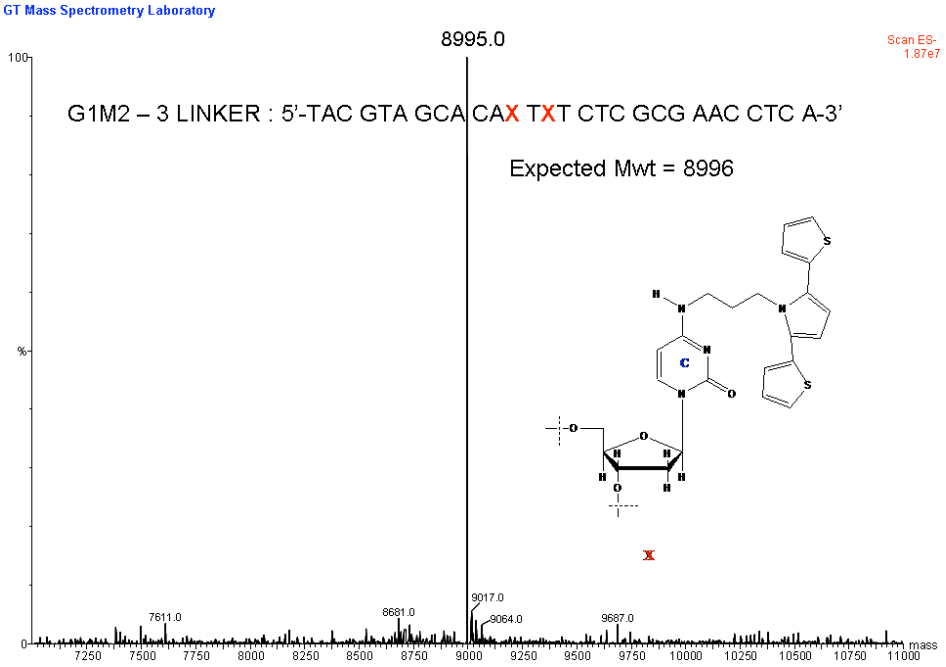

Figure 31 ESI Mass Spectrum of G1M2

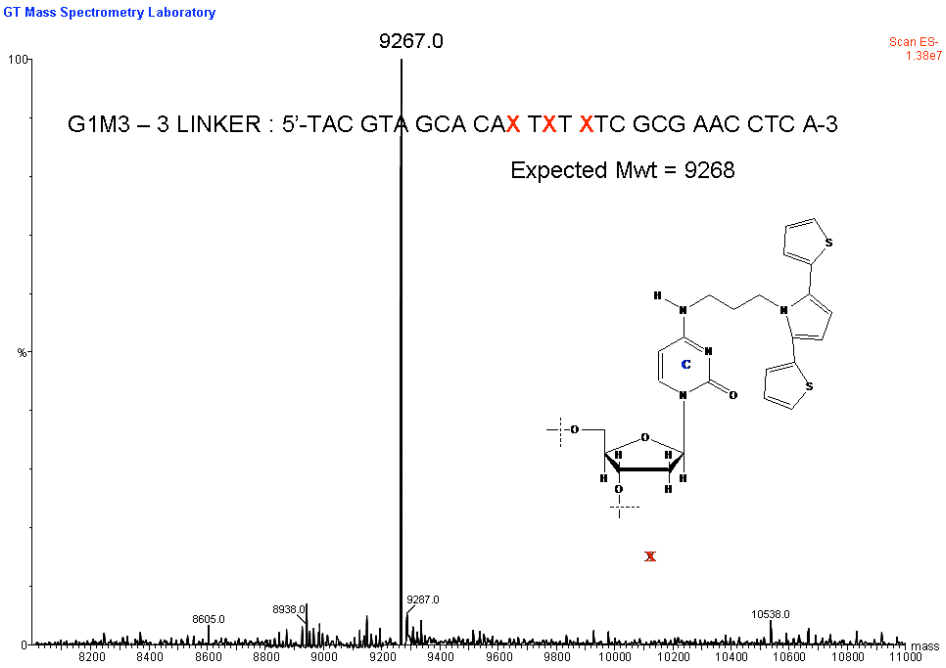

Figure 32 ESI Mass Spectrum of G1M3

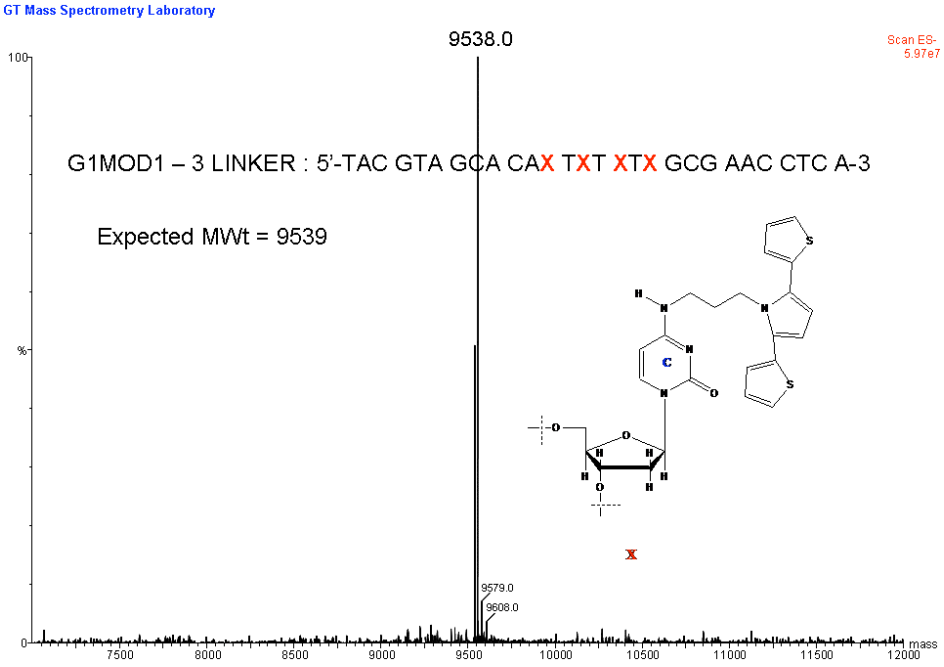

Figure 33 ESI Mass Spectrum of G1MOD1

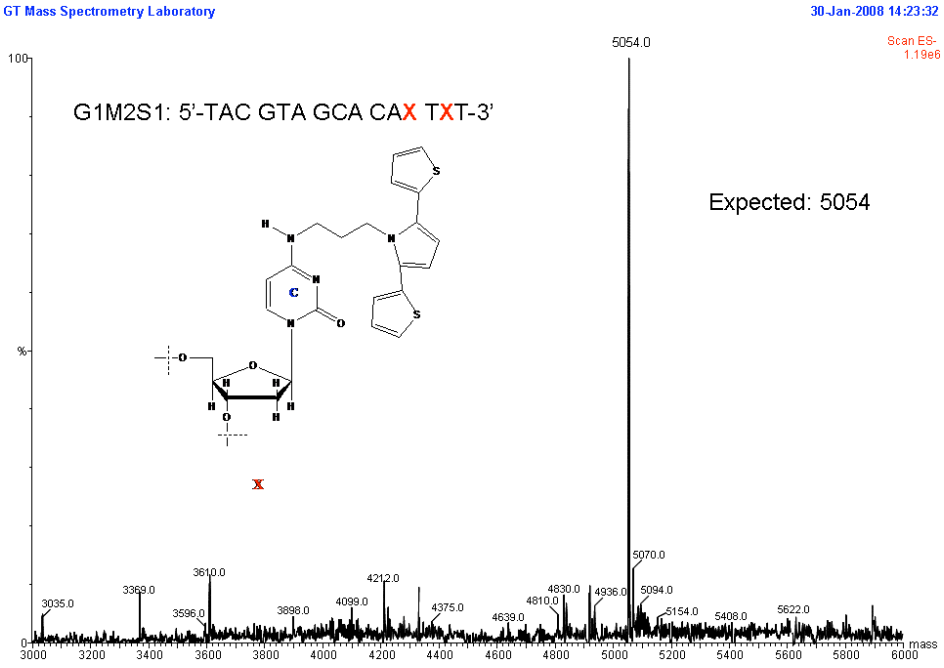

Figure 34 ESI Mass Spectrum of G1M2S1

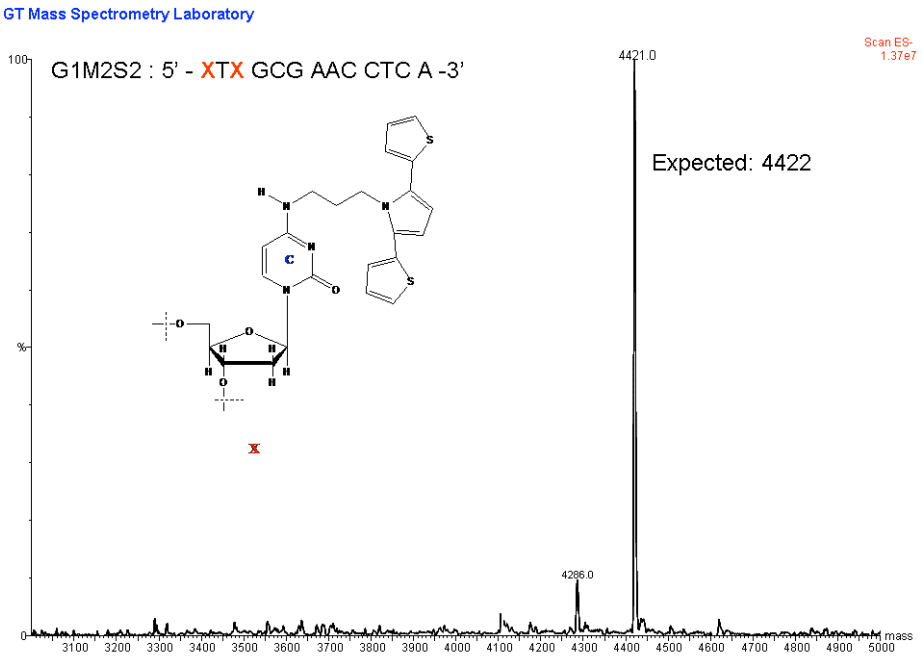

Figure 35 ESI Mass Spectrum of G1M2S2

4.2.4.2 Thermal Denaturation Studies

For studies with 2-(1H-pyrrol-1-yl)ethylamine monomer the samples for thermal denaturation studies were prepared by mixing 2.5 μM of unlabeled complementary DNA single strands, 500 mM NaCl, 2 mM Citrate buffer (pH 4.5).

For studies with the monomers 2-(2,5-di(thiophen-2-yl)-1H-pyrrol-1-yl)ethanamine and 3-(2,5-di(thiophen-2-yl)-1*H*-pyrrol-1yl)propan-1-amine the samples were prepared by mixing 2.5 μM of unlabeled complementary DNA single strands, 500 mM NaCl, 20 mM sodium phosphate buffer (pH 7) or 10 mM citrate buffer(pH 4.5).

The samples were hybridized at 90^0C for 10 minutes and cooled down to room temperature gradually. Hybridized samples were transferred to UV transparent quartz cells with 1 cm path length. The melting temperatures of the samples were monitored by their UV absorption at 260 nm using CARY 1E Spectrophotometer. Several melting ramps starting from 15^0C to 90^0C at 1^0C/min rate were recorded. The plot of wavelength vs. 1st derivative of the absorbance gave us the melting temperatures.

4.2.4.3 Circular Dichroism Studies

The samples used in thermal denaturation studies were used in CD experiments to determine the secondary structure of the DNA duplexes studied.

The spectral resolution was 0.2 nm and the bandwidth was 1 nm. The CD spectra shown through out the work are the average of 5 scans (scan rate 200-400 nm).

4.2.5 Oligomerization and UV-VIS Studies

Horseradish peroxidase (HRP), type II (200 units/mg) was purchased from Sigma Aldrich Co., St. Louis MO. A solution of HRP was prepared (2 mg in 2 ml) and used as a stock solution for the oligomerization. Hydrogen peroxide (H_2O_2; 30%) was purchased from Fisher Scientific, Pittsburg, PA and diluted to 0.3% in deoionized water for use. The DNA duplexes were prepared in either in 10 mM citrate buffer (pH 4.5) containing 500 mM NaCl or in 20 mM sodium phosphate buffer (pH 7) containing 500 mM NaCl.

After the addition of 5 µL HRP to DNA samples, oligomerization was initiated by the addition of 2 µL of H_2O_2. UV-VIS spectra were recorded starting with the addition of HRP until reaction was completed.

4.2.6 Preparation of Radiolabaled DNA

DNA single strands were labeled at their 5' end using [γ-^{32}P]ATP and T4-Polynucleotide Kinase (PNK) enzyme.

5 µL of 200-300 µM of the desired ssDNA, 2 µL of PNK buffer, 1 µL of [γ-^{32}P]ATP, 2 µL of T4-PNK enzyme and 10 µL nano pure water were incubated at 37^{0}C for 45 minutes. After incubation the DNA sample was suspended in 10 µL of denaturing loading dye composed of 3',3'',5',5''-tetrabromophenolsulfonphthalein (bromophenol blue) in 4:1 water-formamide for visualization purposes. The labeled DNA was purified on a 20% polyacrylamide denaturing gel. Purified DNA was visualized by autoradiography and the desired band was cut from the gel. The excised gel piece was eluted with 800 µL of elution buffer (0.5 M NH_4OAc, 10 mM $Mg(OAc)_2$, 1.0 mM EDTA and 0.1% SDS) at 37^{0}C for 12 hours. The DNA was precipitated from the elution buffer by adding 2 µL of glycogen and 800 µL of 100% ethanol and centrifuging at 13000 rpm for 1 hour. The nonradioactive supernate was removed and the DNA was twice washed with 100 µL of 80% ethanol and air dried. Nanopure water was added to adjust the counts to 10,000 cpm/µL

4.2.7 Gel Electrophoresis

The samples for oligomerization were prepared by hybridizing a mixture of the unlabeled and radiolabeled (10,000 cpm) oligonucleotides with the complementary strands in 10 mM Citrate Buffer (pH 4.5) and 500 mM NaCl at 90^0C and slowly cooling to room temperature. The single strand samples were prepared the same way except for the absence of the complementary strand. The hybridized samples were divided into two, the control was set aside. 5 uL HRP (1 mg/ml) and 2 uL H_2O_2 (0.3%) was added to each sample and left to oligomerize for 2 hours. After the reaction was complete both the oligomerized and control samples were precipitated with cold ethanol (100 µL) in the presence of glycogen (1.25 µL, 20 mg/mL), washed with 80 % ethanol (2 x 100 µL) and dried. The counts for the dried samples were adjusted by addition of formamide-dye solution (1500 cpm). The samples for heated at 90^0C for 10 minutes, cooled in ice and were loaded to a 20 % 19:1 acrylamide:bis-acrylamide gel (or 20% 29:1 acrylamide:bis-acrylamide gel) containing urea (7 M) at 70 watts. The gels were dried visualized by autoradiography.

4.2.8 Molecular Modeling Studies

Geometry optimizations were performed in HyperChem 7.5 using standard molecular mechanics methods based on amber94 force field and a conjugate gradient method with a termination value of the RMS gradient of 0.01 kcal/mol/Å.

In depth molecular modeling studies were conducted in Dr. Steve Harvey's lab at Georgia Institute of Technology by Amanda McCook and Jared Gossett.

4.3 Results and discussion

4.3.1 DNA Conjoined Oligomers

We have conducted studies with monomers 2-(2,5-di(thiophen-2-yl)-1H-pyrrol-1-yl)ethanamine(SNS1) and 3-(2,5-di(thiophen-2-yl)-1*H*-pyrrol-1yl)propan-1-amine (SNS) at pH 7 and pH 4.5. Monomer SNS1 has a two-carbon linker which limits the flexibility of the monomer in the major groove. SNS has a 3-carbon linker and molecular modeling studies by HyperChem showed that the monomers line up in the major groove before oligomerization and after oligomerization the structure of the duplex does not seem to be disturbed.(See Figure 36)

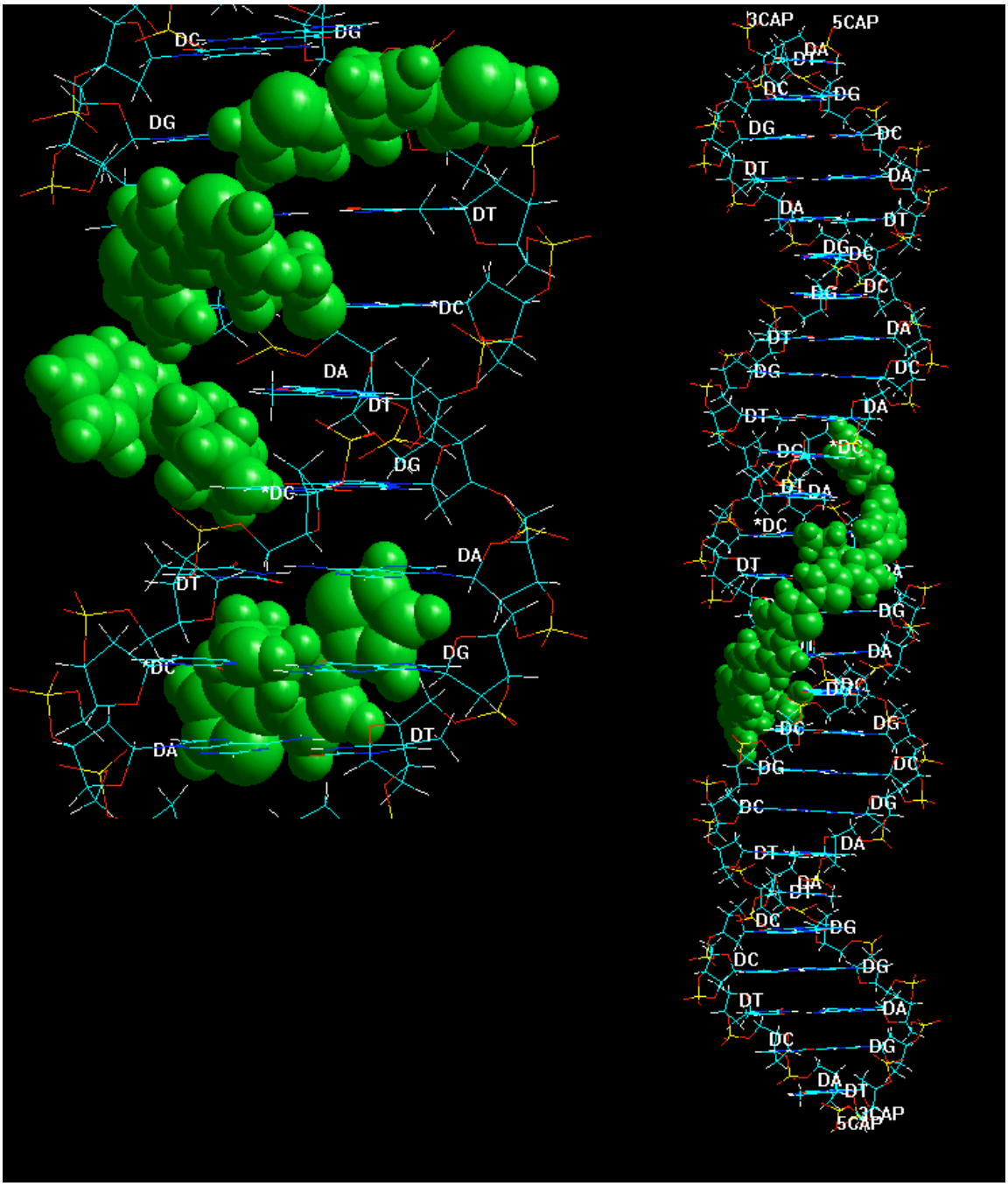

Figure 36 HyperChem Modeling of 4 SNS modifications

The experiments conducted with SNS1 monomer showed no concrete signs of oligomerization so we focused on the SNS modified sequences.

To maintain the integrity of the duplex DNA we first started our experiments at pH 7, previous work has shown that HRP was barely effective at this pH.[125] After some unsatisfactory results at this pH we shifted our focus on experiments at pH 4.5 and have seen that DNA conserved it's duplex structure under the conditions we have set and oligomerization took place.

Figueras et al. studied the absorption properties of poly(2,5-di-(2-thienyl)pyrrole.[147] Their results showed that the monomer 2,5-di-(2-thienyl)pyrrole dissolved in acetonitrile exhibited a band at 340 nm which they assigned to the π-π^* transition of the system. The same absorption wavelength for the monomer was reported by Ferraris and Hanlon.[148] After electrochemical polymerization they observed the formation of a new band at 427 nm which they assigned as π-π^* transition. In a later work the oxidized polymer presented 4 peaks at 594 nm, 639 nm, 749 nm and 814 nm. They attributed these peaks to dications (bipolarons) along the polymeric chain and saw that the bands decreased in time as a result of self reduction.[149]

In another study by Tarkuc et al. examined poly(6-(2,5-di(thiophen-2-yl)-1H-pyrrole-1-yl)hexan-1-amine),P(PTHA), via spectroelectrochemistry.[150] They observed that P(PTHA) has a peak absorbance at 334 nm and that upon doping peaks at 470 nm and 970 nm emerge and increase while the peak at 334 nm decreases.

4.3.2 SNS Monomer

The monomer 3-(2,5-di(thiophen-2-yl)-1*H*-pyrrol-1yl)propan-1-amine(SNS) was synthesized as shown in Figure 26 with 79% yield as a dark yellow syrup.

We dissolved 1 umole SNS in 100 uL acetonitrile and added 900 uL citrate buffer at pH 4.5. The monomer was examined by UV-Vis spectroscopy. A band at ~305 nm was observed which is the neutral monomer absorption. After the addition of HRP no measurable difference was observed. With the addition of H_2O_2 a sharp decrease in the 305 nm monomer peak and the formation of a peak ~500 nm was observed. Within 45 minutes the monomer absorption peak almost disappeared. We followed the reaction with TLC which showed us that the starting material was completely consumed. At this point a new peak ~360 nm emerged. To complete the oxidation we added 10% APS to the solution and the monomer absorption peak completely disappeared, the peak at ~360 nm shifted to ~385 nm. The absorption in the 600-900 nm region was observed to increase with

the oxidation process. These results are in accordance with the literature.[148,149,150]

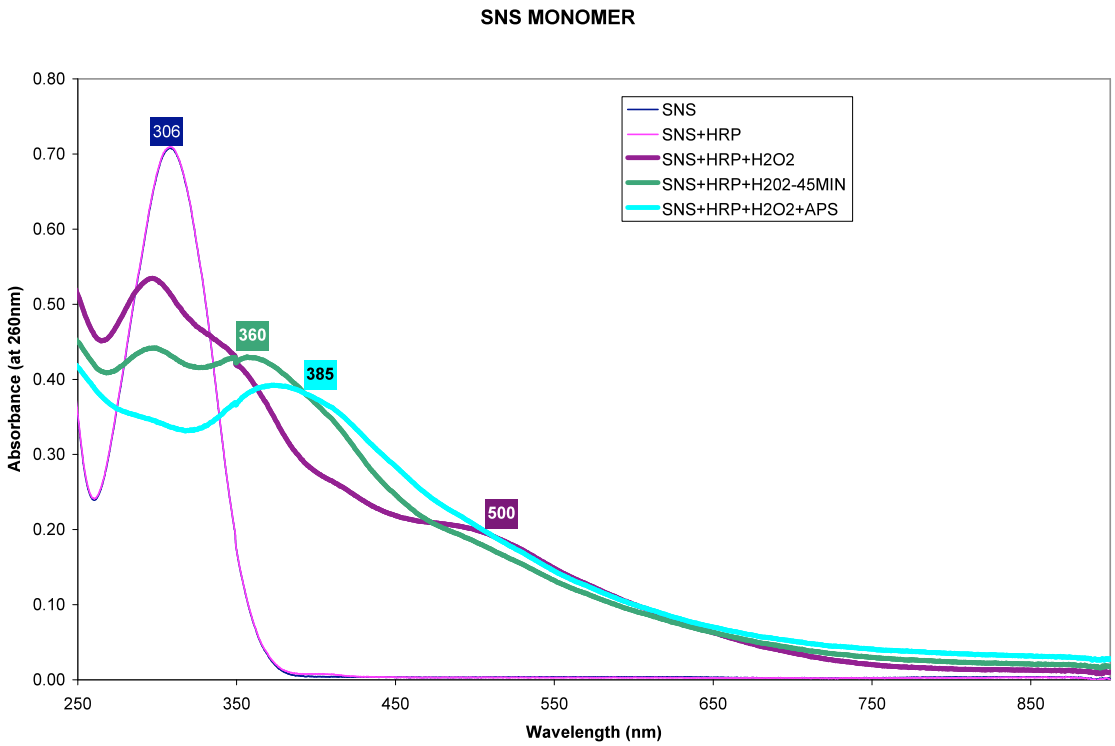

Figure 37 Absorption Spectrum of oligomerized SNS monomer pH4.5

4.3.3 Single Modification

DNA oligonucleotides G1U, G1C and G1M1 shown in Table 5 were synthesized. G1M1 contains a single modified cytosine bearing covalently attached 3-(2,5-di(thiophen-2-yl)-1*H*-pyrrol-1yl)propan-1-amine(SNS) monomer represented with **X**.

Table 5 DNA sequences G1C, G1U, G1M1

G1UC	G1C **:** 5'-TGA GGT TCG CGA GAG AGT GTG CTA CGT A-3' G1U : 3'-ACT CCA AGC GCT CTC TCA CAC GAT GCA T-5'
G1M1C	G1C **:** 5'-TGA GGT TCG CGA GAG AGT GTG CTA CGT A-3' G1M1 : 3'-ACT CCA AGC G**X**T CTC TCA CAC GAT GCA T-5'

The presence of a single SNS monomer in the major groove of the duplex G1M1C lowers the melting temperature by ~3°C when compared to the unmodified duplex G1UC (Table 6), the circular dichroism (CD) spectrum of both complexes are similar (Figure 38), showing the modified duplex maintains an overall B-Form structure.

Table 6 Melting Temperatures for G1UC and G1M1C-Single Modification

DNA	**Modification**	**Tm/°C** **pH 7**	**Tm/°C** **pH 4.5**
G1UC	Unmodified	85	74
G1M1C	1***X** modified	81	71

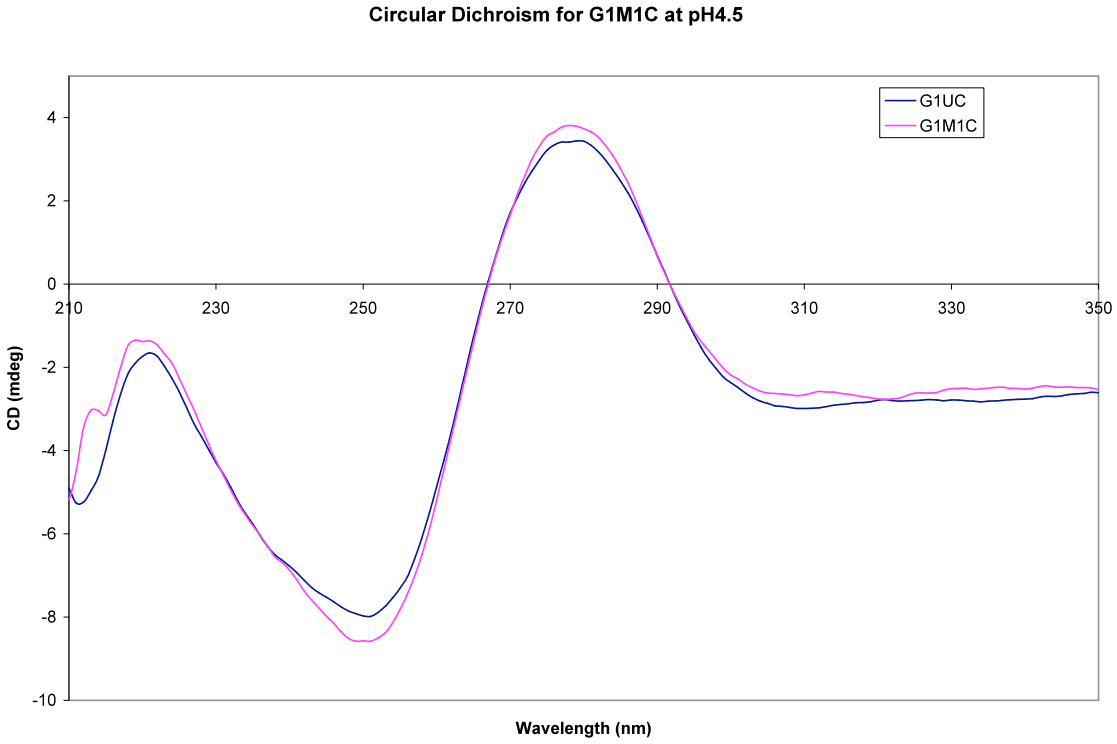

Figure 38 Circular Dichroism for G1M1C at pH4.5

The treatment of duplex G1M1C at pH 7 with HRP and H_2O_2 at room temperature showed the formation of a band at ~460 nm and no other observable bands over the course of 1 hour. We attribute this peak to the π-π^* transition of the oxidized monomer but the absence of other peaks leads us to conclude that oligomerization did not take place. (Figure 39)

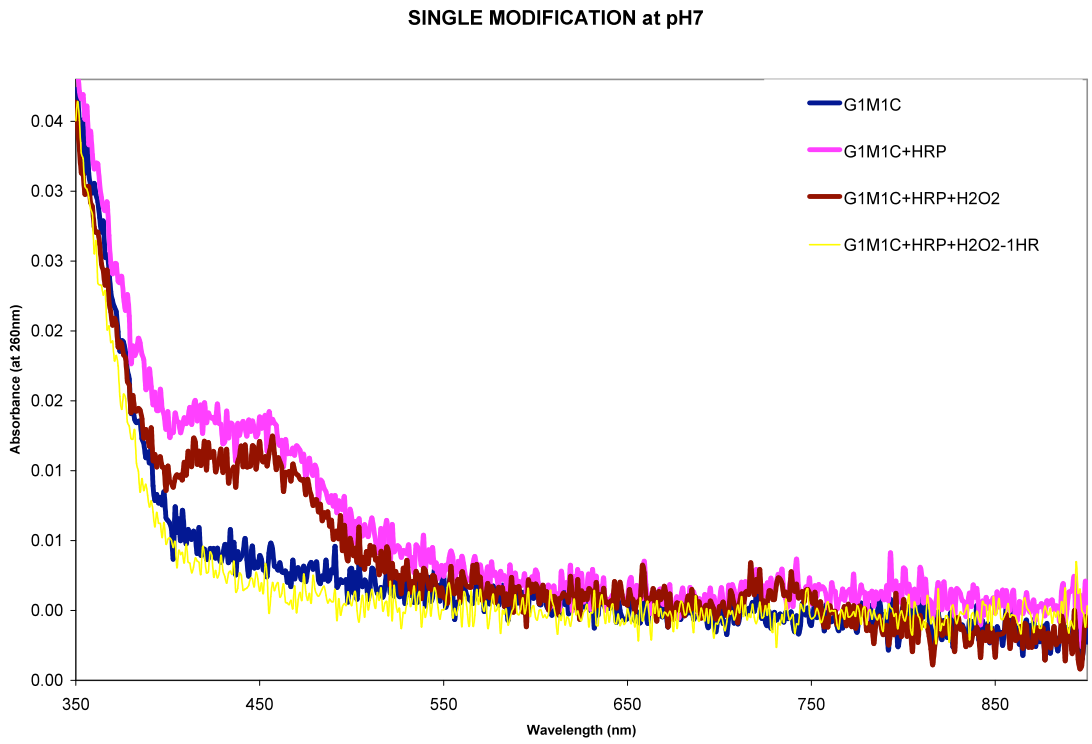

Figure 39 Absorption Spectrum of G1M1C-Single SNS modification at pH7

At pH 4.5 the treatment of the duplex with HRP and H_2O_2 gave rise to a sharp peak at ~460 nm, a broadband peak between 550-700 nm and a peak at ~730 nm. The monomer absorption band at 325 nm was observed to decrease with the addition of HRP and H_2O_2 and with time as the reaction proceeded. We attribute the formation of the bands to the oxidation of the monomer and formation of dications in solution (Figure 40).

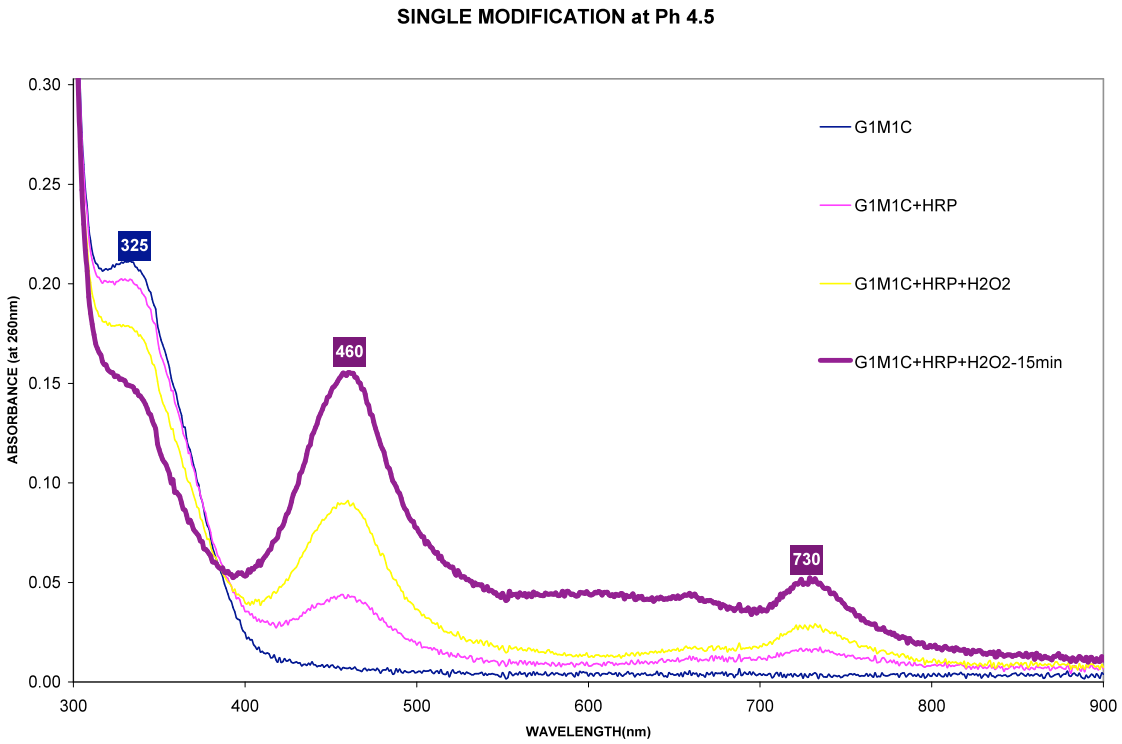

Figure 40 Absorption Spectrum of G1M1C-Single SNS modification at pH4.5

Next, single strand DNA (G1M1) in 500 mM NaCl and 10 mM citrate buffer at pH 4.5 was studied to observe the effects of the template. (Figure 41) With the addition of HRP and H_2O_2 a band at ~430 nm and two broad band peaks formed at ~520 nm and ~820 nm. The monomer peak absorption at 335 nm decreased as reaction proceeded. Within 90 minutes we saw a decrease in the absorption peak ~820 nm which signifies the self reduction of the monomer.

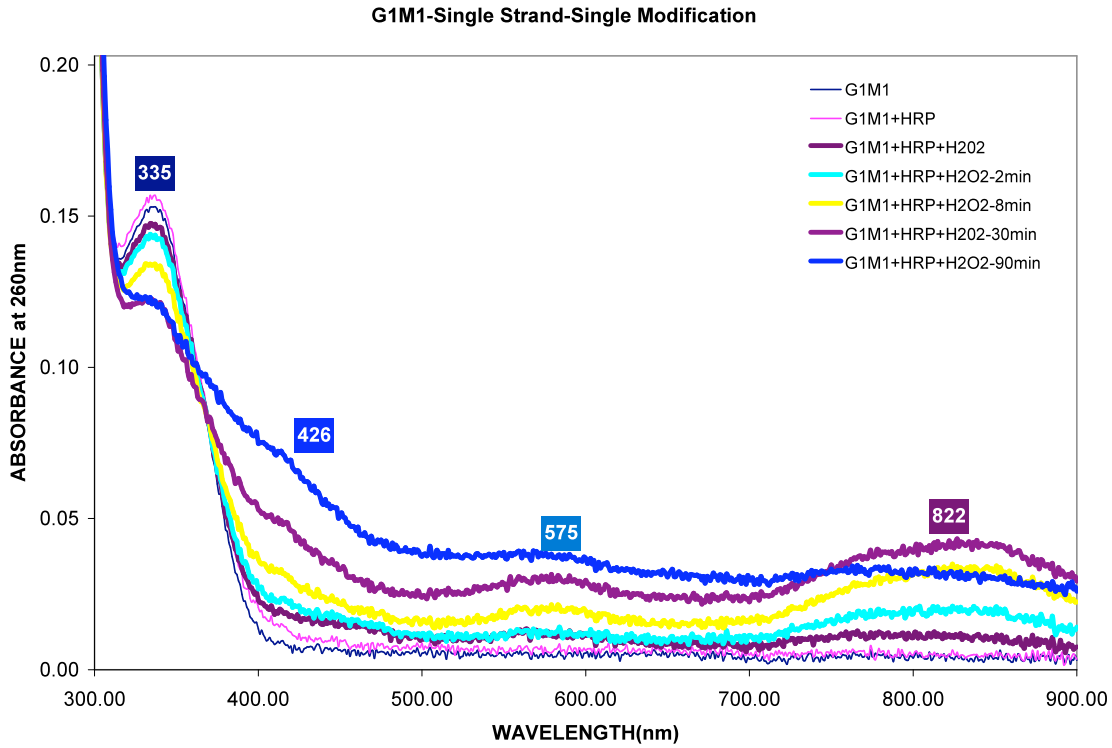

Figure 41 Absorption Spectrum of G1M1-single strand-Single SNS modification at pH4.5

4.3.4 Two Modifications

DNA oligonucleotides G1U, G1C and G1M2 shown in Table 7 were synthesized. G1M2 contains two modified cytosines bearing covalently attached 3-(2,5-di(thiophen-2-yl)-1*H*-pyrrol-1yl)propan-1-amine(SNS) monomers represented with **X**.

Table 7 DNA sequences G1U, G1C, G1M2

G1UC	G1C **:** 5'-TGA GGT TCG CGA GAG AGT GTG CTA CGT A-3' G1U : 3'-ACT CCA AGC GCT CTC TCA CAC GAT GCA T-5'
G1M2C	G1C **:** 5'-TGA GGT TCG CGA GAG AGT GTG CTA CGT A-3' G1M2 : 3'-ACT CCA AGC G**X**T **X**TC TCA CAC GAT GCA T-5'

The presence of two SNS monomers in the major groove of the duplex G1M2C lowers the melting temperature by ~6°C when compared to the unmodified duplex G1UC (Table 8), the circular dichroism (CD) spectrum of both complexes are similar (Figure 42) , showing the modified duplex maintains an overall B-Form structure.

Table 8 Melting Temperatures for G1UC and G1M2C-Two Modifications

G1UC	Unmodified	85	74
G1M2C	2***X** modified	79	68

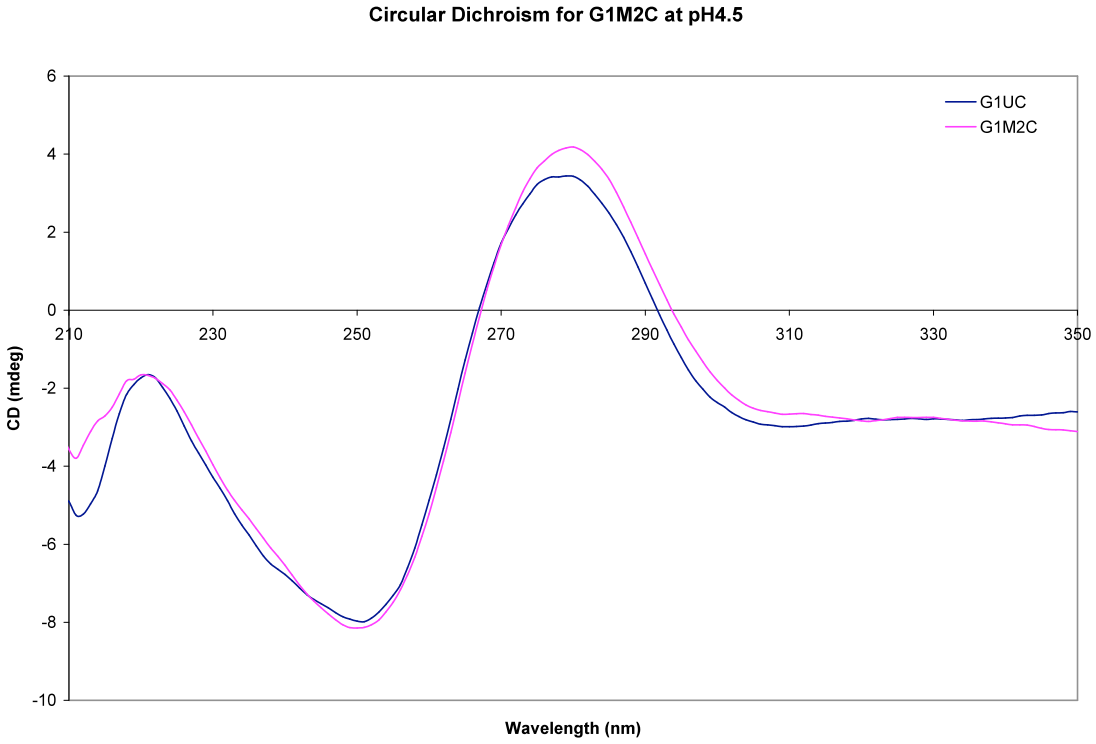

Figure 42 Circular Dichroism for G1M2C at pH4.5

The treatment of duplex G1M2C at pH 7 with HRP and H_2O_2 at room temperature showed the formation of a broadband peak at ~800 nm, a broadband absorption peak between 500-700 nm and the decrease of the monomer band at 325 nm. (Figure 43)

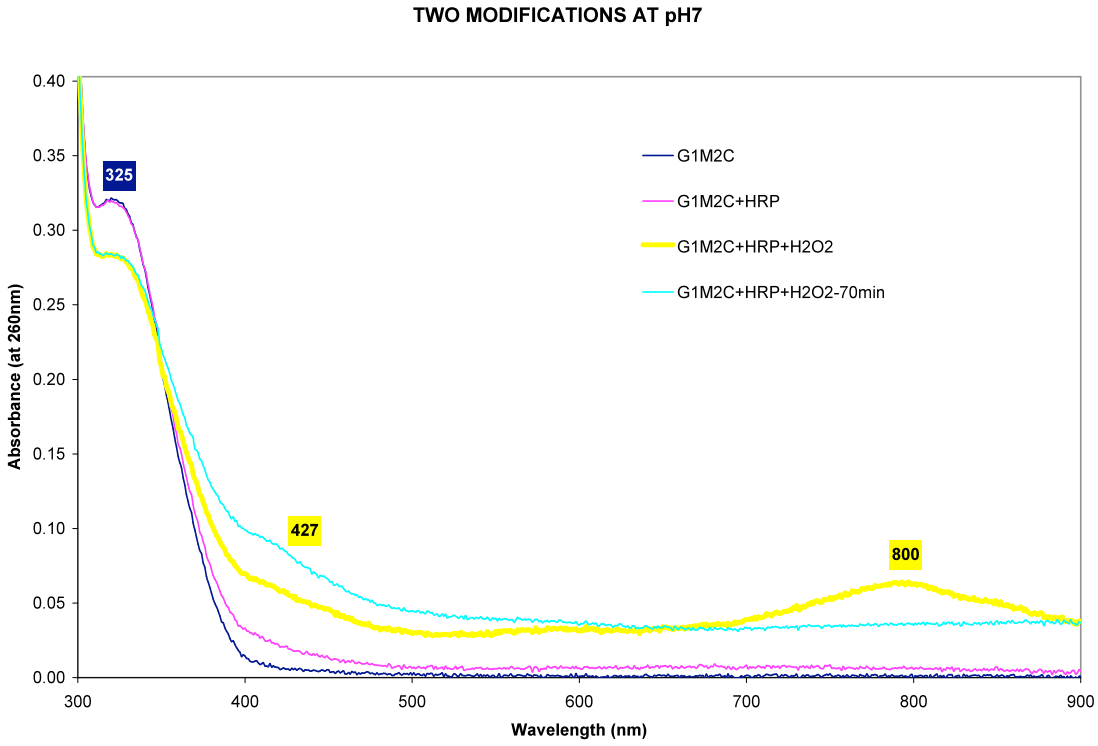

Figure 43 Absorption Spectrum of G1M2C-Two SNS modifications at pH7

At pH 4.5 the treatment of the duplex with HRP and H_2O_2 gave rise to a significantly sharper broad band peak at ~820 nm, a peak at ~465 nm and a significant decrease in the monomer absorption band at 325 nm.(Figure 44) The appearance of the absorption peak at 820 nm signifies the formation of the dimer.

The experiments at pH 7 were conducted with 10uM G1M2C whereas the experiments at pH4.5 were with 2uM G1M2C. The oligomerization reaction at pH 7 with 2uM DNA showed no significant change in the absorption spectrum.

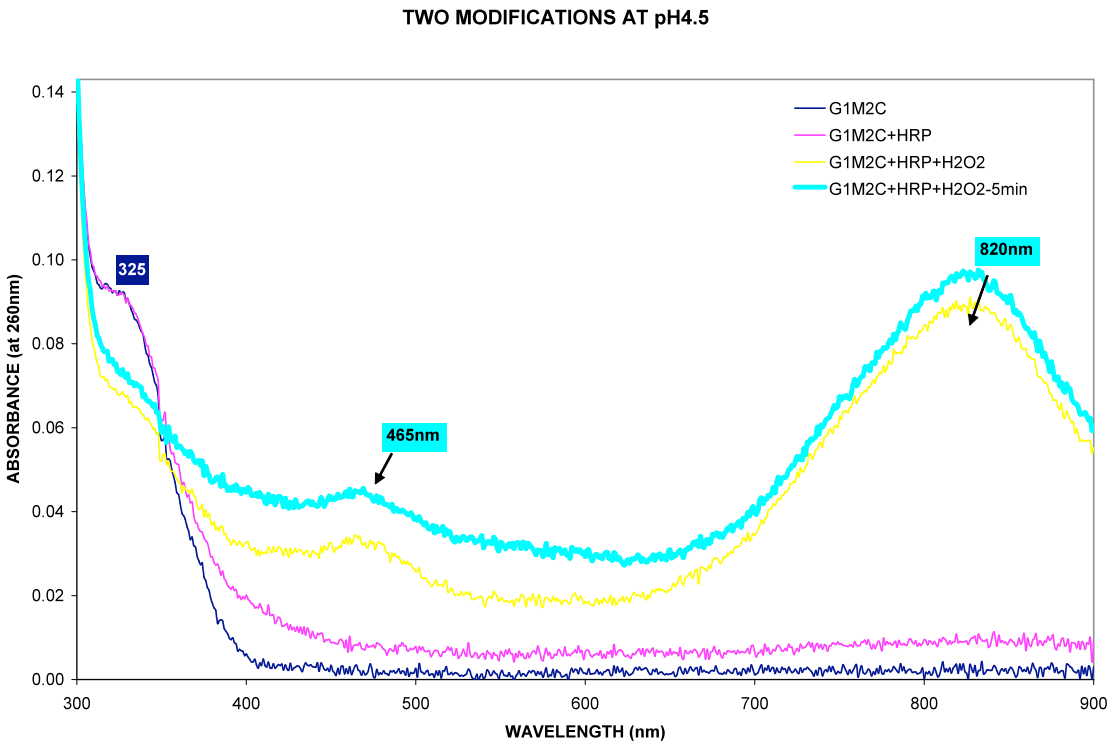

Figure 44 Absorption Spectrum of G1M2C-Two SNS modifications at pH4.5

4.3.5 Three Modifications

DNA oligonucleotides G1U, G1C and G1M3 shown in (Table 9) were synthesized. G1M3 contains three modified cytosines bearing covalently attached 3-(2,5-di(thiophen-2-yl)-1*H*-pyrrol-1yl)propan-1-amine(SNS) monomer represented with **X**.

Table 9 DNA sequences G1U, G1C, G1M3

G1UC	G1C **:** 5'-TGA GGT TCG CGA GAG AGT GTG CTA CGT A-3' G1U : 3'-ACT CCA AGC GCT CTC TCA CAC GAT GCA T-5'
G1M3C	G1C **:** 5'-TGA GGT TCG CGA GAG AGT GTG CTA CGT A-3' G1M3 : 3'-ACT CCA AGC G**X**T **X**T**X** TCA CAC GAT GCA T-5'

The presence of three SNS monomers in the major groove of the duplex G1M3C lowers the melting temperature by ~10°C when compared to the unmodified duplex G1UC (Table 10), the circular dichroism (CD) spectrum of both complexes are similar (Figure 45), showing the modified duplex maintains an overall B-Form structure.

Table 10 Melting Temperatures for G1UC and G1M3C-Three Modifications

DNA	**Modification**	**Tm/°C** **pH 7**	**Tm/°C** **pH 4.5**
G1UC	Unmodified	85	74
G1M3C	3***X** modified	76	64

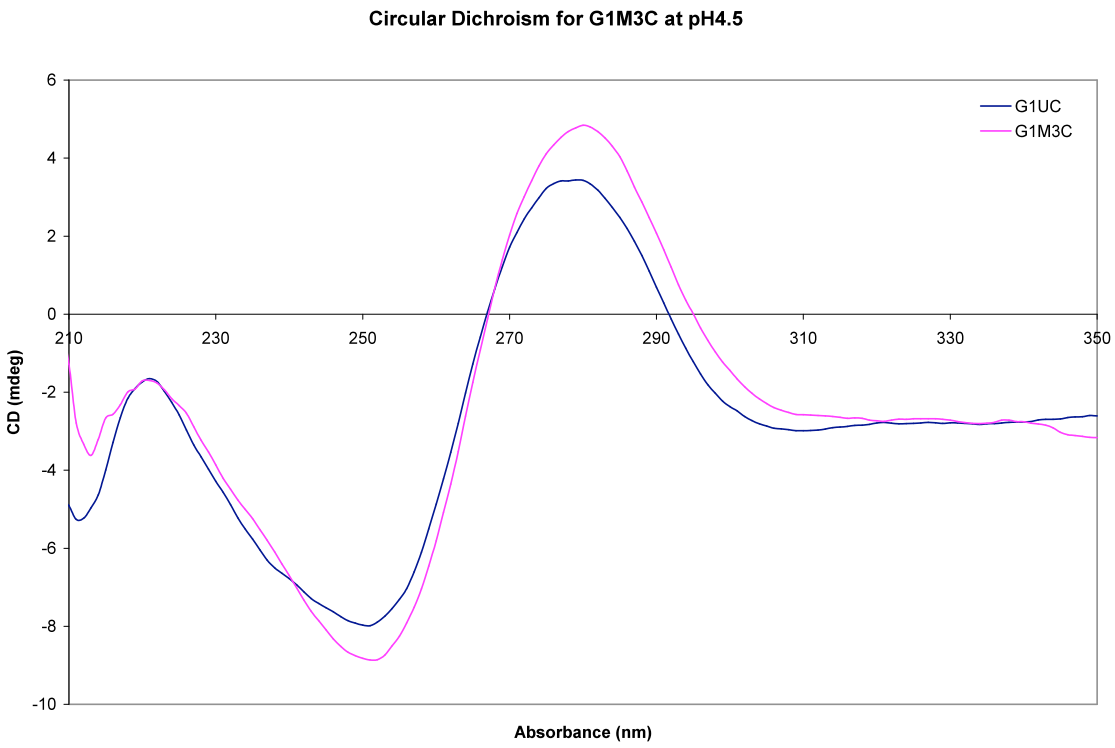

Figure 45 Circular Dichroism for G1M3C at pH4.5

The treatment of duplex G1M3C at pH 7 with HRP and H_2O_2 at room temperature showed no significant change in the absorption spectrum.(Figure 46)

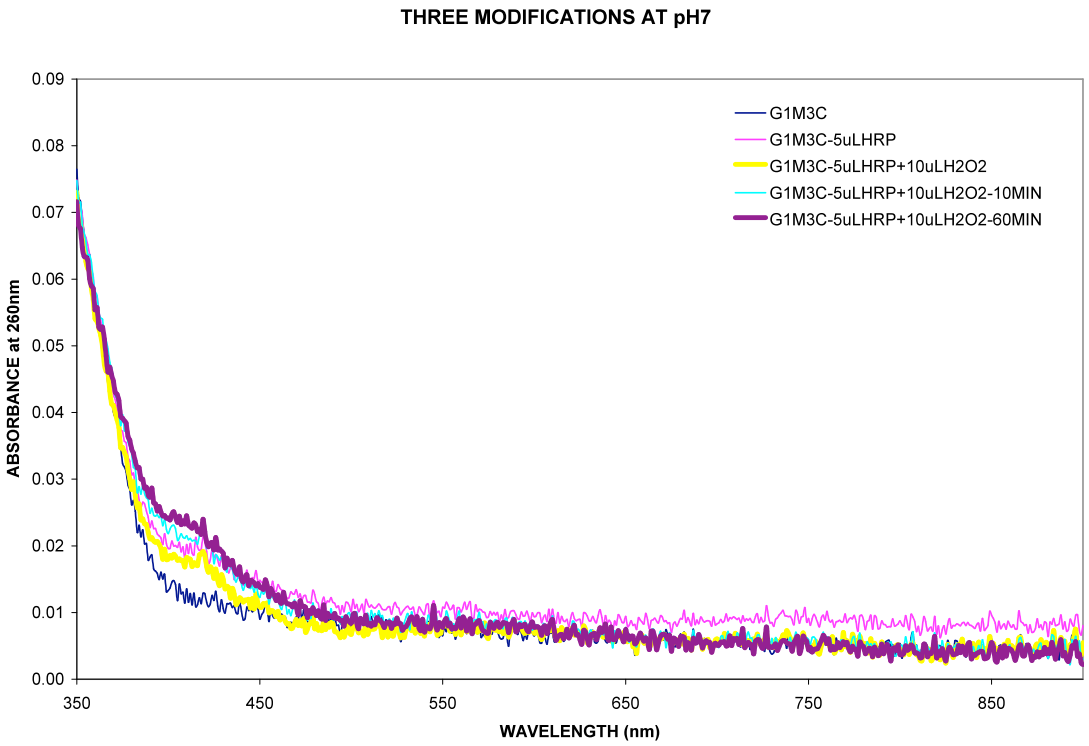

Figure 46 Absorption Spectrum of G1M3C-Single modification at pH7

At pH 4.5 the treatment of the duplex with HRP and H_2O_2 gave rise to a broadband peak at ~425 nm, a broad band peak between 500-700 nm, and increase in absorption tailing towards Near IR region. The monomer absorption band at 325 nm decreased as reaction proceeded (Figure 47)

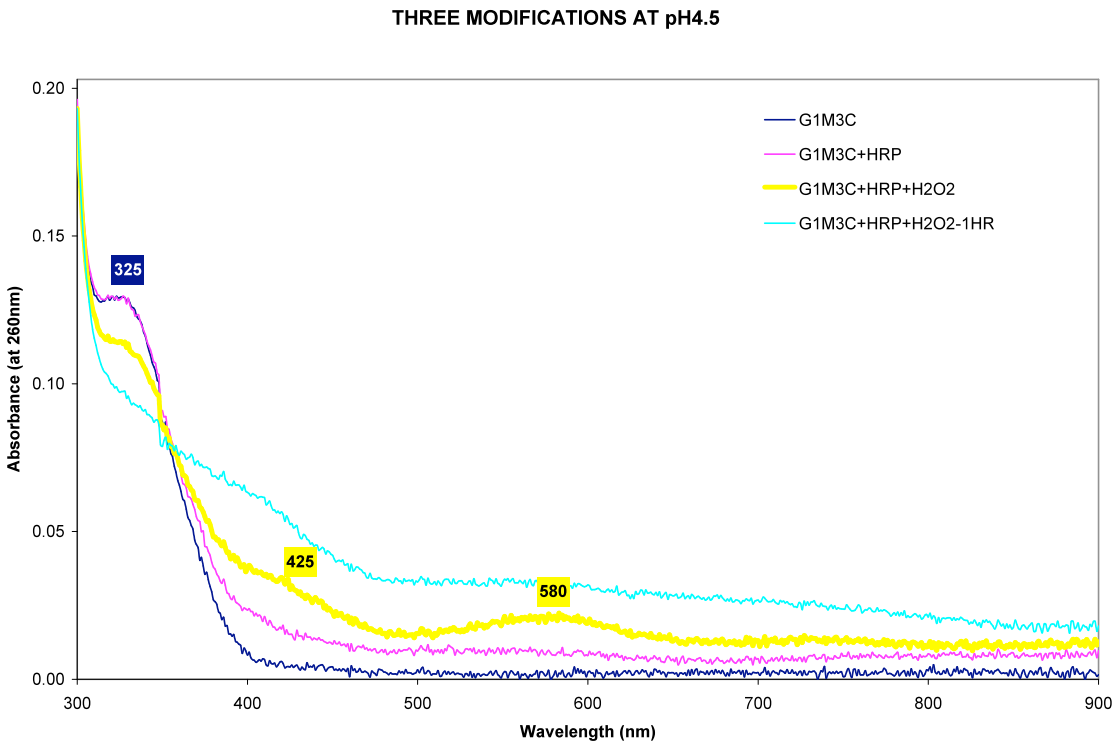

Figure 47 Absorption Spectrum of G1M3C-Single modification at pH4.5

As the number of monomers increase a red shift in the absorption peaks is expected.[151] When compared with the 2-modified G1M2C (Figure 44) we see the shift of the peak at ~465 nm to a broad band peak at ~580 nm. The peak at ~820 nm observed for G1M2C is absent in the case of G1M3C. The trimer formed would absorb in the near IR region. The experimental conditions for oligomerization with HRP does not permit us to observe the near IR region as water has high absorption in that area and it masks the absorption of the oligomers formed.

4.3.6 Four Modifications

DNA oligonucleotides G1U, G1C and G1MOD1 shown in Table 11 were synthesized. G1MOD1 contains four modified cytosines bearing covalently attached 3-(2,5-di(thiophen-2-yl)-1*H*-pyrrol-1yl)propan-1-amine(SNS) monomer represented with **X**.

Table 11 DNA sequences G1U, G1C, G1MOD1C

G1UC	G1C **:** 5'-TGA GGT TCG CGA GAG AGT GTG CTA CGT A-3' G1U : 3'-ACT CCA AGC GCT CTC TCA CAC GAT GCA T-5'
G1MOD1C	G1C **:** 5'-TGA GGT TCG CGA GAG AGT GTG CTA CGT A-3' G1MOD1 : 3'-ACT CCA AGC G**X**T **X**T**X** T**X**A CAC GAT GCA T-5'

The presence of a four SNS monomers in the major groove of the duplex G1MOD1C lowers the melting temperature by ~15°C when compared to the unmodified duplex G1UC (Table 12), the circular dichroism (CD) spectrum of both complexes are similar (Figure 48), showing the modified duplex maintains an overall B-Form structure.

Table 12 Melting Temperatures for G1UC and G1MOD1C- Four Modifications

DNA	**Modification**	**Tm/°C pH 7**	**Tm/°C pH 4.5**
G1UC	Unmodified	85	74
G1MOD1C	4***X** modified	73	59

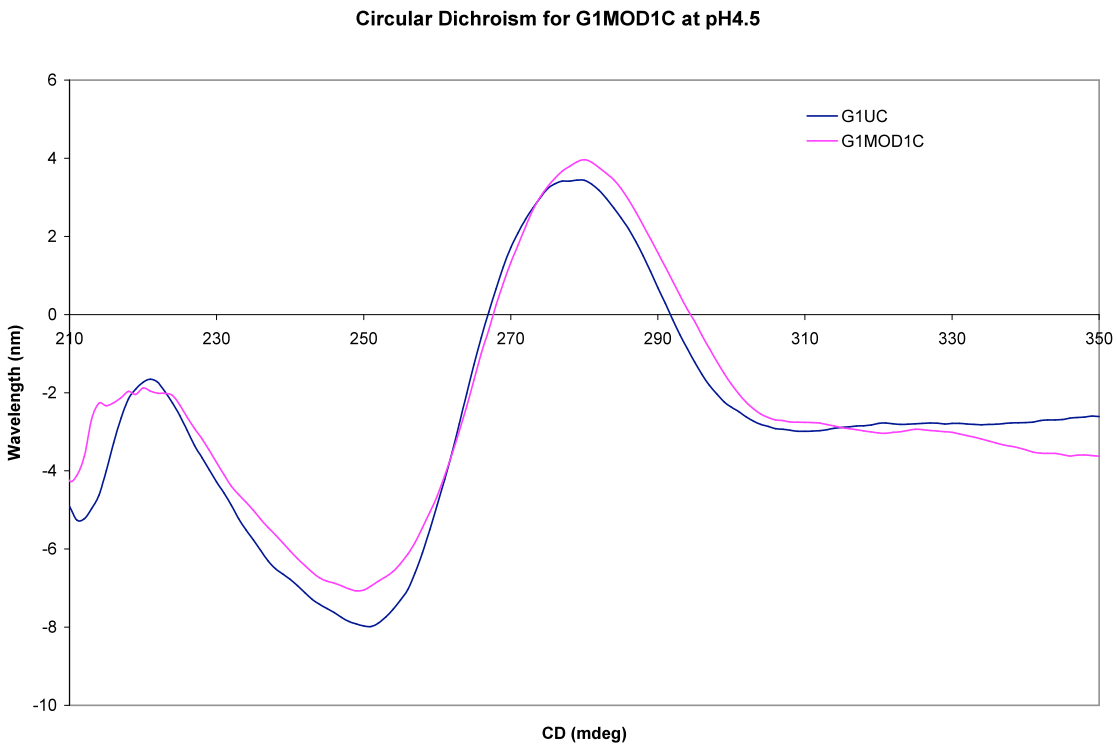

Figure 48 Circular Dichroism for G1MOD1C at pH4.5

The treatment of the duplex G1MOD1C at pH7 with HRP and H_2O_2 gave rise to a broad peak at ~421 nm, a broad band peak between 500-700 nm, and a very small increase in absorption tailing towards near IR region. The monomer absorption band at 325 nm decreased with the addition of H_2O_2 and stayed the same as reaction proceeded signifying once again that oligomerization at pH 7 is very inefficient(Figure 49).

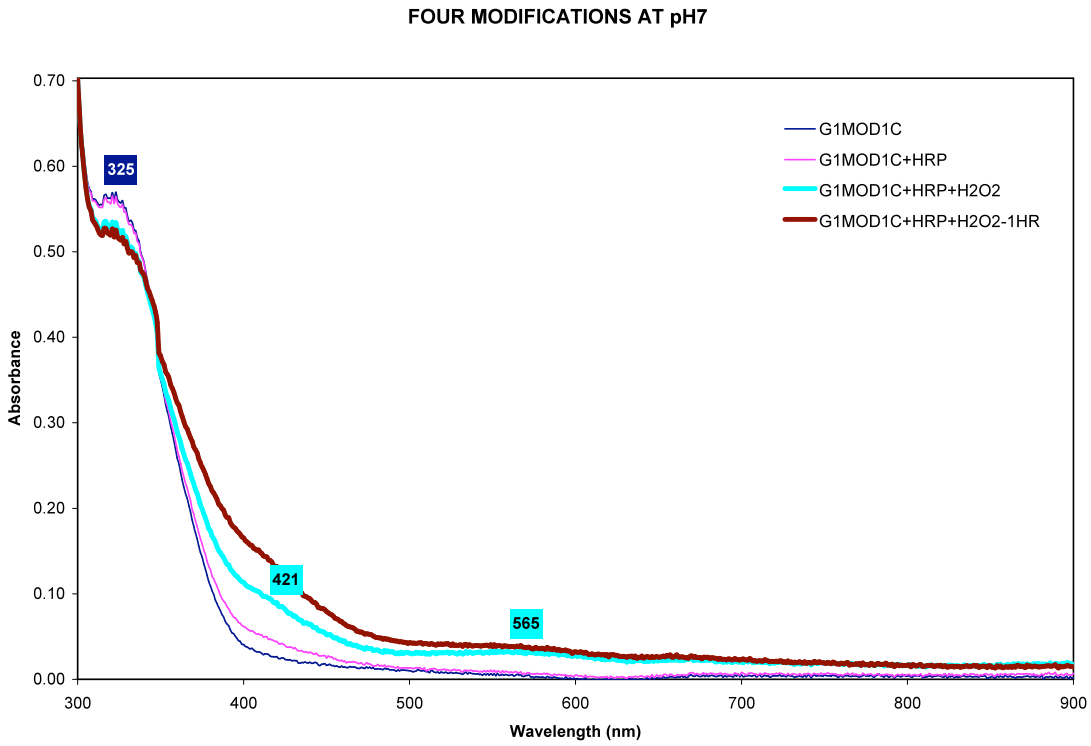

Figure 49 Absorption Spectrum of G1MOD1C-Four modifications at pH 7

At pH4.5 the treatment of the duplex with HRP and H_2O_2 gave rise to a broad peak at ~416 nm, a broad band peak between 500-700 nm, and another broadband absorption peak starting at ~810 nm and tailing towards the Near IR region. The broadband peak at ~810 nm disappeared within seconds but the absorption in that region stayed consistent over the course of 1 hour. The monomer absorption band at 325 nm decreased as reaction proceeded (Figure 50).

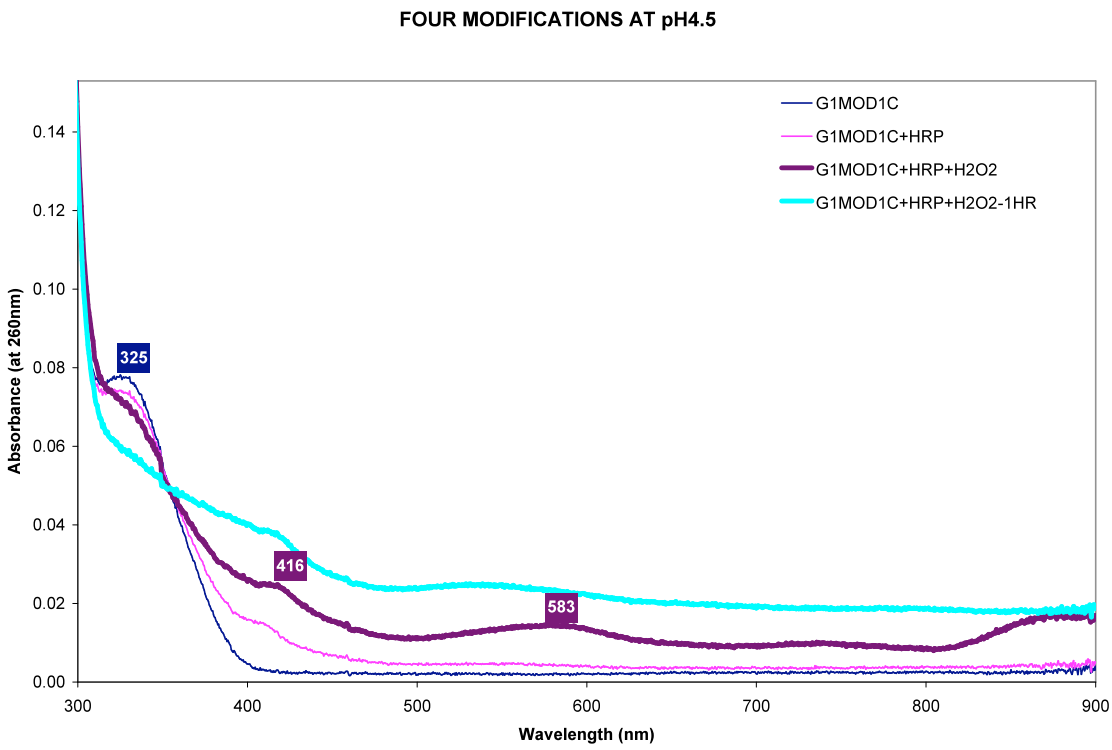

Figure 50 Absorption Spectrum of G1MOD1C-Four modifications at pH 4.5

When the single strand G1MOD1 in 500 mM NaCl and 10 mM citrate buffer at pH 4.5 was studied a similar absorption trend was observed. With the addition of HRP and H_2O_2 two broad band peaks formed at ~410 nm and between 500-700 nm. The absorption increase tailing towards the Near IR region and the decrease in the monomer peak absorption at 325 nm was seen as reaction proceeded (Figure 51).

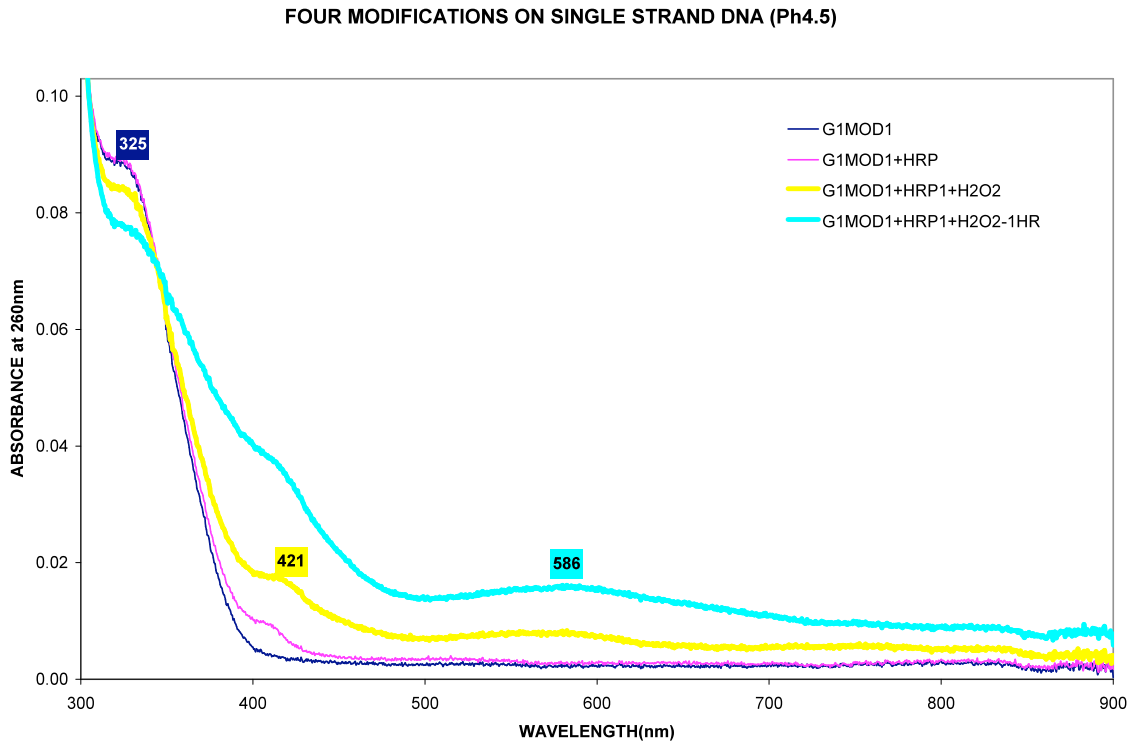

Figure 51 Absorption Spectrum of G1MOD1-Four modifications, single strand at pH4.5

Parallel research in our lab with Dr. Wen Chen showed similar absorption patterns when the number of monomers increased. The disappearance of the sharp peak at 820 nm signifies that oligomerization proceeds rapidly and forms trimers, tetramers and so on.

4.3.7 Ligation Experiments

Sequences G1M2S1 and G1M2S2 were designed to further investigate the oligomerization of DNA templated SNS. Both sequences contain two modified cytosines bearing covalently attached 3-(2,5-di(thiophen-2-yl)-1*H*-pyrrol-1yl)propan-1-amine(SNS) monomer represented with **X** in Table 13.

Table 13 Sequences used in ligation experiments

G1M2S1 : 5' - TAC GTA GCA CA**X** T**X**T - 3'
G1M2S2 : 5' - **X**T**X** GCG AAC CTC A - 3'
G1MOD1 : 5' - TAC GTA GCA CA**X** T**X**T **X**T**X** GCG AAC CTC A - 3'
G1MSC : 5' - TAC GTA GCA CA**X** T**X**T - 3' 5' - **X**T**X** GCG AAC CTC A - 3' 3'- ATG CAT CGT GTG AGA GAG CGC TTG GAG T -5'

The sequences are merely the 4 modified sequence G1MOD1 split in half. The two separate pieces of DNA are brought together in the presence of G1C templating strand that has adjacent sequences complementary to G1M2S1 and G1M2S2. The combination of these three oligomers forms a ternary complex that organizes the SNS monomers so that the two on G1M2S1 and the two on G1M2S2 are adjacent to each other. The experiment was designed to show that when oligomerized the SNS monomers would form bonds with each other and make up a single strand with 4 modifications. (Figure 52)

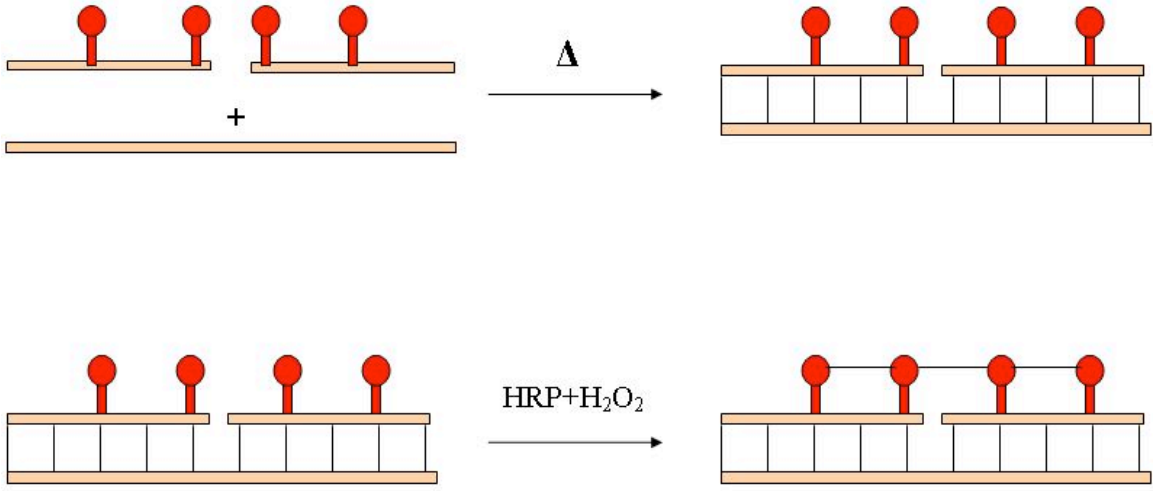

Figure 52 Schematic illustration of ligation experiment

The G1M2S21, G1M2S2 and the complementary strand G1C were hybridized in the presence of 500mM NaCl and 10mM citrate buffer at pH 4.5 forming G1MSC duplex.

The melting temperature of the duplex decreased by another 10°C when compared with the 4 modified G1MOD1C duplex but the CD spectrum showed that the modified G1MSC duplex maintained an overall B-Form structure. See Table 14, Figure 53.

Table 14 Melting Temperatures for unmodified, 4-modified duplexes

DNA	**Modification**	**Tm/°C pH 7**	**Tm/°C pH 4.5**
G1UC	Unmodified	85	74
G1MOD1C	4***X*** modified	73	59
G1MSC	4***X*** modified	N/A	49

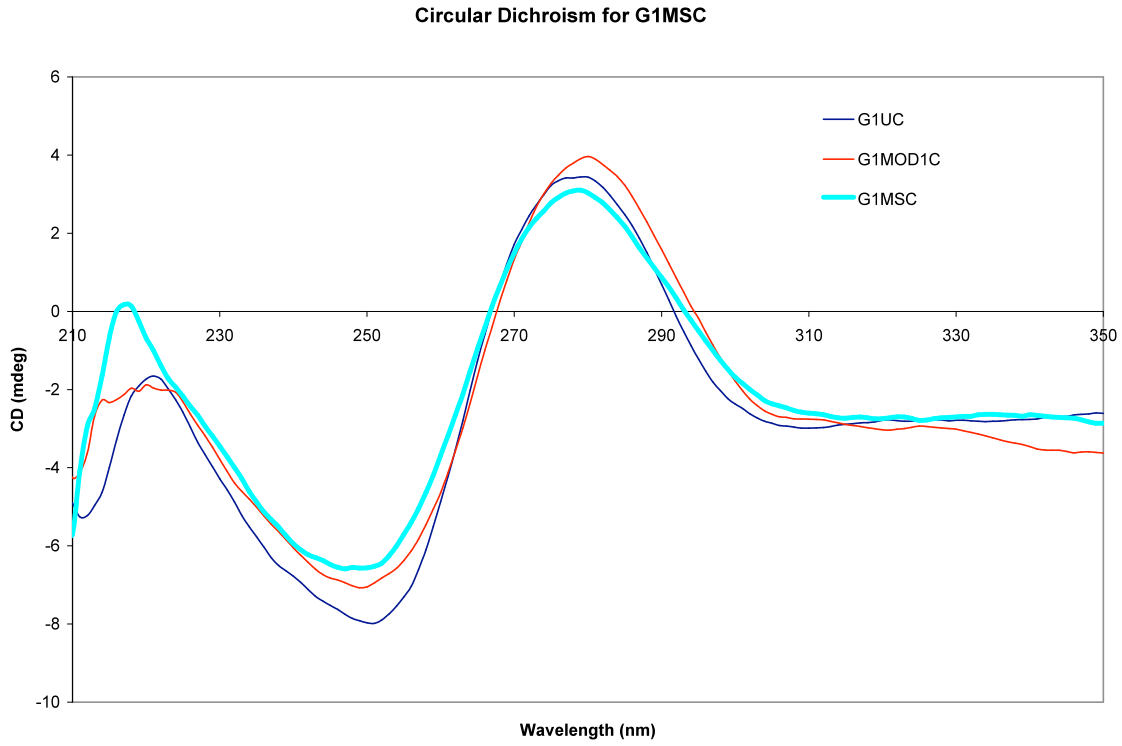

Figure 53 Circular Dichroism for G1MOD1C and G1MSC at pH 4.5

To the solution of single strands G1M2S1(5 uM) and G1M2S2 (5 uM) in 500 mM NaCl and 10 mM citrate buffer we've added HRP, followed by the addition of H_2O_2. The appearance of a peak ~410 nm, a broadband peak between 500-700 nm and an increase in absorption tailing towards the Near-IR region was observed (Figure 54). Same absorption trend was observed for the ligated double strand G1MSC (Figure 55) and the single strand G1M2S1 (Figure 56).

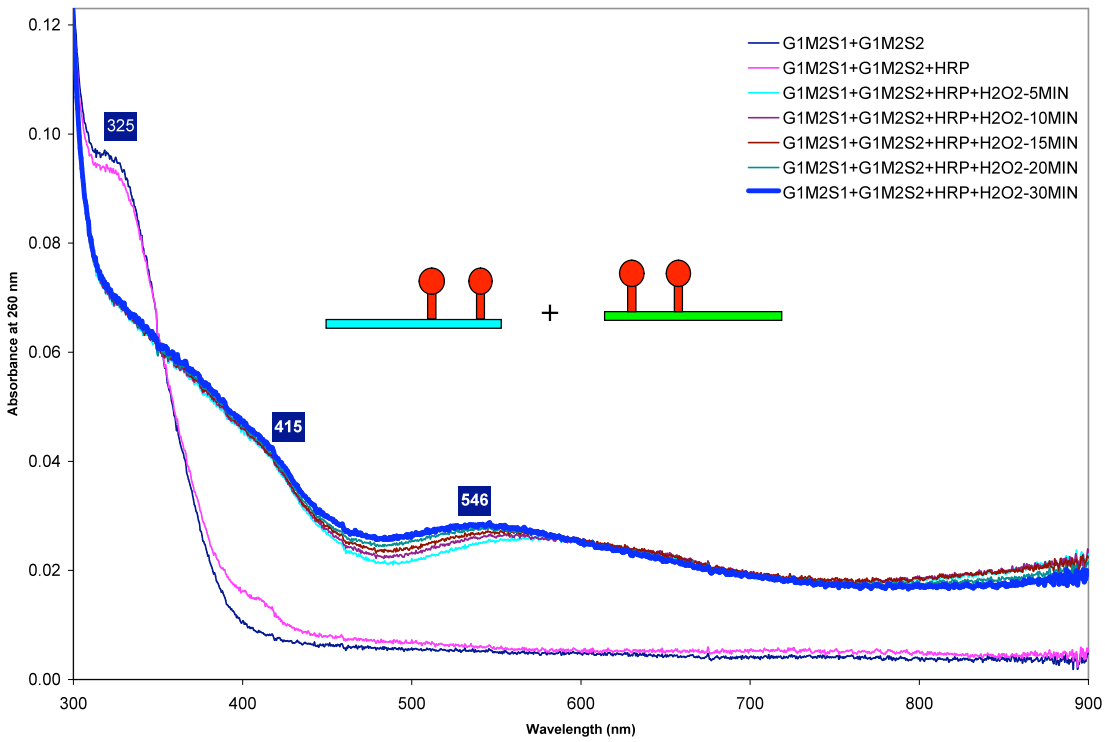

Figure 54 Absorption Spectrum for G1M2S1, G1M2S2 mixture.

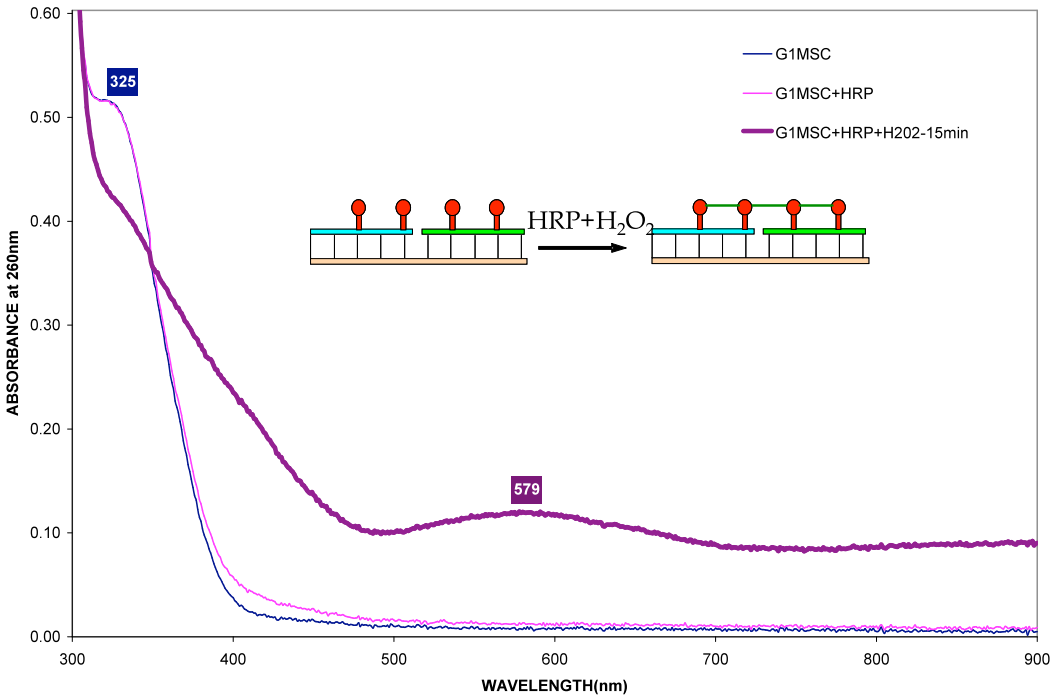

Figure 55 Absorption Spectrum for G1MSC - 4SNS modifications

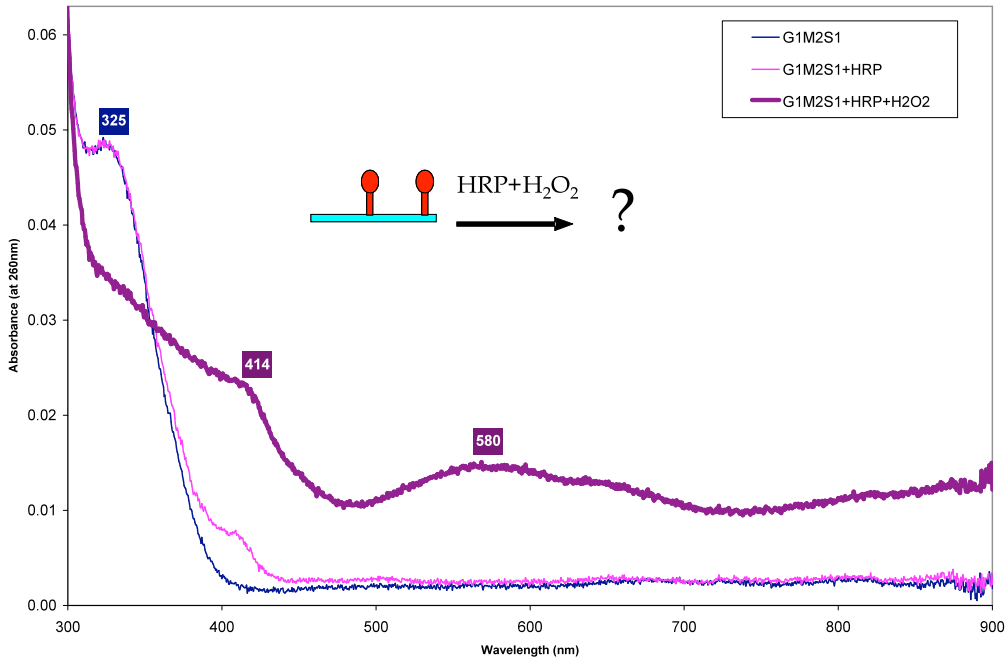

Figure 56 Absorption Spectrum for G1M2S1-single strand-2 SNS modifications

The short single strand sequence G1M2S1 hybridized with the longer complementary strand G1C was studied to assess the role of the template strand. Same conditions of 500 mM NaCl and 10 mM citrate buffer at pH 4.5 were maintained.

With the addition of HRP and H_2O_2 a peak at ~414 nm, a broadband peak between 500-700 nm and a sharp peak at ~830 nm characteristic of the dimer was observed (Figure 57).

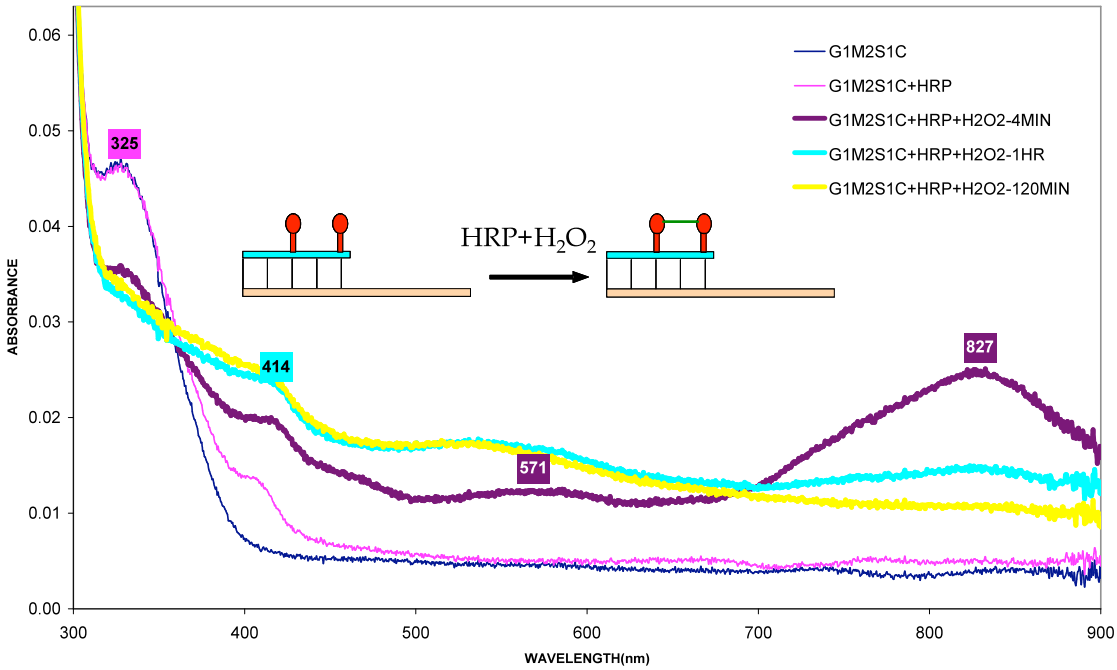

Figure 57 Absorption Spectrum of G1M2S1C

As we mentioned earlier with 3 or more modifications we observe absorption peaks at ~420 nm, a broadband absorption peak between 500-700 nm and an increase in absorption tailing towards the Near IR region. Without the presence of the template strand interstrand and intrastrand oligomerization takes place rapidly and we do not observe the dimer peak at ~820 nm. When the template strand is present the formation of dimer is apparent.

4.3.8 Proof of ligation: Autoradiography

PAGE analysis of the oligomerized sequences gave further proof for the formation of oligomers.

We labeled the short single strand G1M2S1 and the long single strand G1MOD1. Lanes 1 and 2 in Figure 58 show that when single strand G1M2S1 is treated with HRP/H_2O_2 it forms tetramer, pentamer, hexamer and higher order oligomers. For lanes 3 and 4 we see that when G1M2S1 is hybridized with its complementary strand G1C formation of higher order oligomers is limited. The template controls the interstrand oligomerization.

The ligated sample clearly shows the formation of the ligated oligomer as well as a second band corresponding to interstrand oligomerization, lanes 5 and 6, Figure 58. The DNA strands used for oligomerization, G1M2S1 and G1M2S2 have 15 base pairs and 13 base pairs. When ligation takes place we get a strand with 28 base pairs but when interstrand oligomerization takes place a strand with 30 base pairs and another strand with 26 base pairs forms. Since only G1M2S1 is labeled we see the formation of 2 bands corresponding to 28 and 30 base pairs.

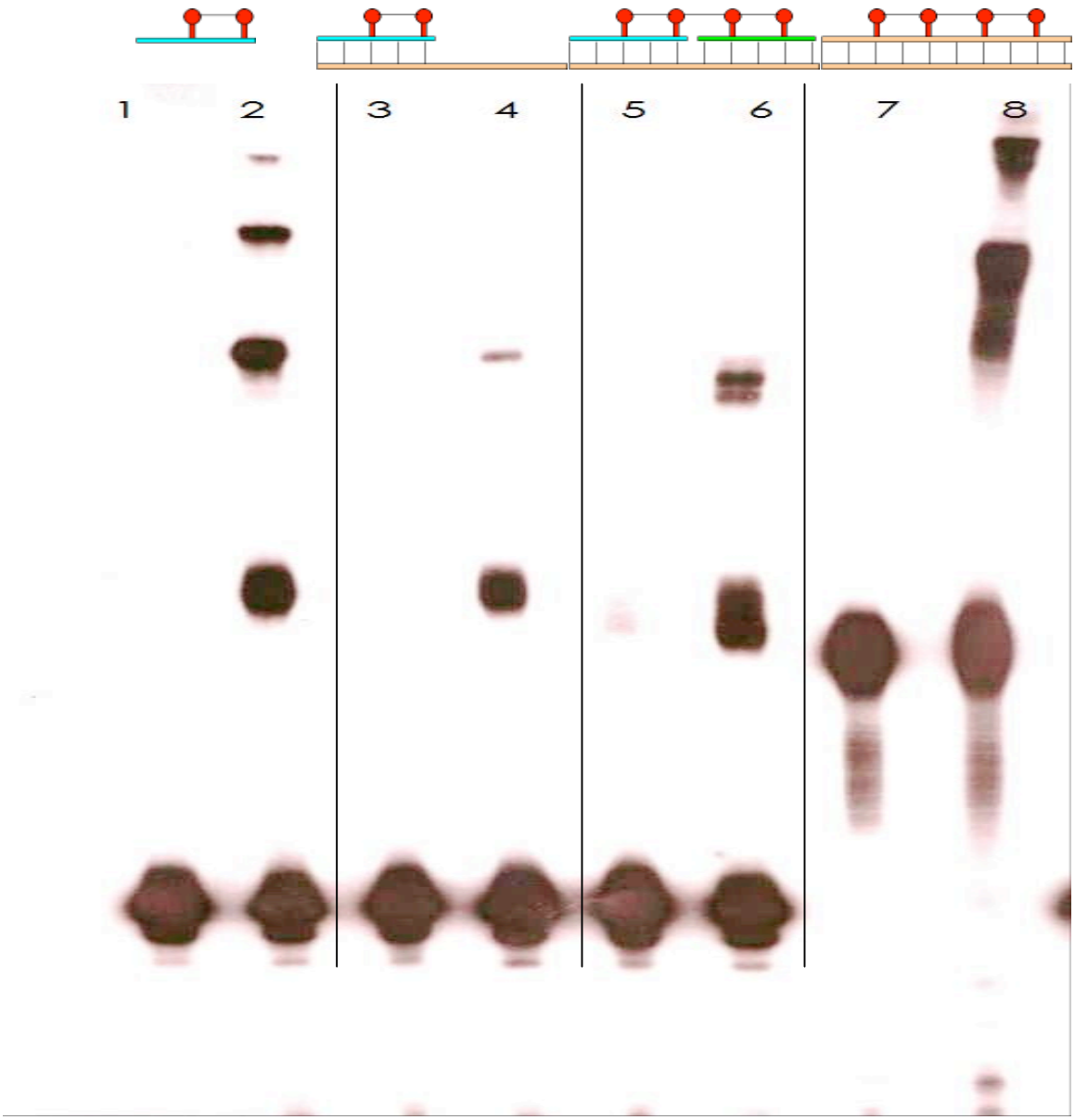

Figure 58 PAGE analysis. Lanes 1,3,5,7 control, Lane 2: G1M2S1P, lane 4:G1M2S1CP, lane 6:G1MSCP and lane 8 :G1MOD1CP where P represents polymerized

G1MOD1C, when oligomerized forms a tetramer that differs from the control by 3 bonds between the monomers. With the 20% 19:1

acrylamide:bis-acrylamide PAGE we couldn't observe the difference between the oligomerized and control samples, Figure 58, lanes 7,8.

Figure 59 shows the PAGE analysis with 20% 29:1 acrylamide:bis-acrylamide gel. The oligomerized sample runs slower than the control signifying the formation of the tetramer.

Figure 59 PAGE analysis. Lane 1: G1MOD1C Lane 2: G1MOD1CP. 20% 29:1 Acrylamide/Polyacrylamide gel.

4.4 Conclusion

Design of DNA-conjoined oligomers offers a convenient way to assemble homo and hetero building blocks into programmable assemblies with a better control on oligomerization process and yield highly ordered and well-defined hybrid materials. We have designed and synthesized a thiophene-pyrrole-thiophene monomer (SNS) and successfully incorporated it in various oligonucleotide sequences by solid phase DNA synthesis. The bridge length (two or three carbon linker) and base position of modifications (alternate base modification) were optimized by molecular mechanics calculations. The introduction of one to four monomeric units in a DNA strand slightly decreased the stability of duplex in a sequential manner. DNA melting and CD studies showed that all these modified oligonucleotides form stable B-form duplexes at room temperature and under the pH conditions we used in this study (pH 7 and 4.5). Enzymatic oligomerizations were tried at pH 7 and pH 4.5 using HRP/H_2O_2 as the oxidant and we observed a better reactivity at pH 4.5, whereas the reactions at pH 7 were marginal.

In order to understand the oligomerization process, we have studied the reactions in different systems starting from SNS monomer alone to oligonucleotides having one, two, three, four and more monomer modifications and established the oligomerization pattern in these systems. For example, SNS monomer in aqueous solutions forms random

polymers which show characteristic absorption spectra of polythiophene-pyrrole-thiophenes(polySNS). On the other hand, singly modified oligonucleotide duplex doesn't form any oligomeric product and shows absorption characteristics of the oxidized monomer. DNA duplexes modified with two monomer units, after oligomerization reaction, show characteristic absorption properties of SNS dimer which establishes the coupling of two monomers under the reaction conditions. Oligonucleotides modified with three or more monomeric units show absorption characteristic to SNS polymer and the position of the absorption bands show slight red shifts when going from three to many modifications. Further we have established the bond formation in these DNA-conjoined monomers by designing a ligation experiment where two oligonucleotides bearing two modifications each were successfully ligated on a template DNA strand. Further evidence of the controlled oligomer formation in modified duplexes come from PAGE experiments where we observed less cross-linking products in modified duplexes compared to modified single strands in solution. Further optimization of the oligomerization efficiency and characterization of the oligomer product are in progress in our laboratory. Also attempts are in progress to make continuous SNS polymers on DNA templates to study the conductivity properties.

REFERENCES

[1] Lodish, B.; Zipursky, M.; Baltimore, D. *Molecular Cell Biology* **1999**, Von Hoffman Press

[2] Avery, O. ; MacLeod, C. ; McCarty, M., *J Exp Med*. **1944**, 79 (2), 137

[3] Franklin, R. ; Gosling, R. *Nature* **1953**, 171, 740

[4] Watson, J. D.; Crick, F. H. C. *Nature* **1953**, 171, 737

[5] Eley, D.D.; Spivet, D.I. *Trans. Faraday Soc.* **1962**, 58, 411

[6] Smart, R. S. *Trans. Faraday Soc.* **1963**, 59, 754

[7] Ames, B. N.; Lee, F. D.; Durston, W. E. *Proc. Natl. Acad. Sci. U.S.A.* **1973**, 70, 782

[8] Demple, B.; Harrison, L. *Annu. Rev. Biochem.* **1994**, 63, 915

[9] Friedman, K. A.; Heller, A. *J. Phys. Chem. B* **2001**, 105, 11859

[10] Norbury, C.J.; Zhivotovsky, B. *Oncogene* **2004**, 23, 2797

[11] Boiteux, S.; Gellon, L.; Guibourt, N. *Free Radic. Biol. Med.* **2002**, 32, 1244

[12] Ventra, M. Di; Zwolak, M., DNA Electronics. In *Encyclopedia of Nanoscience and Nanotechnology*, Nalwa, H. S., Ed. American Scientific Publishers: **2004**; Vol. 2, pp 475

[13] Storm, A.J.; van Noort J. ; de Vries, S.; Dekker, C. *Appl. Phys. Lett* **2001**, 79, 3881

[14] Nogues, C.; Cohen, S.R.; Daube, S.; Apter, N. ; Naaman, R. *J. Phys. Chem. B* **2006**, 110, 8910

[15] Voet, D.; Voet, J.G., *Biochemistry*, 2nd Ed., John Wiley & Sons, Inc., **1995**

[16] Sinden, R. R., *DNA Structure and Function*, Academic Press, **1994**

[17] Campbell, M. K., *Biochemistry*, 2nd Ed., Saunders College Publishers, **1995**

[18] Sarma, M. H.; Sarma, R. H., *DNA Double Helix and The Chemistry of Cancer*, Academic Press, **1988**

[19] Holum, J.R., *Organic and Biologial Chemistry*, John Wiley & Sons Inc., **1996**

[20] Stewart, R.F.; Jensen, L. H., *J. Chem. Phys*. **1964**, 40, 2071

[21] Drew, H. R.; Dickerson, R. E. *Journal of Molecular Biology* **1981**, 151, 535

[22] Dickerson, R. E.; Drew, H. R.; Conner, B. N.; Wing, R. M.; Fratini, A. V.; Kopka, M. L. *Science* **1982**, 216, (4545),475

[23] Champ, P.C.; Maurice, S.; Vargason, J.M.; Camp, T.; Ho, P.S. *Nucleic Acids Res.* **2004**, 32, 6501

[24] Rich, A.; Zhang, S. *Nature Rev. Genet.* **2003**, 4, 566

[25] Eley, D. D. *Research* **1959**, 12, 293

[26] Eley, D. D.; Spivey, D. I. *Transactions of the Faraday Society* **1962**, 58, 411

[27] Burrows, C.J.; Muller, J.G. *Chem. Rev.* **1998**, 98, 1109

[28] Conwell, E. *Top. Curr. Chem.* **2004**, 237, 73

[29] Pogozelski, W. K.; Tullius, T. D. *Chem. Rev.* **1998**, 98, 1089

[30] Armitage, B. *Chem. Rev.* **1998**, 98, (3), 1171

[31] Dizdaroglu, M.; Von S. C.; Schulte F. D. *J. Am. Chem. Soc.* **1995**, 97, 2277

[32] Sancar, A. *Annual Review of Biochemistry* **1996**, 65, (1), 43

[33] Kow, Y. W. *Annals of the New York Academy of Sciences* **1994**, 726, 178

[34] Kanvah, S.; Schuster, G. B. *J. Am. Chem. Soc.* **2004**, 126, 7341

[35] Demple, B.; Harrison, L. *Annu. Rev. of Biochem.* **1994**, 63, 915

[36] Poulsen, H. E.; Prieme, H. Loft, S. *Eur. J. Cancer Prev.* **1998**, 7, (1), 9

[37] Hasty, P.; Vijg, J. *Science* **2002**, 296, 1250

[38] Armitage, B.; Yu, C.; Devadoss, C.; Schuster, G. B. *J. Am. Chem. Soc.* **1994**, 116, (22), 9847

[39] Macgregor, R. B. *Analytical Biochemistry* **1992**, 204, (2), 324

[40] Breslin, D. T.; Schuster, G. B. *J. Am. Chem. Soc.* **1996**, 118, (10), 2311

[41] Turro, N. J. *Modern Molecular Photochemistry* **1978**, Benjamin-Cummings Publication Co., Inc., California.

[42] Chow, C. S.; Barton, J. K. *Methods Enzymol.* **1992**, 212, 219

[43] Pratviel, G.; Pitie, M.; Bernadou, J.; Meunier, B. *Angew. Chem. Int. Ed. Engl.***1991**, 30, 702

[44] Burger, R. M. *Chem. Rev.* **1998**, 98, 1153

[45] Kochevar, I.; Dunn, D. A. *Biorg. Photochem.* **1990**, 1, 273

[46] Lee, C. C.; Rodgers, M. A. *Photochem. Photobiol.* **1987**, 45, 79

[47] Mei, H.; Barton, J. K. *Proc. Natl. Acad. Sci. U.S.A.* **1988**, 85, 1339

[48] Croke, D. T.; Perrouault, L.; Sari, M. A.; Battioni, J. P.; Mansuy, D.; Helene, C. ; Le Doan, T. *J. Photochem. Photobiol.B* **1993**, 18, 41

[49] Hiort, C.; Goodisman, J.; Dabriowiak, J. C. *Biochemistry* **1996**, 35, 12354

[50] Ito, K.; Inoue, S.; Yamamoto, K.; Kawanishi, S. *J. Biol. Chem.* **1993**, 268, 13221

[51] Nunez, M.; Barton, J.K. *Curr. Opin. Chem. Biol.* **2000**, 4, 199

[52] Fhalman, R.P.; Sharma, R.D; Sen, D. *J. Am. Chem. Soc.* **2002**, 124, 12477

[53] Olson, E.J.C. ; Hu, D.; Horman, A.; Barbara, P.F. *J. Phys. Chem. B* **1997**, 101, 299

[54] Santhosh, U. ; Schuster, G.B. *J. Am. Chem. Soc.,* **2002**, 124, 10986

[55] Williams, T.T.; Dohno, C. ; Stemp, E.D.; Barton, J.K. *J. Am. Chem. Soc.* **2004**, 126, 8148

[56] Krebs, F. C.; Laursen, B. W.; Johannsen, I.; Faldt, A.; Bechgaard, K.; Jacobsen, C. S.; Thorup, N.; Boubekeur, K. *Acta Crystallographica Section B* **1999**, 55, (3), 410

[57] Reynisson, J. ; Schuster, G.B.; Howerton, S.B.; Williams, L.D.; Barnett, R.N.; Cleveland, C.L.; Landman, U.; Harrit, N.; Chaires, J.B. *J. Am. Chem. Soc.* **2003**, 125, 2072

[58] Lewis, F. D.; Letsinger, R. L.; Wasielewski, M. R. *Acc. Chem. Res.* **2001**, 34, (2), 159

[59] Giese, B.; Dussy, A.; Meggers, E.; Petretta, M.; Schwitter, U. *J. Am. Chem. Soc.* **1997**, 119, 11130

[60] Moore, J. N.; Phillips, D.; Nakashima, N.; Yoshihara, K. *J. Chem. Soc., FaradayTrans. 2* **1987**, 83, 1487

[61] Gasper, S. M.; Schuster, G. B. *J. Am. Chem. Soc.* **1997**, 119, 12762.

[62] Schuster, G.B. ; Landman, U. *Top Curr Chem* **2004,** 236, 139

[63] Murphy, C. J.; Arkin, M. R.; Jenkins, Y.; Ghatlia, N. D.; Bossmann, S. H.; Turro, N. J.; Barton, J. K. *Science* **1993**, 262, 1025

[64] Kelley, S. O.; Holmlin, E. R.; Stemp, E. D. A.; Barton, J. K. *J. Am. Chem. Soc.* **1997**, 119, 9861

[65] Hall, D. B.; Barton, J. K. *J. Am. Chem. Soc.* **1997**, *119*, 5045

.

[66] Kelley, S. O.; Holmlin, R. E.; Stemp, E. D. A.; Barton, J. K. *J. Am. Chem. Soc.* **1997**, *119*, 9861

[67] Wan, C.; Fiebig, T.; Schiemann, O.; Barton, J. K.; Zewail, A. H. *Proc. Natl. Acac. Sci. U.S.A.* **2000**, *97*, 14052

[68] Giese, B. *Acc. Chem. Res.* **2000**, *33*, 631

[69] Turro, N. J.; Barton, J. K. *J. Biol. Inorg. Chem.* **1998**, 3, 201

[70] Adams, D.M. ; Brus, L.; Chidsey, C. E. D. ; Creager, S.; Creutz, C.; Kagan, C. R; Kamat, P. V.; Lieberman, M. ; Lindsay, S. ; Marcus, R. A. ; Metzger, R. M.; Michel-Beyerle, M. E.; Miller, J. R. ; Newton, M. D. ; Rolison, D. R. ; Sankey, O. ; Schanze, K. S.; Yardley J. ; Zhu, X. *J. Phys. Chem. B* **2003**, 107, 6668

[71] Weiss, E. A. ; Ahrens, M. J.; Sinks, L. E.; Gusev, A. V. ; Ratner M. A.; Wasielewski, M. R. *J. Am. Chem. Soc.* **2004**, 126, 5577

[72] Endres, R. G. ; Cox, D. L.; Singh, R. R. P. *Rev. Mod. Phys.* **2004**, 76, 195

[73] Filoramo, A. ; Dekker, C.; Sivan, U.; Schonenberger, C.; Michel-Beyerle, M. E.; *Phantoms Newsl.* **2003**, 4

[74] Schuster ,G. B., *Long-Range Charge Transfer in DNA I*, Springer, Heidelberg, **2004**

[75] Schuster, G. B. *Long-Range Charge Transfer in DNA II*, Springer, Heidelberg, **2004**

[76] Jortner, J. ; Bixon, M. ; Voityuk, A. A.; Rosch, N. *J. Phys. Chem. A* **2002**, 106, 7599

[77] Lewis, F. D. ; Liu, J.; Zuo, X.; Hayes, R. T. ; Wasielewski, M. R. *J. Am. Chem. Soc.* **2003**, 125, 4850

[78] Henderson, P. T. ; Jones, D. ; Hampikian, G.; Kan, Y.; Schuster, G. B. *Proc. Natl. Acad. Sci. USA*, **1999**,96, 8353

[79] Barnett, R. N. ; Cleveland, C. L. ; Joy, A.; Landman, U. ; Schuster, G. B. *Science* **2001**, *294, 567*

[80] O'Neill, M. A. ; Becker, H.-C.; Wan, C. ; Barton, J. K. ; Zewail, A. H. *Angew. Chem., Int. Ed.* **2003**, 42,5896

[81] Voityuk, A. ; Siriwong, K. ; Rosch, N. *Angew. Chem., Int. Ed.* **2004**, 43, 624

[82] Liu, C.-S. ; Schuster, G. B. *J. Am. Chem. Soc.* **2003**, 125, 6098

[83] Liu, C.-S. ; Hernandez, R.; Schuster, G. B. *J. Am. Chem. Soc.* **2004**, 126, *2877*

[84] O'Neill, M. A. ; Barton, J. K. *J. Am. Chem. Soc.* **2004**, 126, 11471

[85] Schuster, G. B. *Acc. Chem. Res.* **2000**, 33, 253

[86] Steenken, S. ; Jovanovic, S. V. *J. Am. Chem. Soc.***1997**, 119, 617

[87] Seidel, C. A. M.; Schulz, A. ; Sauer, M. H. M. *J. Phys. Chem.* **1996**, 100, 5541

[88] Lan, T.; McLaughlin, L. W. *Bioorg. Chem.* **2001**, 29, 198

[89] Moran, S. ; Ren, R.; Rumney, R.-F. I.; Kool, E. T. *J. Am. Chem. Soc.* **1997**, 19, 2056

[90] Schweitzer, B.: Kool, E. *J. Org. Chem.* **1994**, 59, 7238

[91] Bhat, C.C. *Synthetic Procedures in Nucleic Acid Chemistry*, New York interscience, **1968**, 521

[92]Xiao-Feng, R. ; Schweitzer, B. ; Sheils, C. ; Kool, E. *Angew Chemie. Int. Ed. Engl.* **1996,** 35, 743

[93] Schweitzer, B.; Kool, E. *J. Am. Chem. Soc.* **1995**, 117, 1863

[94] Roginskaya, M.; Bernhard, W. A. ; Razkazovskiy, Y. *J. Phys. Chem. B* **2004**, 108, 2432

[95] Gray, D. M. ; Hung, S.-H. ; Johnson, K. H. *Methods Enzymol.* **1995**, 246, 19

[96] Lan, T. ; McLaughlin, L. W. *J. Am. Chem. Soc.* **2000**, 122, 6512

[97] Woods, K. K. ; Lan, T. ; McLaughlin, L. W.; Williams, L. D. *Nucleic Acids Res.* **2003**, 31, 1536

[98] Guckian, K. M. ; Krugh, T. R. ; Kool, E. T. *Nat. Struct. Biol.* **1998**, 5, 954

[99] Steenken, S. *Chem. Rev.* **1989**, 89, 503

[100] Sheu, C. ; Foote, C. S. *J. Org. Chem.* **1995**, 60, 4498

[101] Barnett, R. N. ; Cleveland, C. L. ; Landman, U. ; Boone, E. ; Kanvah, S. ; Schuster, G. B. *J. Phys. Chem. B* **2003**, 107, 3525

[102] Li, E. ; Shi, G. ; Hong, X. ; Wu, P. *J. Appl. Polymer Sci.* **2004**, 93, 189

[103] Michl, J. ; Bonacic-Koutecky, V. *Electronic Aspects of Organic Photochemistry*, John Wiley & Sons, New York, **1990**

[104] Dohno, C. ; Stemp, E. D. A.; Barton, J. K. *J. Am. Chem. Soc.* **2003**, 125, 9586.

[105] Sanii, L. ; Schuster, G. B. *J. Am. Chem. Soc.* **2000**, 122, 11545

[106] Misiaszek, M. ; Crean, C. ; Joffe, A. ; Geacintov, N. E. ; Shafirovich, V. *J. Biol. Chem.* **2004**, 279, 32106

[107] Takada, T. ; Kawai, K. ; Fujiska, M. ; Majima, T. *Proc. Natl. Acad. Sci. USA* **2004**, 101, 14002

[108] Voityuk, A. A. ; Jortner, J. ; Bixon, M. ; Rösch, N. *Chem. Phys. Lett.* **2000**, 324, 430

[109] Senthilkumar, K. ; Grozema, F. C. ; Guerra Fensca, C. ; Bickelhaupt, F. M.; Siebbeles, L. D. A. *J. Am.Chem. Soc.* **2003**, 125, 13658

[110] Voityuk, A. A. ; Rösch, N. *J. Phys. Chem. B* **2002**, 106, 3013

[111] Giese, B. ; Spichty, M. ; Wessely, S. *Pure Appl. Chem.* **2001**, 73, 449

[112] Chen, J.; Seeman, N.C. *Nature*, **1991**, 350, 631

[113] Czlapinski, J.L.; Sheppard, T.L. *J. Am. Chem. Soc.* **2001**, 123, 8618

[114] Garner, Z.J.; Liu, D.R. *J Am. Chem. Soc.* **2001**, 123, 6961

[115] Li, X ; Liu, D.R. *Angew. Chem. Int. Ed.* **2004**, 43, 4848

[116] Seeman, N.C.; Wang, H. ; Yang, X; Liu, F; Mao, C; Sun, W ; Wenzler, L; Shen, Z; Sha, R. Yanm H; et al. *Nanotechnology* **1998**, 9, 257

[117] Mirkin, C.A. ; Letsinger, R.L.; Mucic, R.C.; Storhoff, J.J. *Nature* **1996**, 382, 607

[118] Seeman, N.C. *Nature (London)* ***2003***, 421, 427

[119] Simmel, F.C.; Dittmer, W. U. *Small* **2005**, 1, 284

[120] Yurke, B.; Turberfield, A.J.; Mills, A.P. Jr.; Simmel, F.C., Neumann, J.L. *Nature* **2000**; 406, 605

[121] Ding, B.; Seeman, N. C. *Science* **2006**, 314, 1583

[122] Braun, E. ; Eichen, Y.Sivan, U.Yoseph, G.B., *Nature* **391**, 775

[123] Richter,J; Seidel, R.; Kirsch, R. ; Mertig, M. Pompe, W.; Plaschke, J. ; Schackert, H.K. *Adv. Mat.* **2000**, 12, 507

[124] Menon, R. ; Yoon, C.O. ; Moses, D.; Heegar,A.J. *Handbook of Conducting Polymers*, 2nd ed. ; Skotheim, T.A., Elsenbaumer, R.L., Reynolds, J.R., Eds.; Marcel Dekker:New York, **1998**, 27

[125] Nabid, M.R.; Entezami, A.A. *Journal of Appl. Poly. Sci.* **2004**, 94, 254

[126] McCullough, L. A; Dufour,B.; Tang, C.; Zhang, R.; Kowalewski, T; Matyjaszweski, K. *Macromolecules* **2007,** *40, 7745*

[127]Liu, W.; Kumar, J.;Tripathy, S. ; Senecal, Kris J.; Samuelson, L. *J.Am. Chem. Soc.* **1999**, 121, 71

[128] Ryu, K.; McEldoon, J.P.; Pokora, A.R.; Cyrus,W.; Dordick,J.S. *Biotechnol. Bioeng.* **1993**, 42, 807

[129] Bae, A.; Hatano, T.; Numata, M.; Takeuchi, M.; Shinkai, S. *Chemistry Letters* **2004**, 33,436

[130] Eichen, Y.; Braun, E.; Sivan, U.; Ben-Yoseph, G. *Acta Polym.* **1998**, 49, 663

[131] Uemura, S.; Shimakawa, T.; Kusabuka, K.; Nakahira, T.; Kobayashi, N. *J. Mater Chem.* **2001**, 11, 267

[132] Kobayashi, N.; Uemura, S.; Kusabuka, K.; Nakahira, T.; Takahashi, H. *J. Mater. Chem.* **2001**, 11 1766

[133] Nagarajan, R.; Liu, W.; Kumar, J.; Tripathy, S. K.; Bruno, F. F.; Samuelson, L. A. *Macromolecules* **2001**, 34, 3921

[134] Nagarajan, R.; Roy, S.;Kumar,J.; Tripathy, S.K.; Dolukhanyan, T.; Sung, C. Bruno, F.;Samuelson, L.A. *J. Macromol. Sci.-Pure Appl. Chem.* **2001**, A38, 1519

[135] Ma, Y. F.; Zhang, J. M.; Zhang, G. J.; He, H. X. *J. Am. Chem. Soc.* **2004**,126, 7097

[136] Datta, B.; Schuster, G. B.; McCook, A.; Harvey, S. C.; Zakrzewska, K *J. Am.Chem. Soc.* **2006**, 128, 14428

[137] Datta, B.; Schuster, G.B. *J. Am. Chem. Soc.* **2008**; 130, 2965

[138] Fischler, M.; Simon, U.; Nir, H.; Eichen, Y.; Burley, G.A.; Gierlich, J.; Gramlich, J.; Carell, T. *Small* **2007**, 3, 1049

[139] Gu, Q.; Cheng, C.; Gonela, R. Suryanarayanan, S. ; Anabathula, S.; Dai, K.; Haynie, D.T. *Nanotechnology* **2006**, 17, R14

[140] Burley, G.A.; Gierlich, J.; Mofid, M.R.; Nir,H.;Tal, S.; Eichen, Y. ; Carell, T. *J. Am. Chem. Soc.* **2006**, 128, 1398

[141] Nguyen, K.; Monteverde, M.; Filoramo, A.; Goux-Capes, L.; Lyonnais, S.; Jegou, P.; Viel, P.; Goffman, M.; Bourgoin, J.-P. *Adv. Mater.* **2008**, *20*, 1099

[142] Srinivasan, S.; Schuster, G.B. *Org. Lett.,* 2008, 10 , 3657

[143] Dutta, P.; Mandal, S.K. *J. Phys. D:Appl. Phys.* **2004**, 37, 2908

[144] Geier , R.G. III; Grindrod, S.C., *J. Org. Chem.*, **2004,** *6404*

[145] De Pablo, M.S. ; Gandasegui, T. ; Vaquero, J.J. ; Navio,J.L.G ; Alvarez-Builla, *J. Tetrahedron* **1992**, 48, 8793

[146] Min., C. ; Verdine, G.L. *Nucleic Acids Res.* **1996**, 24, 3806

[147] Carrasco, J. ; Figueras, A. *Synthetic Metals* **1993**, 61, 253

[148]Ferraris, J.P.; Hanlon, T.R. *Polymer* **1989**, 30, 1319

[149] Otera, T.F.; Figueras A. ; Carrasco, J. ; Brillas, E. *Journal of Electroanalytical Chemistry* **1994**, 370, 231

[150] Tarkuc, S.; Ak, Metin; Onurhan, E.; Toppare, L. *Journal of Macromolecular Science w, Part A: Pure and Applied Chemistry* **2008**, 45, 164

[151] Melo, J.S.; Elisei, F. ; Becker, R.S., *Journal of Chemical Physics* **2002**, 117, 4428